Australian Government
Department of Defence
Defence Science and
Technology Organisation

Determination of Small Crack Stress Intensity Factors for an American Society for Testing Materials (ASTM) Middle Tension Test Specimen by Finite Element Method

Callum Wright

Air Vehicles Division
Defence Science and Technology Organisation

DSTO-TR-2628

ABSTRACT

Improved small-crack stress intensity factors are important for accurate fatigue crack growth prediction. This report presents accurate small-crack stress intensity factor distributions for the American Society for Testing Materials middle tension test specimen, derived in three dimensions utilising the advanced finite element method code StressCheck for a parametric study of a range of small crack sizes and shapes. This information was not readily available in reference books. The results have been presented in tabulated normalised form for future reference and clearly show the influence of the specimen notch on the variation of stress intensity factors.

RELEASE LIMITATION

Approved for public release.

Published by

Air Vehicles Division
DSTO Defence Science and Technology Organisation
506 Lorimer St
Fishermans Bend, Victoria 3207 Australia

Telephone: (03) 9626 7000
Fax: (03) 9626 7999

AR-015-156
November 2011

APPROVED FOR PUBLIC RELEASE

Determination of Small Crack Stress Intensity Factors for an American Society for Testing Materials (ASTM) Middle Tension Test Specimen by Finite Element Method

Executive Summary

DSTO has expended significant effort to improve the cost effectiveness of air platforms subjected to the unique Australian operational conditions. This work often places DSTO at the forefront of full-scale fatigue testing. In support of these efforts, DSTO conducts research into the more fundamental aspects of metal fatigue and crack growth while seeking to improve understanding, techniques and predictions. A prime outcome of this research is to improve the understanding of fatigue and thereby potentially reduce the total life costs for military air platforms. Most current crack growth models rely on an assessment of geometry correction or stress intensity factors to provide transferability between different cracking configurations. It is therefore important to ensure that calculations of these parameters are sufficiently accurate to produce reliable crack growth modelling.

Geometry correction factors relate the stress intensity factor for a crack in any arbitrary geometry to that of a crack in an infinite plate, and these are easily produced from finite element analysis. Therefore, this report documents the generation of stress intensity factors for small cracks in the American Society of Testing Materials Middle Tension test specimen, utilising advanced three dimensional p-element finite element method. The American Society of Testing Materials Middle Tension test specimen was chosen as it is an internationally recognised test with a large amount of available test data and it often shows the short crack phenomenon. Several cases are considered; including corner cracks, near corner (surface) cracks, and centrally located (surface) cracks. These cases apply to a geometric problem that is not in the open literature and will therefore increase the pool of scientific knowledge. The more complex case of irregular initiation sites will not be covered by this report. The reported work developed a large set of valuable results for short cracks within the American Society of Testing Materials Middle Tension test specimen. The results are presented in the usable form of tabulated values of stress intensity factors.

The results show that the stress intensity factors, and therefore the geometry correction factors, may characterise the behaviour of the early portion of crack growth for the specimen. However, the method of measurement of that early portion of crack life is likely to have significant influence on the experimental data for this region. Before a conclusive recommendation could be made, it is felt necessary that the experimental techniques behind the source data be investigated.

This page is intentionally blank

Author

Callum Wright
Air Vehicles Division

Callum Wright is a Masters qualified Aerospace Engineer who joined the Air Vehicles Division, DSTO, in 2002 after a 12 year career in the Royal Australian Air Force. His RAAF career included time at the Aircraft Research and Development Unit (ARDU) and the Directorate of Technical Airworthiness, Aircraft Structural Integrity Section (ASI-DGTA). He has been involved with the International Follow-On Structural Test Project (IFOSTP), the BAe Hawk Mk127 full scale fatigue test and Aircraft Structural Integrity Management on F/A-18 Hornet, Pilatus PC9, Hawk Mk127, C130J Hercules, Airborne Early Warning and Control Aircraft and Air to Air Refuelling Aircraft. He has been working in Long Range Research projects for several years and is currently the Task Leader for the AVD Enabling Research Program (former called Long Range Research).

This page is intentionally blank

Contents

1. Introduction

DSTO has often been at the forefront of full-scale airframe fatigue testing in an effort to improve the cost effectiveness of platforms subjected to the unique Australian operational conditions [1]. In support of these efforts, DSTO conducts research into the more fundamental aspects of fatigue and crack growth while seeking to improve understanding, techniques and predictions. A prime outcome of this work is to improve the understanding of fatigue and thereby potentially reduce the total life costs for military air platforms.

In light of this, DSTO has been seeking to develop improved crack growth models that apply to typical air platform load spectra and material regimes. One such example is Molent et al. [2]. In this example, the centre portion of crack growth data—that displays exponential crack growth behaviour— is utilised and the Paris crack growth law [3] is manipulated to improve the prediction. This centre portion is marked as Zone 2 in Figure 1. The technique is fairly robust at making predictions when the behaviour fits a exponential growth pattern. However, it fails to reasonably predict the crack growth in the other zones of measured data; namely Zones 1 and 3 from Figure 1. Failing to accurately predict the early life can have a significant impact on the accuracy of the failure time.

With the work of Molent et al. [2], it was shown that the crack growth behaviour was exponential only during periods where the geometry correction factor was constant. Geometry correction factor is related to the stress intensity factor, as described in Section 2. Assuming that a change in the geometry correction factor changes the exponential relationship, Molent supposed that such a variation may be responsible for the transition region of Zone 1. Zone 3 is known to be the zone were tearing starts to occur just prior to specimen failure and, as such, is not expected to behave in the same stable manner as Zone 2 and was thus ignored in this report. However, the interpretation of the Zone 1 behaviour is more subjective; it could be due to the method of crack length measurement, changes in geometry correction factor or another small crack phenomenon. These changes in geometry correction factor could be due to the relative shape of the crack to the local geometry, or for the time from the initiation at an irregular defect to the time when the crack becomes self-similar, or when it develops its long term stable shape. Hence, it was felt necessary to understand the variations of geometry correction factor for small cracks.

The example cited above, Figure 1, is from a standard ASTM Middle Tension test specimen [4] under constant amplitude loading. Geometry correction factors for centreline asymmetric small cracks in the ASTM Middle Tension test specimen [4] layout were not available in the literature. Specifically, single-sided semicircular and elliptical crack information was not available for the ASTM Middle Tension test specimen [4]. The only data found related to centreline symmetric through cracks [5], which highlighted the need for information on non-through cracks for this specimen type. As there are no handbook solutions to determine the geometry correction factors for small cracks in this specimen it was therefore necessary to use another technique, such as finite element methods.

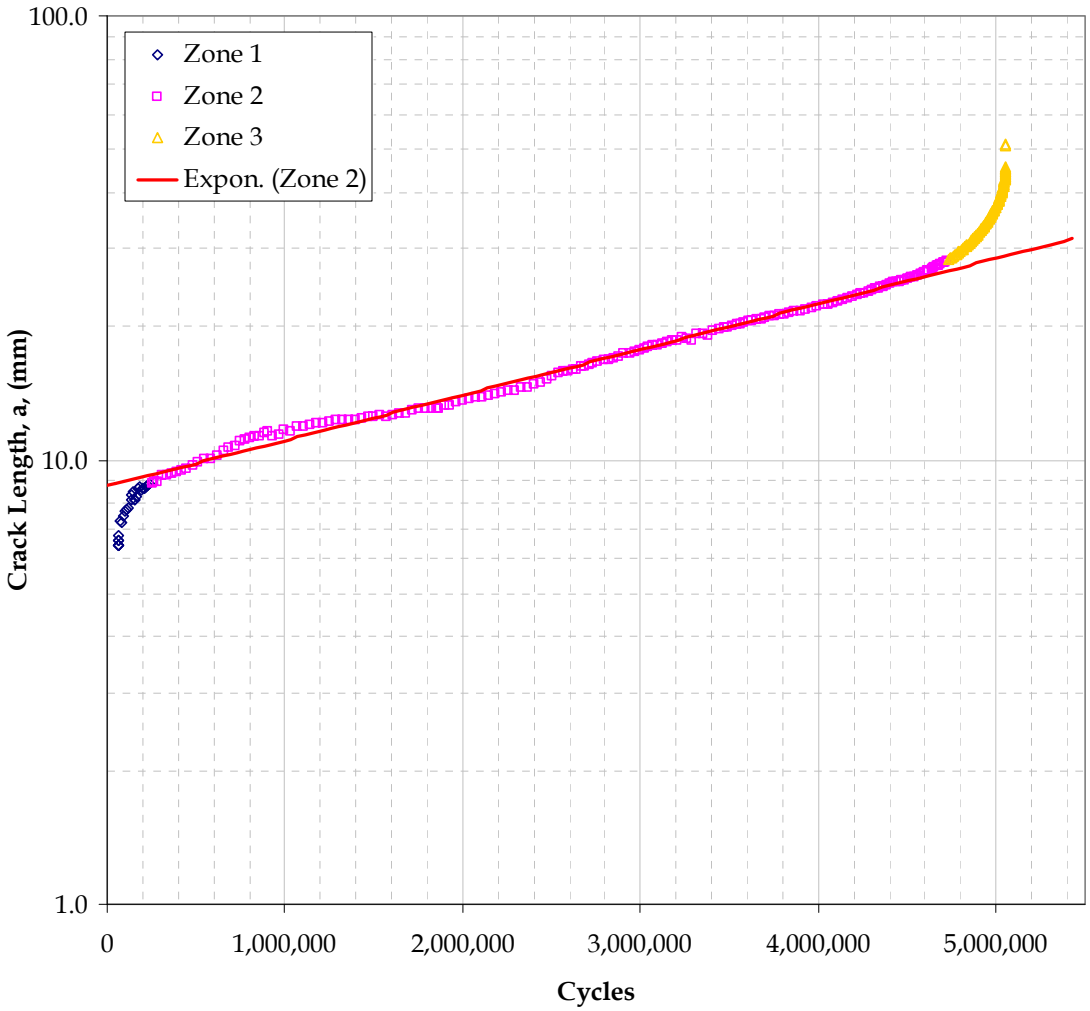

Figure 1: ATSM standard middle tension test specimen crack growth rate data example. The test data is generated using an ASTM standard middle tension test specimen, with a width: of 101.6 mm (4 inches) and thickness of 1.5975 mm (0.0625 inches). The trend line through the Zone 2 data highlights the exponential behaviour of this data.

Investigation into the behaviour of small cracks is becoming increasingly common as researchers try to understand the contributing factors to the variation of crack behaviour at this small scale. Therefore, this work would have the secondary benefit of adding to information available for small crack geometry correction factors. This is a valuable contribution to the available body of scientific knowledge.

This report utilises advanced finite element method to assess whether there are changes in geometry correction factor for small cracks in the ASTM Middle Tension test specimen [4]. The finite element method will employ advanced high order polynomial elements, commonly referred to as p-elements, to aid in expedient and robust solutions. Several cases will be considered; including corner initiated cracks, near corner initiated cracks, and centrally initiated cracks, as shown in Figure 2. The more complex case of irregular initiation sites—Figure 2 (d)—will not be covered by this report. The report derives stress intensity factors,

which are readily convertible to geometry correction factors, as shown in Section 2, for specific local stress cases.

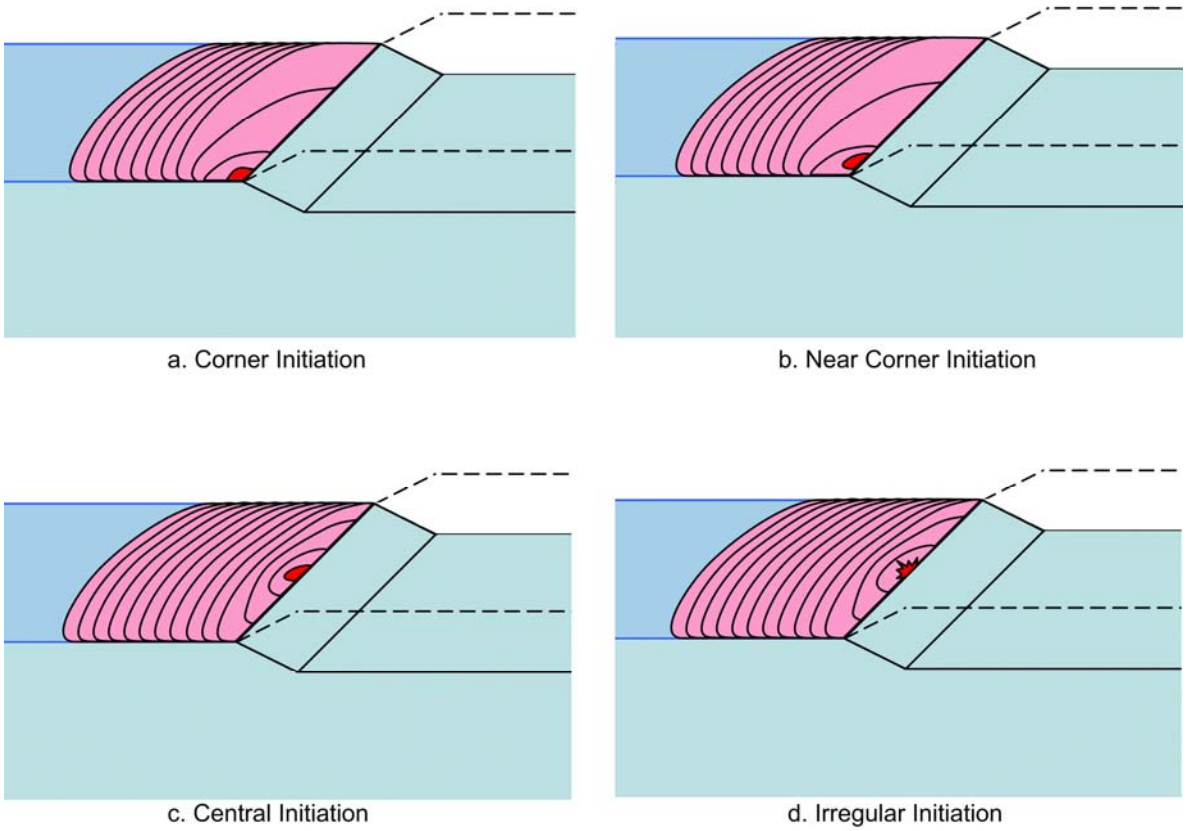

Figure 2. Possible crack initiation sites

2. Numerical Approach

2.1 Geometry Correction Factors

2.1.1 Explanation

It is worth understanding the origin, meaning and use of geometry correction factors, otherwise known as β factors, before putting them into practice. 'β factor' is a term that relates the stress intensity factor for a crack in any arbitrary geometry to that of a crack in an infinite plate.

For example, Broek [6] outlines and defines β factors in his book on the practical use of fracture mechanics. In this book linear elastic fracture mechanics (LEFM) is discussed and the stress intensity factor (K) is derived after performing a J-integral (also known as the Contour Integral Method) within the stress field around the crack-tip in an infinite plate. By taking only the most significant term in the series expansion Broek [6] obtains:

$$K = \sigma\sqrt{\pi a} \tag{1}$$

Where 'K' is the stress intensity factor, 'σ' is the far field stress and 'a' is the crack length.

This provides the reference case of the stress intensity factor for an infinite plate. However infinite plates do not exist in reality so this is then modified to account for a finite plate width and the formula is adjusted to:

$$K = \sqrt{\sec\left(\frac{\pi a}{W}\right)}\left(\frac{a}{L}\right)\sigma\sqrt{\pi \cdot a} \tag{2}$$

Where 'W' is plate width , 'L' is plate length and 'K', 'σ' and 'a' are defined previously.

This simplifies through the introduction of β to:

$$K = \beta\left(\frac{a}{L}\right)\sigma\sqrt{\pi a} \tag{3}$$

Where:

$$\beta = \sqrt{\sec\left(\frac{\pi a}{W}\right)} \tag{4}$$

for a centre crack in a plate of finite width. Therefore, the β factor of equation 4 provides the correction from a finite plate to an infinite plate. Note that different stress intensity factors are defined for different types of loading associated with the crack extension methods, see Figure 3. The example cited here applies to the stress intensity factor under Mode I loading.

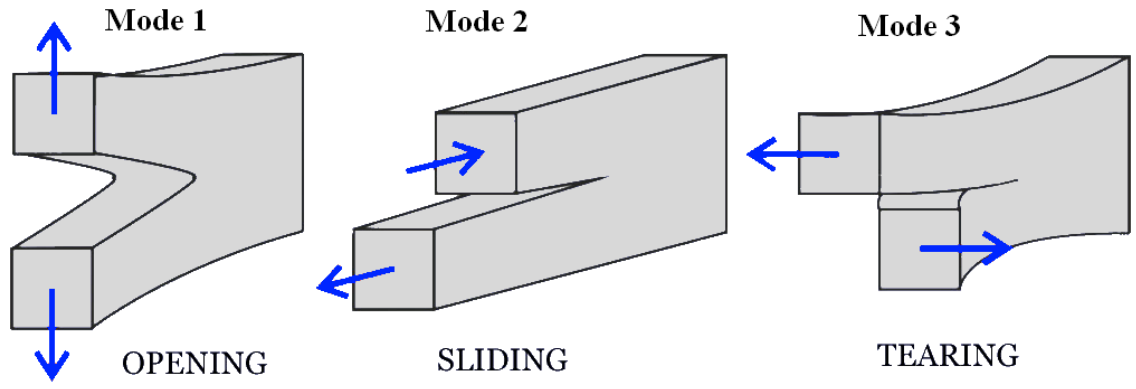

Figure 3. Crack extension modes

β factors can be derived for all crack geometry problems—relating them to a crack in an infinite plate.

2.1.2 Developing β factors for complex geometry

There is a large amount of literature—including Rooke et al. [7], Sih [8], Tada et al. [9] and Murakami et al. [5]—that provide β factors for predetermined geometries. These solutions have been derived through a variety of methods and can often be used to develop bounding cases or acceptable engineering solutions. However, occasionally these do not match the real-world geometric layout and relative loading. As such, an approximate method of combining these is required to provide acceptable engineering estimations. The two techniques employed are superposition and compounding. To understand if these are applicable to this problem it is important to first understand how they work.

2.1.2.1 Superposition

Superposition is the technique used to adjust the β factor for variations in the mode of loading [6]. For example, if a specimen was simultaneously subjected to Mode 1 bending and tension, the total stress intensity would be the summation of the stress intensities for each case. The case in this paper is loaded in simple uni-axial tension, so the superposition technique will not be needed.

2.1.2.2 Compounding

Compounding refers to the combination of various geometric effects. The idea being to combine simple geometric cases—such as for finite boundaries and stress concentrations—to give an accurate total β factor. For example, a semi-circular crack in a finite plate could be represented by compounding the β factors for the finite width, the back free surface and front free surface—resulting in a correctly bound mathematical representation.

One of the challenges in establishing compounded solutions is to determine how to divide the problem into appropriate boundary effects. In short, the sub-structured elements must continue to behave in the same way as the parent for the division to be valid. For example, a finite plate could be divided into half, length ways, because there will be no stresses acting across the split. However, a plate with a crack in the middle will not behave in a similar manner if split in half, length ways, because stresses will cross the boundary at the crack. The centre crack is likely to open more when it becomes an edge crack in the segregated sections. Therefore, this division is not valid as the sub-structured elements would not behave like the parent. [6]

The model under consideration here is not symmetrical and as such compounding is not applicable. This leads to the conclusion that stress intensity factors cannot be derived from text book solutions. As such, there is a requirement to undertake numerical modelling to develop the β factors.

2.2 Numerical Modelling

For more complicated geometry it is often more appropriate to develop β factors with numerical methods. This allows for estimations to be made for geometries that are not easily broken out into the predetermined geometries listed in text books. It can also speed up the processing of multiple cases to find the influence of configuration variations on the solution. This study is interested in variations of crack geometry, including non-symmetrical cases, and

has therefore opted to use a numerical method, specifically the commercially available code called StressCheck by Engineering Software Research and Development, Inc. (ESRD). Not all modelling tools extract geometry factors in the same manner and some use approximations that impact on the robustness of the solution within certain regions. It is therefore useful to assess the specific methodology employed by StressCheck to understand any possible limitations.

StressCheck is an advanced 'p-version' computational analysis program for the determination of stresses [10]. All finite element methods provide approximate solutions for the determination of stress and most finite element codes are based on 'h-version' solutions, which limit the ability of the user to readily-assess the convergence of the solution. However, 'p-version' solutions provide for multiple approximations of higher orders to forecast the convergence of a solution and measure the robustness through error estimation. Of course, this error estimation only considers the accuracy of the finite element solution, not of the idealisations employed in constructing the model.

2.2.1 Theory of geometry factor determination in StressCheck

StressCheck includes tools to indirectly calculate the geometry factor, through determination of Mode 1 (K_1) and Mode 2 (K_2) stress intensity factors [11]. K_1 and K_2 are computed using an extraction via the contour integral method. This is done by taking a section normal to a tangent at the crack edge and extracting stress and displacement information along a circular path contained in the cutting plane, centred on the crack tip, shown in Figure 4. This is essentially a 2-D approximated solution for a slice in a 3-D body. Multiple slices can be taken to map the stress intensity factor around the crack front. One limitation of this simplification is that only K_1 and K_2 can be determined, with K_3 working out of the plane of the slice, as per Figure 3. For most cases, and specifically in this case, this approximation will not significantly inhibit the veracity of the solution. However, when through thickness stresses develop, such as near a free surface the method needs to be corrected—these corrections will be described later.

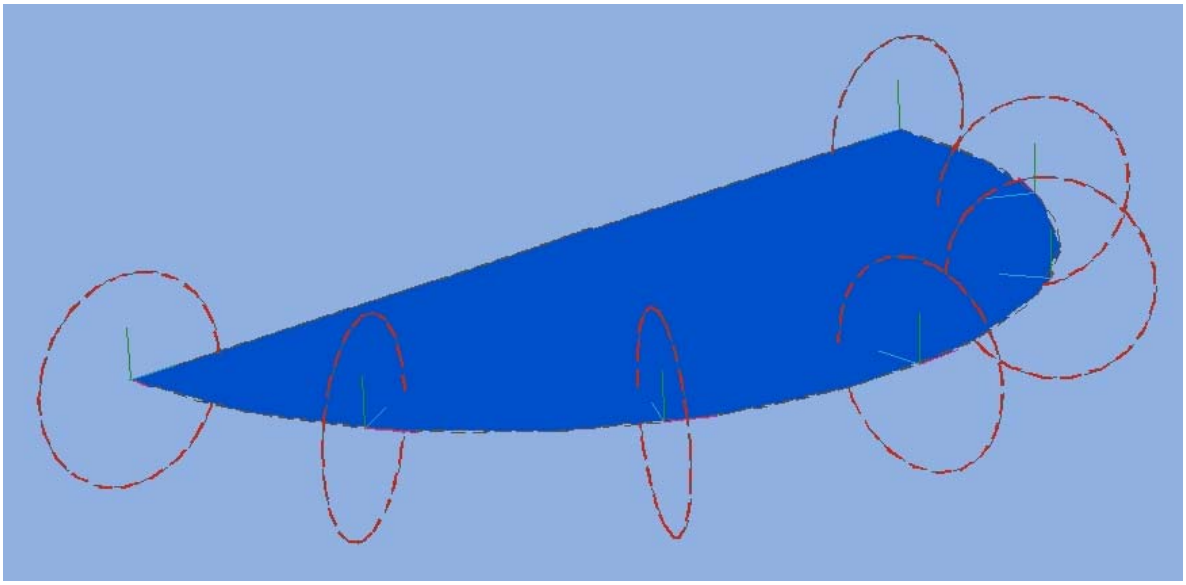

Figure 4. A semi-circular crack in 3-D, shown from within the body, with the 2-D extractions taken in sections normal to the tangent of the crack front

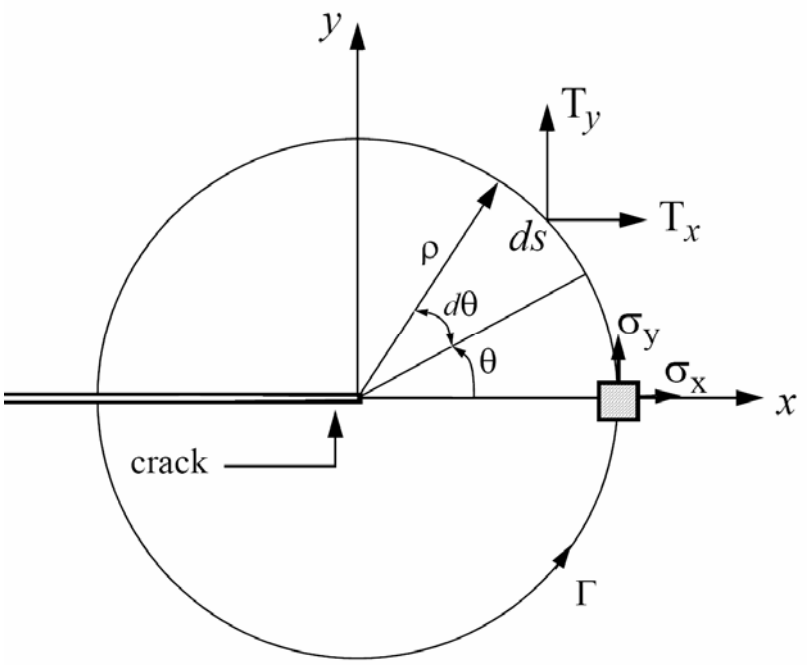

Figure 5.This representation of the 2-D slice provides definition of terms employed in the J-Integral and Contour Integral Method at the crack tip

2.2.1.1 StressCheck method for determining K_1 and K_2.

As per the Master Guide [11], StressCheck uses the contour integral method to determine K_1 and K_2. The calculation is based on the 2-D case which applies to either plane-stress or plane-strain. In both cases the stress intensity factors of the 2-D slice are simplified to the first terms of the asymptotic expansion of the solution near the crack tip:

$$K_1 = \left(\sqrt{2\pi}\right) A_1^{(1)} \tag{5}$$

and

$$K_2 = \left(\sqrt{2\pi}\right) A_1^{(2)} \tag{6}$$

Where the asymptotic expansion is:

$$A_1^{(m)} \approx \int_{\Gamma} \left(W_m T_{FE} - u_{FE} T^{(W_m)} \right) ds \tag{7}$$

This is the basis of a mathematical approach often referred to as an interaction method. In an interaction method an assumed solution is compared and operated against the actual solution to determine the missing relationship, in this case K_1 and K_2. So stresses around the J-Integral, Figure 5, are compared with theoretical values to determine the relative quantities of K_1 and K_2.

Within equation 7, T_{FE} is the traction vector along Γ due to the finite element solution, such that along Γ:

$$T_{FE} = \begin{bmatrix} T_x \\ T_y \end{bmatrix}_{FE} = \begin{bmatrix} \sigma_x \cos\theta + \tau_{xy} \sin\theta \\ \tau_{xy} \cos\theta + \sigma_y \sin\theta \end{bmatrix}_{FE} \tag{8}$$

where (along Γ):

$$u_{FE} = \begin{bmatrix} u_x \\ u_y \end{bmatrix}_{FE} \tag{9}$$

which leaves the extraction function and the associated traction vector to be defined. Firstly, the extraction function:

$$W_m = \frac{\rho^{-\frac{1}{2}}}{D^{(m)}} \left\{ \Psi^{(m)}(\theta) \right\} \tag{10}$$

where:

$$D^{(1)} = \pi(2\kappa - 1) \tag{11}$$

$$D^{(2)} = \pi(2\kappa + 3) \tag{12}$$

With κ for plane-strain as:

$$\kappa = (3 - 4\nu) \tag{13}$$

With κ for plane-stress as:

$$\kappa = \frac{(3-\nu)}{1+\upsilon} \tag{14}$$

With the comparative displacement fields:

$$\Psi^{(1)}(\theta) = \begin{bmatrix} \left(\kappa - \frac{1}{2}\right)\cos\left(\frac{\theta}{2}\right) - \frac{1}{2}\cos\left(\frac{3\theta}{2}\right) \\ \left(\kappa + \frac{1}{2}\right)\sin\left(\frac{\theta}{2}\right) - \frac{1}{2}\sin\left(\frac{3\theta}{2}\right) \end{bmatrix} \tag{15}$$

$$\Psi^{(2)}(\theta) = \begin{bmatrix} \left(\kappa + \frac{3}{2}\right)\sin\left(\frac{\theta}{2}\right) + \frac{1}{2}\sin\left(\frac{3\theta}{2}\right) \\ -\left(\kappa - \frac{3}{2}\right)\cos\left(\frac{\theta}{2}\right) - \frac{1}{2}\cos\left(\frac{3\theta}{2}\right) \end{bmatrix} \tag{16}$$

Returning to the traction vector due to the extraction function:

$$T^{(W_m)} = \frac{G\rho^{-\frac{3}{2}}}{D^{(m)}}\left\{\mathrm{Y}^{(m)}(\theta)\right\} \tag{17}$$

where G is the modulus of rigidity and

$$\mathrm{Y}^{(1)}(\theta) = \begin{bmatrix} \left(\frac{3}{2}\cos\left(\frac{\theta}{2}\right) + \frac{1}{2}\cos\left(\frac{5\theta}{2}\right)\right)\cos(\theta) + \left(\frac{1}{2}\sin\left(\frac{5\theta}{2}\right) - \frac{1}{2}\sin\left(\frac{\theta}{2}\right)\right)\sin(\theta) \\ \left(\frac{1}{2}\sin\left(\frac{5\theta}{2}\right) - \frac{1}{2}\sin\left(\frac{\theta}{2}\right)\right)\cos(\theta) + \left(\frac{5}{2}\cos\left(\frac{\theta}{2}\right) - \frac{1}{2}\cos\left(\frac{5\theta}{2}\right)\right)\sin(\theta) \end{bmatrix} \tag{18}$$

And

$$\mathrm{Y}^{(2)}(\theta) = \begin{bmatrix} \left(-\frac{7}{2}\sin\left(\frac{\theta}{2}\right) - \frac{1}{2}\sin\left(\frac{5\theta}{2}\right)\right)\cos(\theta) + \left(\frac{1}{2}\cos\left(\frac{5\theta}{2}\right) + \frac{3}{2}\cos\left(\frac{\theta}{2}\right)\right)\sin(\theta) \\ \left(\frac{1}{2}\sin\left(\frac{5\theta}{2}\right) + \frac{3}{2}\cos\left(\frac{\theta}{2}\right)\right)\cos(\theta) + \left(-\frac{1}{2}\sin\left(\frac{\theta}{2}\right) + \frac{1}{2}\sin\left(\frac{5\theta}{2}\right)\right)\sin(\theta) \end{bmatrix} \tag{19}$$

Once the values of K_1 and K_2 have been determined, the geometry factor, β, is found simply with this relationship for each mode:

$$\beta_1 = \frac{K_{1\_total}}{\sigma\sqrt{\pi a}} \tag{20}$$

$$\beta_2 = \frac{K_{2\_total}}{\sigma\sqrt{\pi a}} \tag{21}$$

2.2.1.2 Extending the solution of K1 and K1$_I$ for a 3-D stress field.

To account for a 3-D stress field, StressCheck determines the ratio of out of plane stress to the in-plane stress at the zero degree point on the radius of integration:

$$\gamma = \left| \frac{\sigma_z}{\sigma_x + \sigma_y} \right| \tag{22}$$

If $\gamma > 0.1$ then κ is selected as for the plain strain condition:

$$\kappa = \kappa_1 = (3 - 4\nu) \tag{23}$$

Otherwise, if $\gamma \leq 0.1$ then κ is adjusted proportionally using:

$$\kappa = \kappa(\gamma) = \kappa_1 + (\kappa_2 + \kappa_1)\left(\frac{2\gamma}{\gamma_1} + 1\right)\left(1 - \frac{\gamma}{\gamma_1}\right)^2 \tag{24}$$

Where:

$$\gamma_1 = 0.1 \tag{25}$$

Figure 6 shows the typical zones of γ within a cracked body. This provides an understanding of how the solution 2-D case is extended to account for a 3-D stress field, as would be seen on most 3-D cracks.

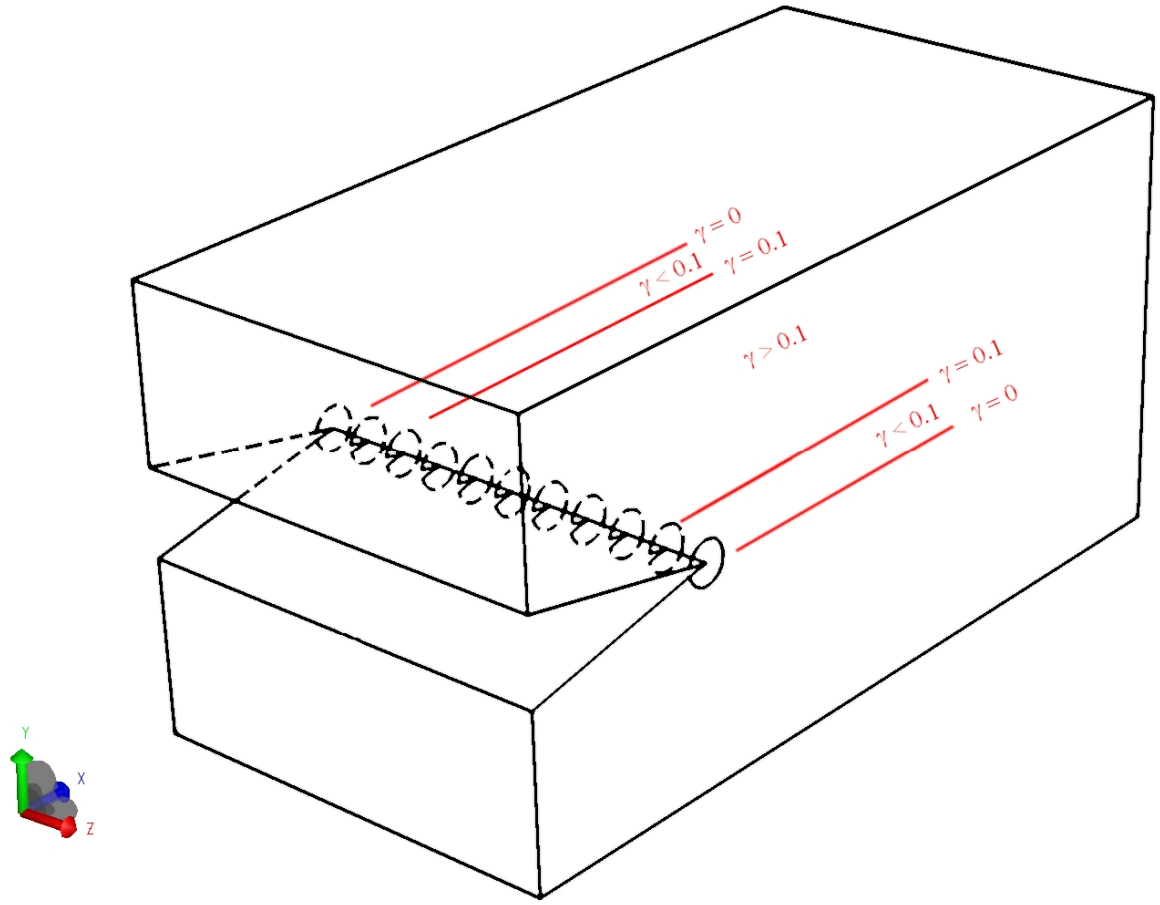

Figure 6. Graphical presentation showing the typical zones of γ within the cracked body

3. Model Development

This activity is seeking to extract stress intensity factors from very small cracks—ranging from 0.08 mm to 1 mm—in a standard ASTM test specimen and assess the change in the stress intensity factors with various crack parameters. Several models were developed in this study, starting with a global model to establish a representative local stress and displacement field and then sub-structured models to improve efficiency without impacting on the resulting accuracy.

3.1 Geometry Definition

The data set shown in Figure 1 was gathered from a standard ASTM middle tension (MT) test specimen [4]. As such, the model considered within this report will also be based on this type of specimen. Figure 7 and Table 1 provide the details of the specific specimen dimensions that are under consideration. These dimensions differ from those of the specimen that generated the data in Figure 1. However, as this report sets out to produce comparative assessments it does not impact on the results of the study.

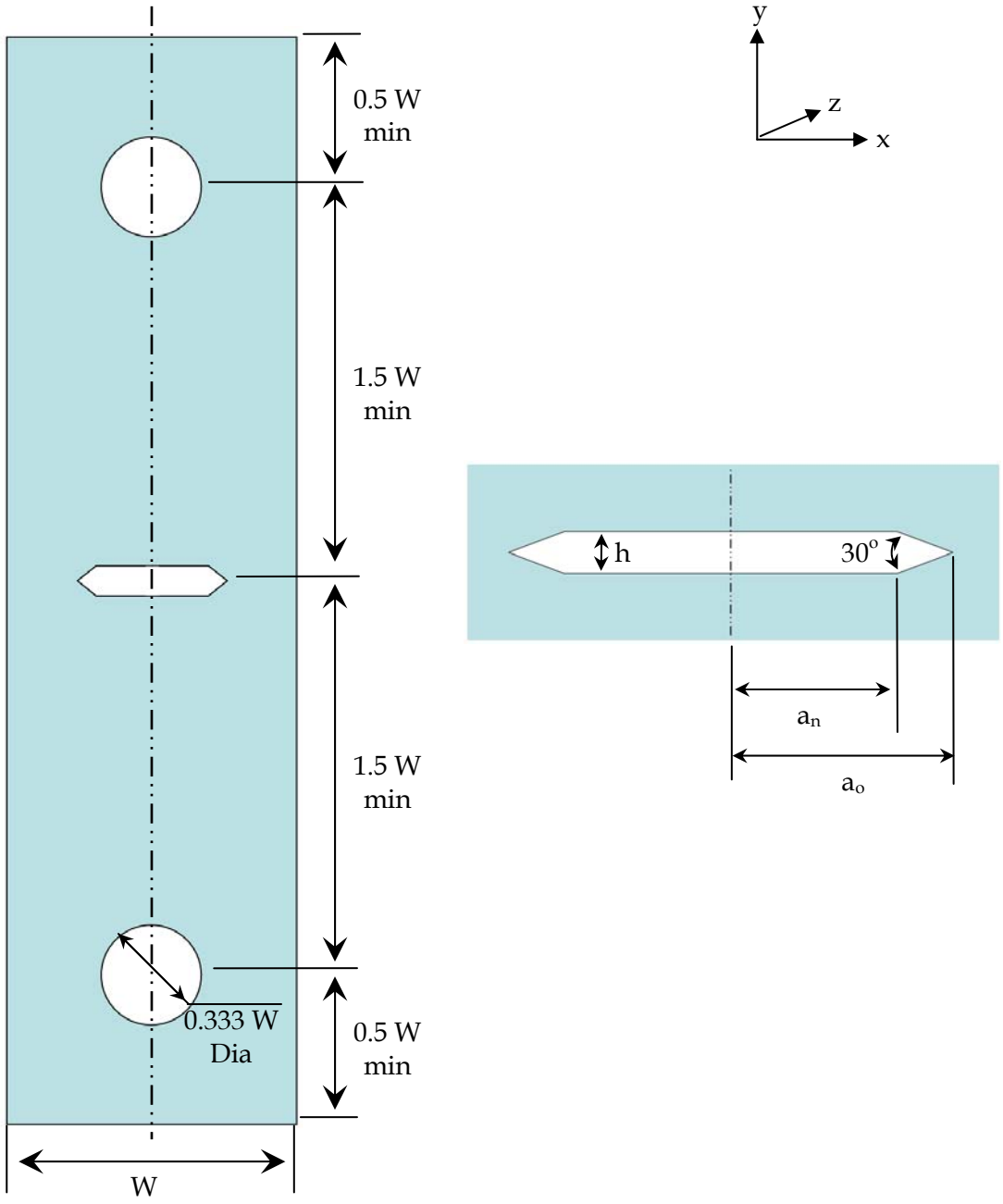

a. Specimen dimensions b. Notch dimensions

Figure 7. ASTM standard middle-tension specimen for fatigue crack growth rate testing

The ASTM MT specimen has a notch at the centre and is either loaded through grips or with pins a set distance back from the notch, as in this case. The symmetrical nature of this specimen allows for the model to be simplified, and so initially a global model will be developed, with symmetry about the notch. The global model will be used to determine the most appropriate geometric simplification and displacements for a sub-structured model.

Table 1. Dimensions of middle-tension specimen used in this analysis.

Dimension	Value
W	100 mm
h	1 mm
a_n	9.13 mm
a_o	10 mm
thickness	12.5 mm

3.2 Modelling Overview

When constructing the models, many of the global parameters were kept consistent. All models were constructed with the axis of loading parallel to the Y axis. The crack and plane of symmetry lay in the XZ plane. The model was always built as "linear elastic" in StressCheck under the "other units" option, with all dimensions entered as SI units. The material selected was aluminium alloy 7075-T6 from the standard StressCheck material library, again using SI units.

Each model was set up with a symmetry plane through the plane of the crack—in other words the centre of the specimen was along the Y axis. This was done using the StressCheck "symmetry" boundary condition, which is a simple way of preventing movement across this plane (in the Y axis), whilst still allowing movement in the X and Z axis. There was also three point restraints applied to prevent free body movement.

Stress check uses "p-element" solutions, rather than the more common "h-element" solutions. This allows for higher order elements and solutions to be calculated without the need for high levels of mesh refinement. All models were tested with low order "p-elements" and final extracts were nominally made from solutions with a "p-element" order of 5. In some cases 5^{th} order elements were not used, but each case will be identified separately, for example in Figure 8.

A substructured model was required to reduce the computational run time and was developed by analysing the model of a half coupon. This first model of the half coupon is referred to as the global model, see Figure 8. The half coupon model was originally analysed with symmetry about the crack surface and constructed to extract displacements at one third of the halved model length from the crack surface. Following this a sub-structured model was built that consisted only of the inner sixth of the coupon (one third of the halved model) run with a plane of symmetry, in-plane with the crack, see Figure 9.

Unfortunately, there were instabilities and limitations with the chosen code, StressCheck, which required models to be redeveloped when new code versions became available. Models were developed for StressCheck versions 7.0.6, 7.1.0 and 7.1.1 before eventually being completed in version 8.0. In short, issues were generally centred on the stability of some methods of geometry construction and meshing. This seemed to be particularly evident for the large range of element sizes required in these models. Refer to Appendix C for more detailed discussions of some of these issues. These issues may not always be apparent in the result produced, and this highlights the importance of robust verification and validation of results—as was conducted for this activity.

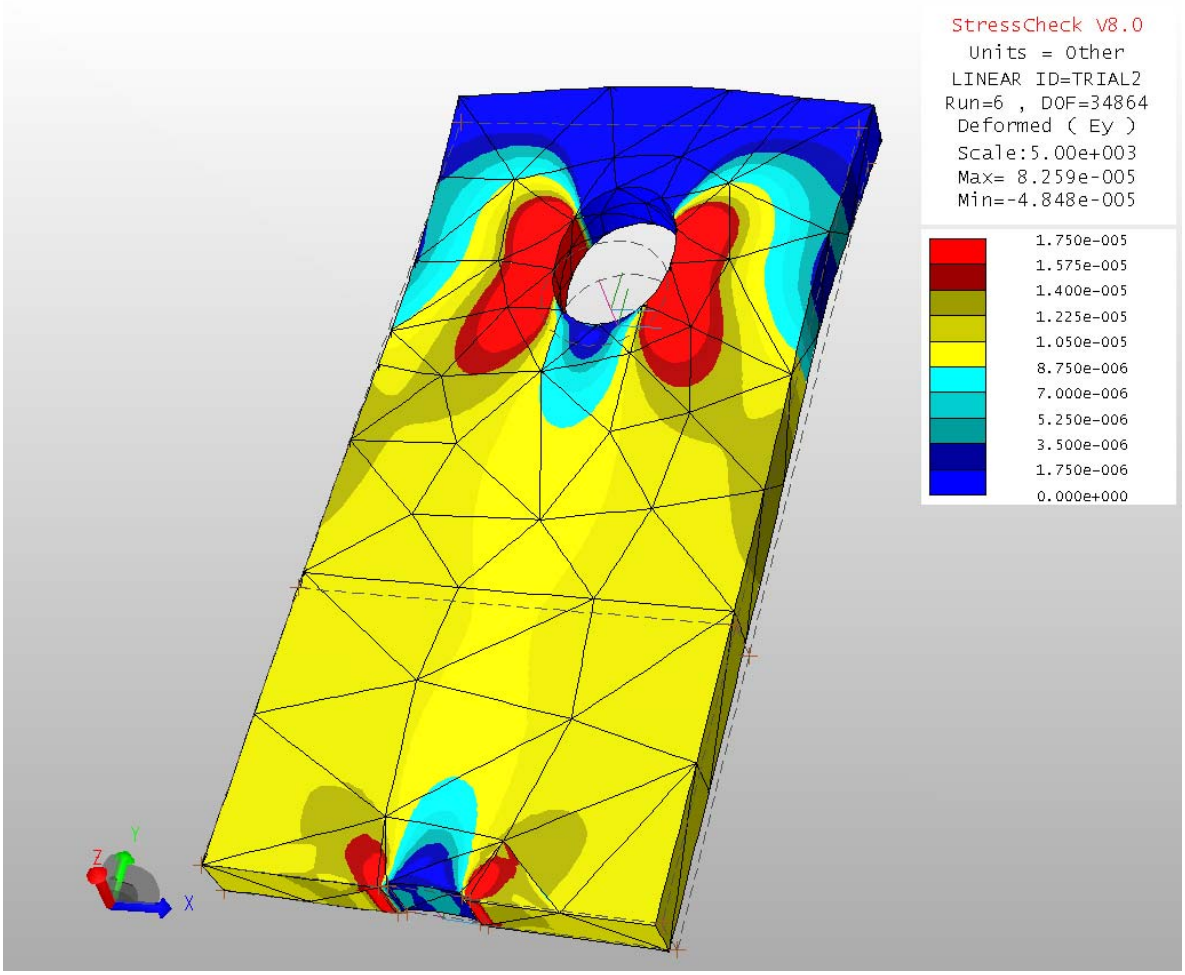

Figure 8. Initial symmetry model of middle-tension specimen. This plot shows the uncracked global model subjected to a bearing load (1 kN) at the pin joint. It depicts strain (E_y) generated from a 6th order polynomial solution by StressCheck version 8.0. Of interest is the consistent displacement at the one third height (near parallel dashed and solid line).

3.3 Global Model

The first step in this process was to develop an uncracked global model and determine a stress field distribution. This generated displacement data for sub-structuring.

This initial model used symmetry about the notch and only modelled one half of the coupon, Figure 8. It used a bearing traction load at the pin hole with symmetry and fixed constraints to generate the displacement and stress distributions. This showed that dividing the half model into thirds would provide a substantially reduced model size with a relatively simple fixed displacement constraint at the new edge.

For the purposes of this study, a simple traction load was selected such that it ensured the model remained within the elastic range, except at the points approaching singularity near the

notch tip. A load of 1 kN in the Y axis was selected. StressCheck is able to distribute this load around the surface of the loading hole in a sinusoid manner, representing the load transferred from a pin.

Details of the construction of this global model are contained in Appendix A. They are presented in a step by step account to enable creation in StressCheck.

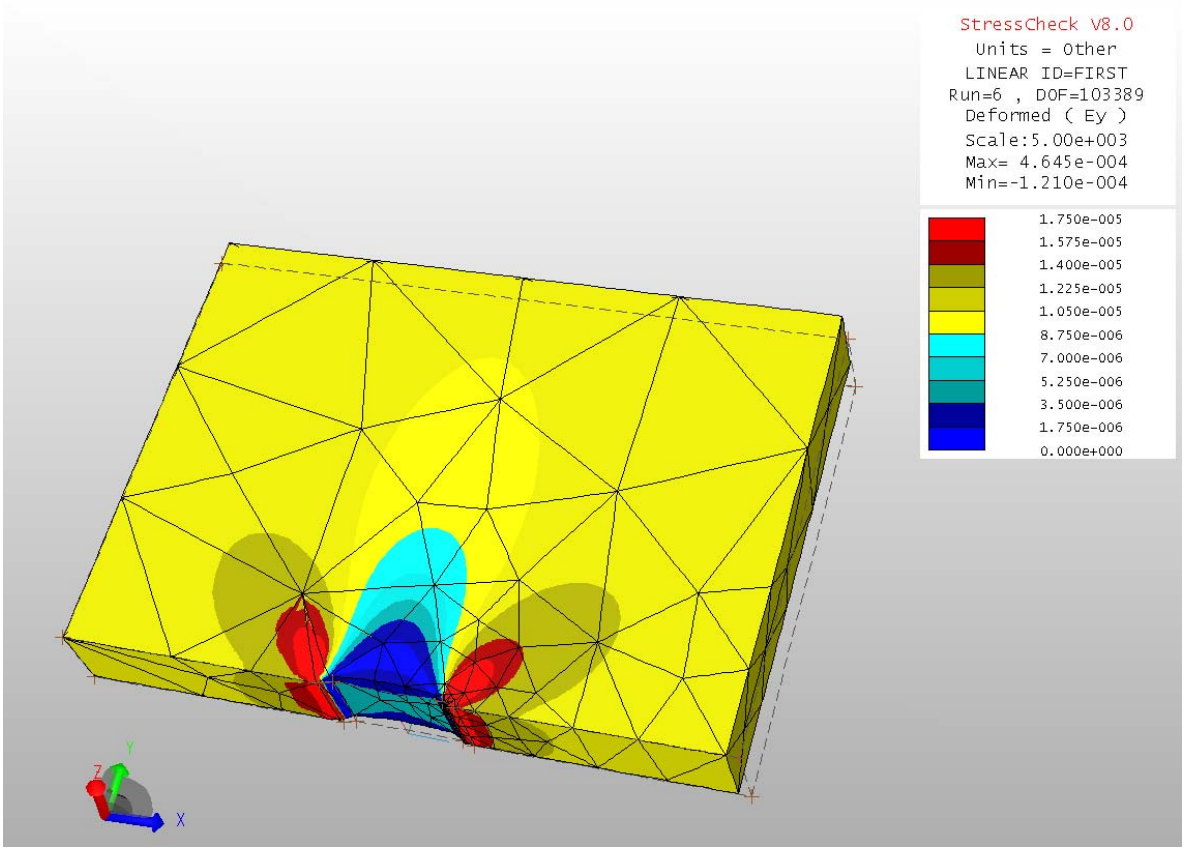

Figure 9. Sub-structured symmetry model of middle-tension specimen. This plot shows the uncracked sub-structured model subjected to the derived fixed displacement along the loaded edge. It depicts strain (E_y) generated from a 6th order polynomial solution by StressCheck version 8.0.

3.4 Sub-structured Model

Once the size of the sub-structured model was determined, a parametric model was developed that allowed for changes to the crack size and location. The model permitted StressCheck to undertake an automated parametric study and provide results more quickly. Details of the construction of this sub-structured model are contained in Appendix B. They are presented in a step by step account to enable creation in StressCheck.

At this point it is important to note that for the discussions herein 'notch size' is the size of initial notch and 'crack size' refers to the size of the defect growing from the original notch.

As can be seen by a comparison of Figure 8 and Figure 9, there is consistent lobes with comparable magnitudes for the displacements. The coarseness of the global model does lead to minor irregularities, part of the reason for substructuring, but on the whole the match is good. Therefore the sub-structuring applied is considered valid and representative.

3.5 Validation Test Case

To validate the modelling assumptions, a simple test case was carried out that compares a simple handbook solution with a simplified crack in a finite plate, modelled with assumptions consistent to those used in the main models.

3.5.1 Handbook baseline

Geometry correction factors have been investigated quite extensively and existing solutions can be found in many texts, such as those by Rooke et al. [7], Sih [8], Tada et al. [9] and Murakami et al. [5]. The following derivations will be based on Murakami et al. [5].

This work considers a middle tension specimen [4] with compliant dimensions and geometry as shown in Figure 7 and Table 1. So to determine the β factor for this specimen a centre notch in a plate with finite width and thickness is considered. Therefore adapting Murakami [5] for this case gives:

$$\beta = \left(1 - 0.25\alpha^2 + 0.06\alpha^4\right) \cdot \sqrt{\sec\left(\frac{\alpha\pi}{2}\right)} \tag{26}$$

Where:

$$\alpha = \frac{2a_o}{W} \tag{27}$$

$\alpha = 0.2$

Therefore, a comparison β factor is:

$\beta = 1.024$

Table 2. Data for K_1 extracted from a simple StressCheck model of a crack in the centre of the specimen also showing the calculated β by extraction point and averaged β for the full crack front, plane strain and plane stress regions

Extraction Number	Normalised Location	K_1 extraction (MPa √m)	β
0	0	4.5	0.957
1	0.027	4.468	0.950
2	0.054	4.619	0.982
3	0.081	4.798	1.020
4	0.108	4.854	1.032
5	0.135	4.869	1.036
6	0.162	4.875	1.037
7	0.189	4.878	1.037
8	0.216	4.882	1.038
9	0.243	4.877	1.037
10	0.270	4.877	1.037
11	0.297	4.874	1.037
12	0.324	4.872	1.036
13	0.351	4.87	1.036
14	0.378	4.867	1.035
15	0.405	4.864	1.034
16	0.432	4.863	1.034
17	0.459	4.869	1.036
18	0.486	4.861	1.034
19	0.514	4.865	1.035
20	0.541	4.865	1.035
21	0.568	4.865	1.035
22	0.595	4.866	1.035
23	0.622	4.868	1.035
24	0.649	4.866	1.035
25	0.676	4.872	1.036
26	0.703	4.878	1.037
27	0.730	4.871	1.036
28	0.757	4.879	1.038
29	0.784	4.878	1.037
30	0.811	4.879	1.038
31	0.838	4.876	1.037
32	0.865	4.87	1.036
33	0.892	4.858	1.033
34	0.919	4.794	1.020
35	0.946	4.612	0.981
36	0.973	4.473	0.951
37	1	4.503	0.958
Average of total set:			1.024
Average of plane strain set:			1.036
Average of plane stress set:			0.963

3.5.2 Simplified numerical model of a crack in a finite plate

By running a model with a simple crack in a centre of the specimen the values of K_1 can be extracted and β determined from:

$$\beta = \frac{K_{total}}{\sigma\sqrt{\pi a}} \tag{28}$$

For this calculation K_{total} is the K_1 extracted from StressCheck and the σ is the far-field stress of the uncracked specimen, determined from the applied displacement.

$$\sigma = 0.839MPa \tag{29}$$

Figure 10 shows a StressCheck plot of deformed strain in the y direction for a simple crack in the centre of the sub-structured specimen. The plot is consistent with previous plots, indicating a consistent modelled behaviour for this test case. Table 2 presents the extracted data and calculated β factors. When comparing the results of Table 2 with the comparison β factor (β = 1.024) it shows a near perfect correlation for this simple case of an idealised through crack in a finite plate. This provides confidence in the modelling approach and the derived results.

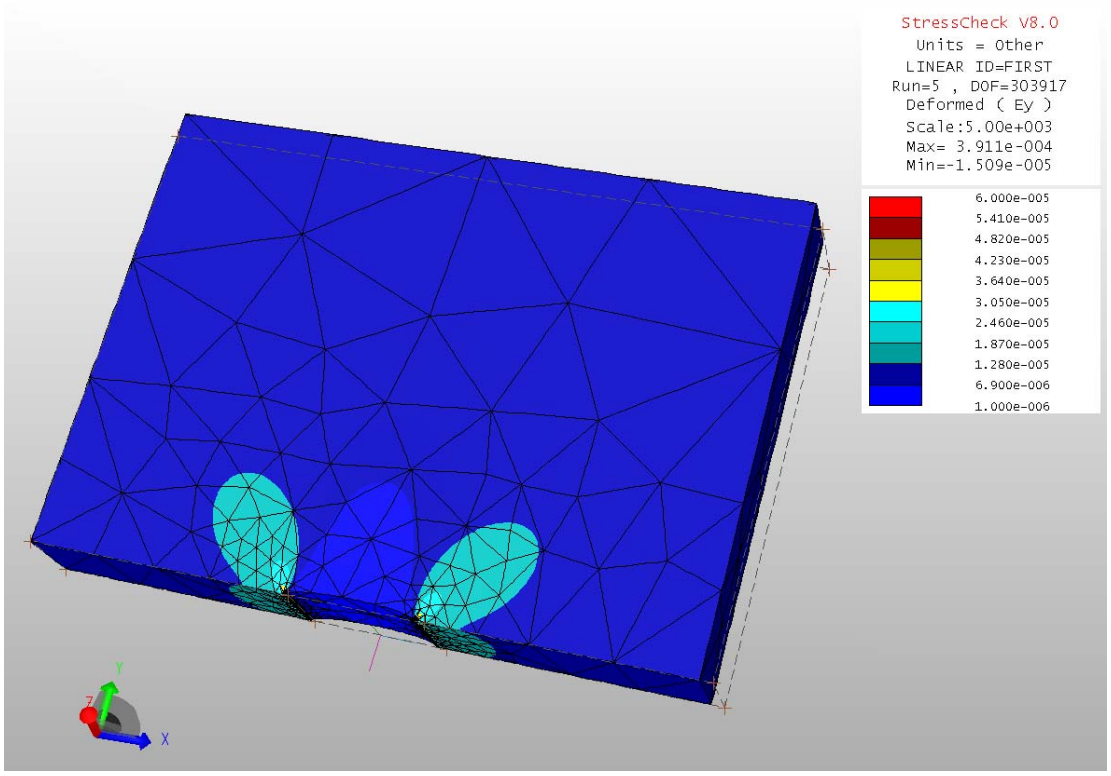

Figure 10. A sub-structured model containing a through thickness centre crack subjected to fixed displacement ($7.8e^{-4}$ mm) along the loaded edge. It depicts strain (E_y) generated from a 5^{th} order polynomial solution by StressCheck version 8.0.

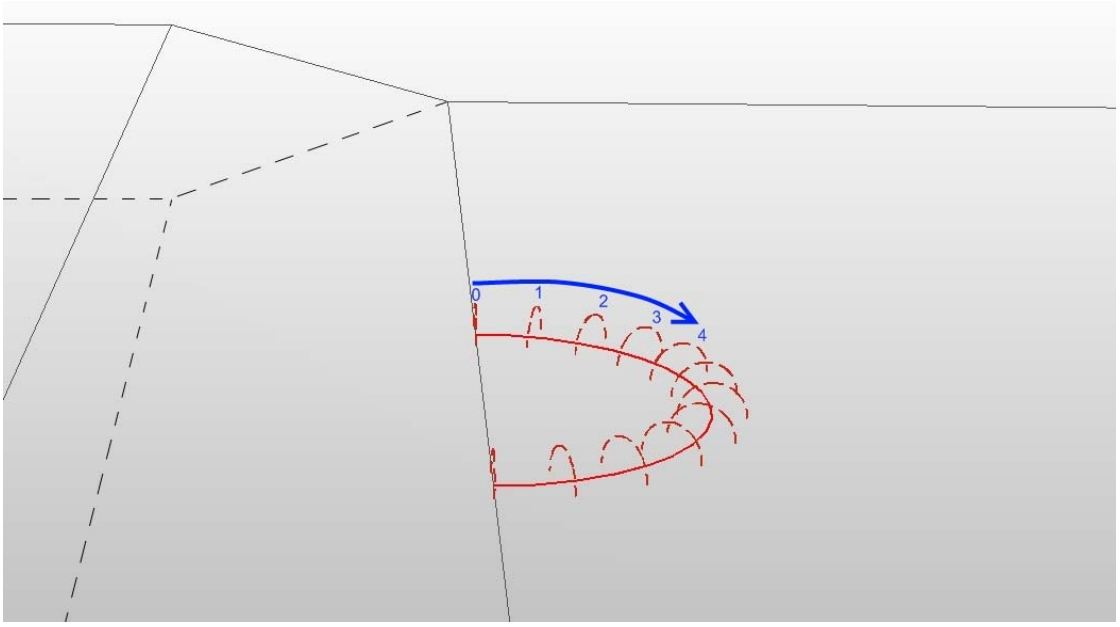

Figure 11. Generalised data extraction locations about a crack front. The crack is shown in the solid red semi-circle with the extractions depicted as the dashed semi-circles. The blue arrow and numbers highlights the ascending direction of the extractions. The extractions only appear as semi-circles due to the symmetry condition of the model.

3.6 Data Extraction and Manipulation

3.6.1 Extractions

Extractions to produce K_1 were conducted around the crack front. They were numbered from where the crack meets the free edge as shown in Figure 11. K_1 was computed using these extractions via the contour integral method, as described in Section 2.2.1. The extraction number listed in all tabulated results refers to these extraction locations. The normalised location is also presented for all tabulated data, which is the location number normalised by the total number of locations. This is equivalent to the normalised arc length or angle because the extractions are equally spaced.

3.6.2 Edge effects

During model development, issues were identified with extraction of K_1 values. It was shown that in areas with tight curvature or in the transition to near surface—from plane strain to plane stress—the modelling accuracy decreases. As a result, a data set was not extracted closer than 5 degrees from a free surface. However in some instances, from viewing the plots of the K_1 about the crack front, it was apparent that the results were erroneous. In these cases, the data set was marked and manually filled—where possible from the symmetric result (see more in Paragraph 3.6.3 below)—or ignored.

Table 3. Example of K_1 data extracted from a symmetrical semi-circular crack in the centre of the thickness of the specimen around the crack boundary. The semi-circular crack has a radius of 0.08 mm.

Extraction Number	Normalised Location	K_1 (MPa √m)			Variation (%)
		Normal	Mirrored	Averaged	
0	0.000	4.962	4.468	4.715	9.9%
1	0.027	4.342	3.985	4.164	8.2%
2	0.054	3.736	3.557	3.646	4.8%
3	0.081	3.326	3.289	3.308	1.1%
4	0.108	3.000	3.077	3.038	-2.6%
5	0.135	2.723	2.891	2.807	-6.2%
6	0.162	2.490	2.726	2.608	-9.5%
7	0.189	2.303	2.588	2.445	-12.4%
8	0.216	2.154	2.473	2.313	-14.8%
9	0.243	2.043	2.381	2.212	-16.6%
10	0.270	1.969	2.312	2.140	-17.4%
11	0.297	1.941	2.253	2.097	-16.1%
12	0.324	1.942	2.212	2.077	-13.9%
13	0.351	1.953	2.177	2.065	-11.5%
14	0.378	1.959	2.141	2.050	-9.3%
15	0.405	1.957	2.097	2.027	-7.2%
16	0.432	1.955	2.052	2.003	-4.9%
17	0.459	1.956	2.012	1.984	-2.9%
18	0.486	1.978	1.980	1.979	-0.1%
19	0.514	1.980	1.978	1.979	0.1%
20	0.541	2.012	1.956	1.984	2.8%
21	0.568	2.052	1.955	2.003	4.7%
22	0.595	2.097	1.957	2.027	6.7%
23	0.622	2.141	1.959	2.050	8.5%
24	0.649	2.177	1.953	2.065	10.3%
25	0.676	2.212	1.942	2.077	12.2%
26	0.703	2.253	1.941	2.097	13.9%
27	0.730	2.312	1.969	2.140	14.8%
28	0.757	2.381	2.043	2.212	14.2%
29	0.784	2.473	2.154	2.313	12.9%
30	0.811	2.588	2.303	2.445	11.0%
31	0.838	2.726	2.490	2.608	8.7%
32	0.865	2.891	2.723	2.807	5.8%
33	0.892	3.077	3.000	3.038	2.5%
34	0.919	3.289	3.326	3.308	-1.1%
35	0.946	3.557	3.736	3.646	-5.0%
36	0.973	3.985	4.342	4.164	-9.0%
37	1.000	4.468	4.962	4.715	-11.0%

3.6.3 Mesh symmetry

During model development it was identified that extraction of K_1 values was being influenced by mesh geometry. This conclusion was reached because extractions from symmetric cases were not returning symmetric values. Investigation showed that the only factor creating a non-symmetric influence in these models was mesh, generated from the automesher. To

reduce this mesh effect the cases were created of mirrored geometric pairs, the extracted results were then averaged to provide the final K_1 values. For example, consider the data of Table 3 graphically presented in Figure 12. This is for a small semicircular crack, 0.08 mm in radius, growing on the centreline of the thickness of the coupon from the notch. This is a symmetrical case and would be expected to return symmetrical data; however there is a variation in K_1 of up to 17.4%, where the variation is calculated as the difference between the 'normal' and 'mirror' results divided by the 'normal' result (refer Table 3 and Figure 12).

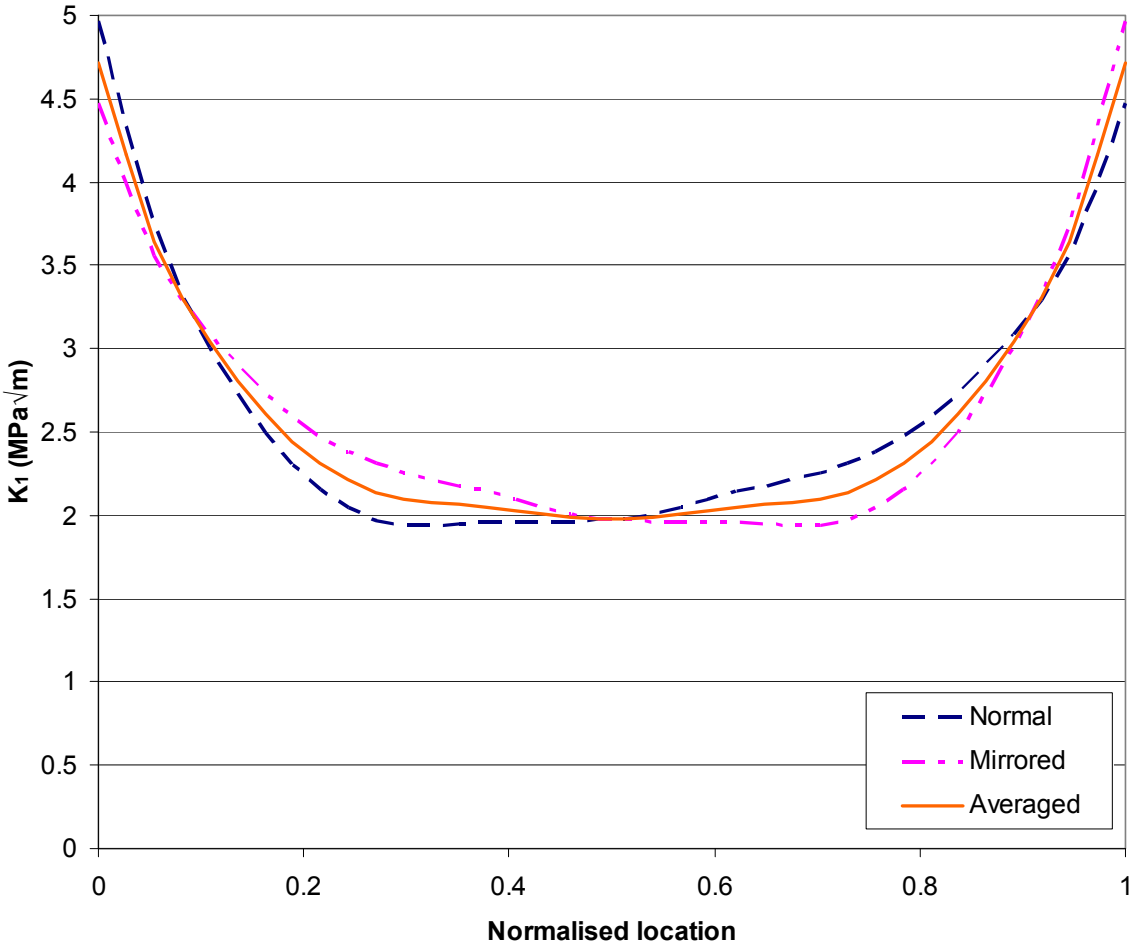

Figure 12. Example of K_1 data extracted from a symmetrical semi-circular crack in the centre of the thickness of the specimen. The semicircular crack has a radius of 0.08 mm. The normal data set is the extraction. The mirrored data set is the mirror of the normal data about the centre line.

This identified variation lead to the averaging of all results and created the nomenclature presented in the tabulated results. Results were generated for a through thickness location, for example at 30% of the thickness. Another case was run that created result for the mirrored location, in this example 70% of thickness. These results were then averaged to remove the potential fluctuations. With this in mind, locations are identified in all proceeding tables as

having a through thickness location, where it is presented as the two percentages of thickness used in the averaging, "70/30" as for the case of the example.

A combination of averaging the results and a significant increase in mesh density was used to minimise the influence of the extraction errors on the results presented here. This highlights that the guidance provided by the software provider [10] is inadequate to reasonably model this case. After these corrections variations typically decreased to approximately 2%.

3.7 Cases Considered

Three main questions have been considered during this investigation:

1. What happens to K_1 as the crack size becomes smaller?
2. What happens to K_1 as the crack location moves through the thickness?
3. What happens to K_1 as the crack grows from a semicircular initiation to a through crack?

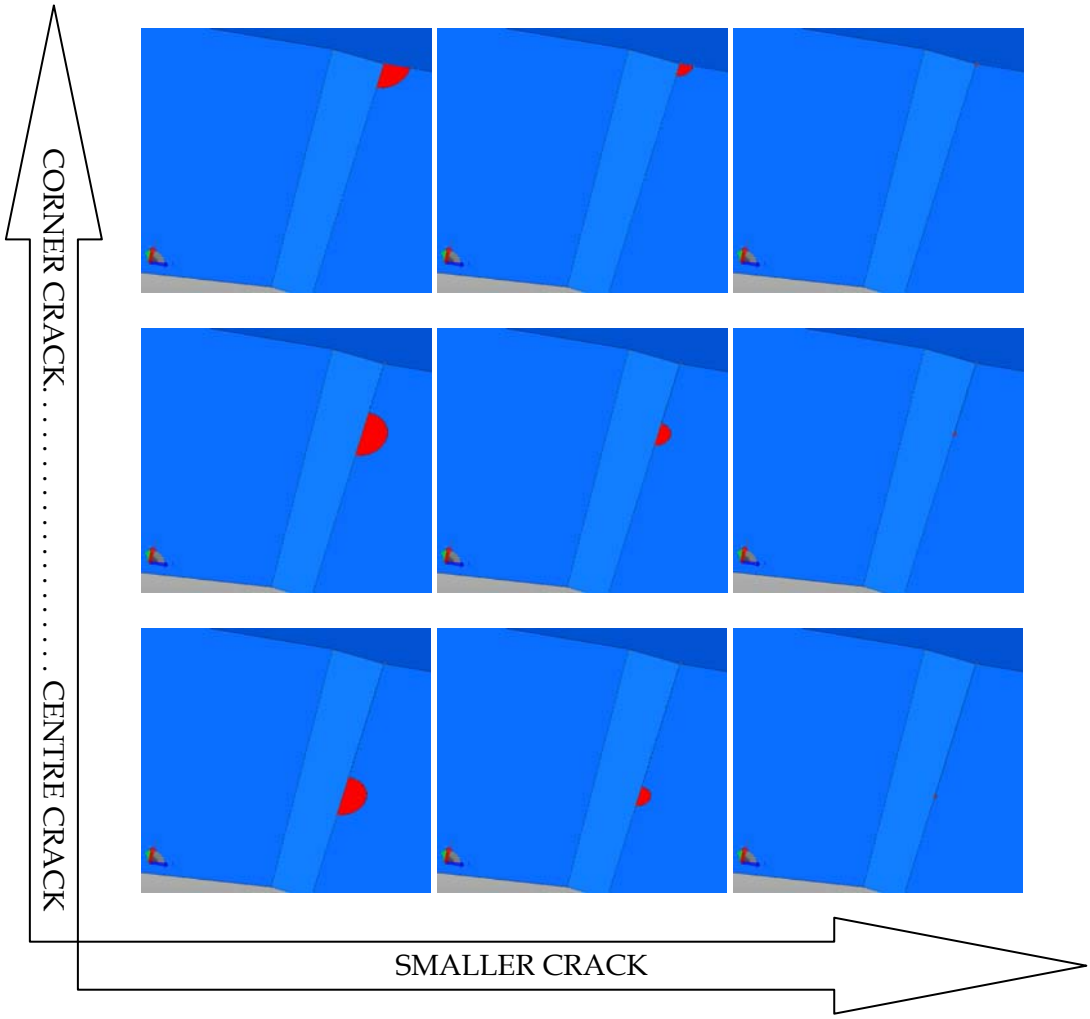

Figure 13. A graphical illustration of the range of crack size and location investigation with circular cracks

To answer these questions, two sets of cases were constructed and presented as matrices of the investigation. The first matrix looks at circular cracks of different sizes at various positions through the specimen thickness. Figure 13 shows the range of investigations pictorially. For this set, some specific attention was paid to the behaviour of cracks near corners, as depicted in Figure 14. In this subset the crack locations were chosen to keep the ratio of the radius and the distance from the corner the same for each case. Table 4 presents the full test matrix.

Table 4. Matrix 1 – Crack size and location investigation with semi-circular cracks. The location (%) shows the two percentage of thicknesses used for the averaged K1 extractions. The number in the table shows the degrees of arc of the crack. Where 'NC' refers to 'near corner'.

Through Thickness Location (%)	Crack Radius (mm)					
	1	0.5	0.3	0.2	0.1	0.08
50/50	180°	180°	180°	180°	180°	180°
55/45	180°	180°	180°	180°	180°	180°
60/40	180°	180°	180°	180°	180°	180°
65/35	180°	180°	180°	180°	180°	180°
70/30	180°	180°	180°	180°	180°	180°
75/25	180°	180°	180°	180°	180°	180°
80/20	180°	180°	180°	180°	180°	180°
85/15	180°	180°	180°	180°	180°	180°
90/10	180°-NC	180°	180°	180°	180°	180°
95/5	128.7°	180°-NC				
97/3			180°-NC			
97.5/2.5		128.7°				
98/2				180°-NC		
98.5/1.5			128.7°			
99/1				128.7°	180°-NC	
99.2/0.8						180°-NC
99.5/0.5					128.7°	
99.6/0.4						128.7°
100/0	90°	90°	90°	90°	90°	90°

The second investigation looks at transitions from the semi-circular crack to an elliptical crack to a through crack, again at different sizes. This is graphically presented in Figure 15. Again this was performed for the same range of crack sizes as used in the first investigation. However, it was limited to cracks that are symmetrical about the centre of the specimen thickness. Table 5 presents the full matrix that was considered during this investigation. In Table 5 the ellipse *aspect ratio* is the ratio of the width radius to the depth radius, for example: "1" is a semi-circle and "3" has the width of the crack three times larger than the depth of the crack. Again, in this set the sizes were chosen in two manners, first a set was selected with consistent ellipse ratios and second a set was chosen with consistent crack width to specimen thickness ratios—to enable comparison of any effects linked to geometric ratios.

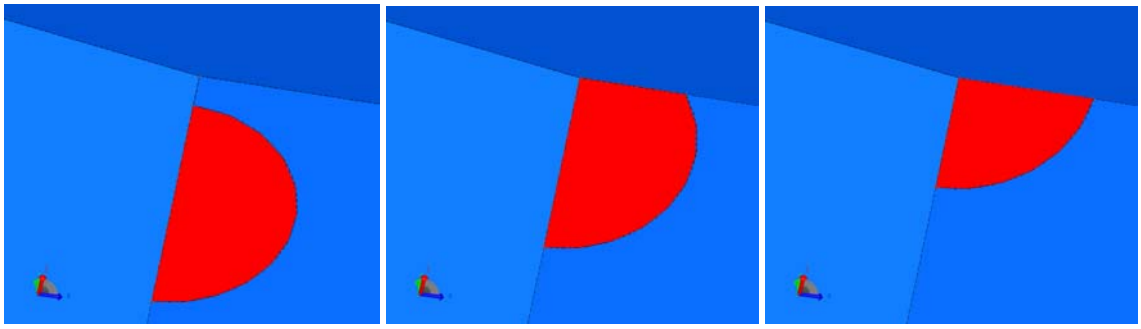

Figure 14. A graphical illustration of the detail of investigation into effects near corners.

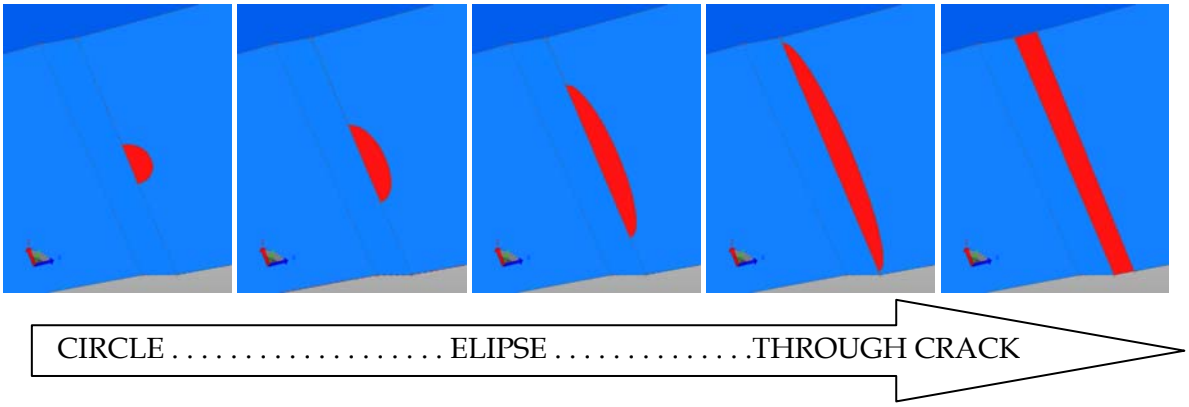

Figure 15. Matrix 2 - A graphical illustration of the crack size and shape investigation with cracks about the centre of the specimen thickness

Table 5. Matrix 2 - Crack size and shape investigation with elliptical cracks about the centre of the specimen thickness

Aspect Ratio	Crack Depth (mm)					
	1	0.5	0.3	0.2	0.1	0.08
1.0	X	X	X	X	X	X
2.0	X	X	X	X	X	X
3.0	X	X	X	X	X	X
4.0	X	X	X	X	X	X
5.0	X	X				
6.0	X	X				
6.1			X			
7.0		X				
7.5				X		
8.0		X				
8.22			X			
9.0		X				
10.0		X				
10.33			X			
11.0				X		
11.67					X	
12.44			X			
13.75						X
14.5				X		
14.56			X			
16.67			X			
18.0				X		
19.33					X	
21.5				X		
23.5						X
25.0				X		
27.0					X	
33.25						X
34.67					X	
42.33					X	
43.0						X
50.0					X	
52.75						X
62.5						X
Infinite (Through crack)	X	X	X	X	X	X

4. Results

4.1 General Results

Figure 16 and Figure 17 provide a general view of a model with a 1 mm semi-circular crack located at 50% through thickness. The figures present the details of the mesh and a plot of the strain in the Y axis (Ey). Figure 16 shows a general overview of the mesh and strain field for the substructured model, whereas Figure 17 provides it for the crack detail.

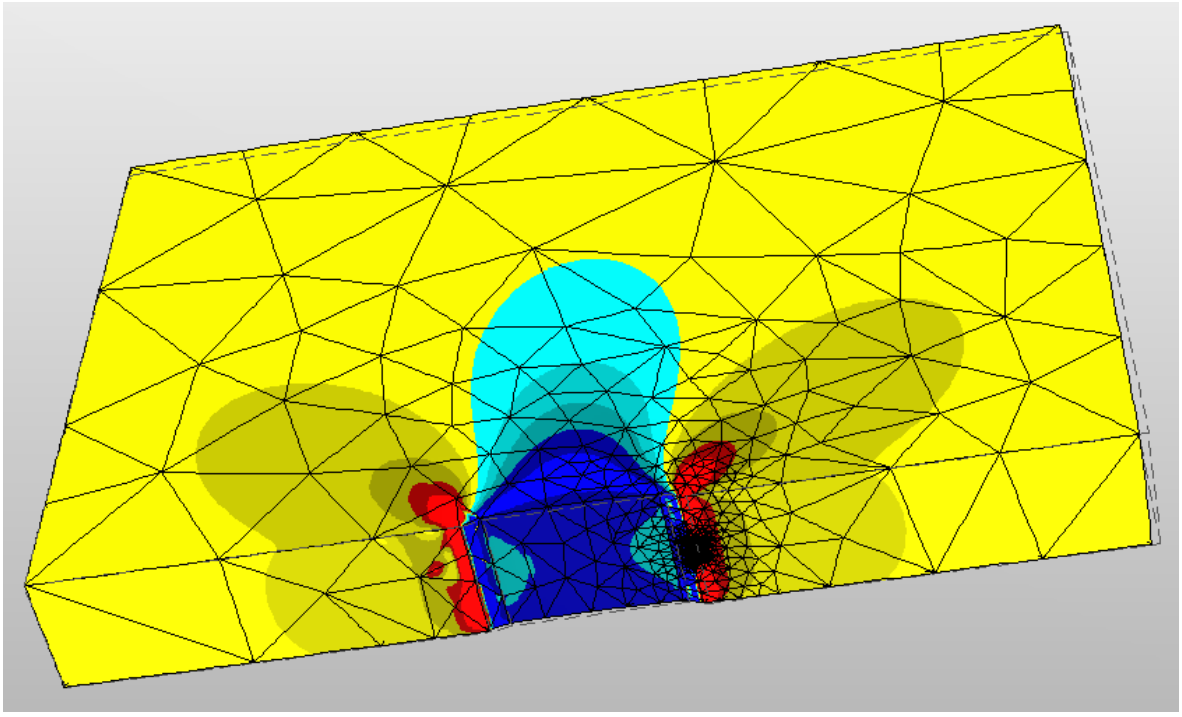

Figure 16. Overview of mesh and Y axis strain (E_y) results for a 1 mm semi-circle crack at 50% through thickness subjected to fixed displacement ($7.8e^{-4}$ mm)

4.2 Variation of Crack Size

The runs used in this section were generally successful with only the centre extraction of the 0.08 mm near corner crack (0.4% and 99.6% of thickness) failing. The judicious selection of near corner crack locations allowed for this high success rate. Detailed results are presented in Appendix D as both raw and processed data.

For most configurations, crack size variation has a very small effect on overall K_1 extracts. From Figure 18 to Figure 21, we see that the K_1 values for semicircular, elliptical and through cracks all vary very little as the size changes. The exception is for the corner crack, Figure 22, where the variation is obvious and effective. Given that the notch is 'crack-like', it is not surprising that the changes in K_1 are small for these relatively small cracks.

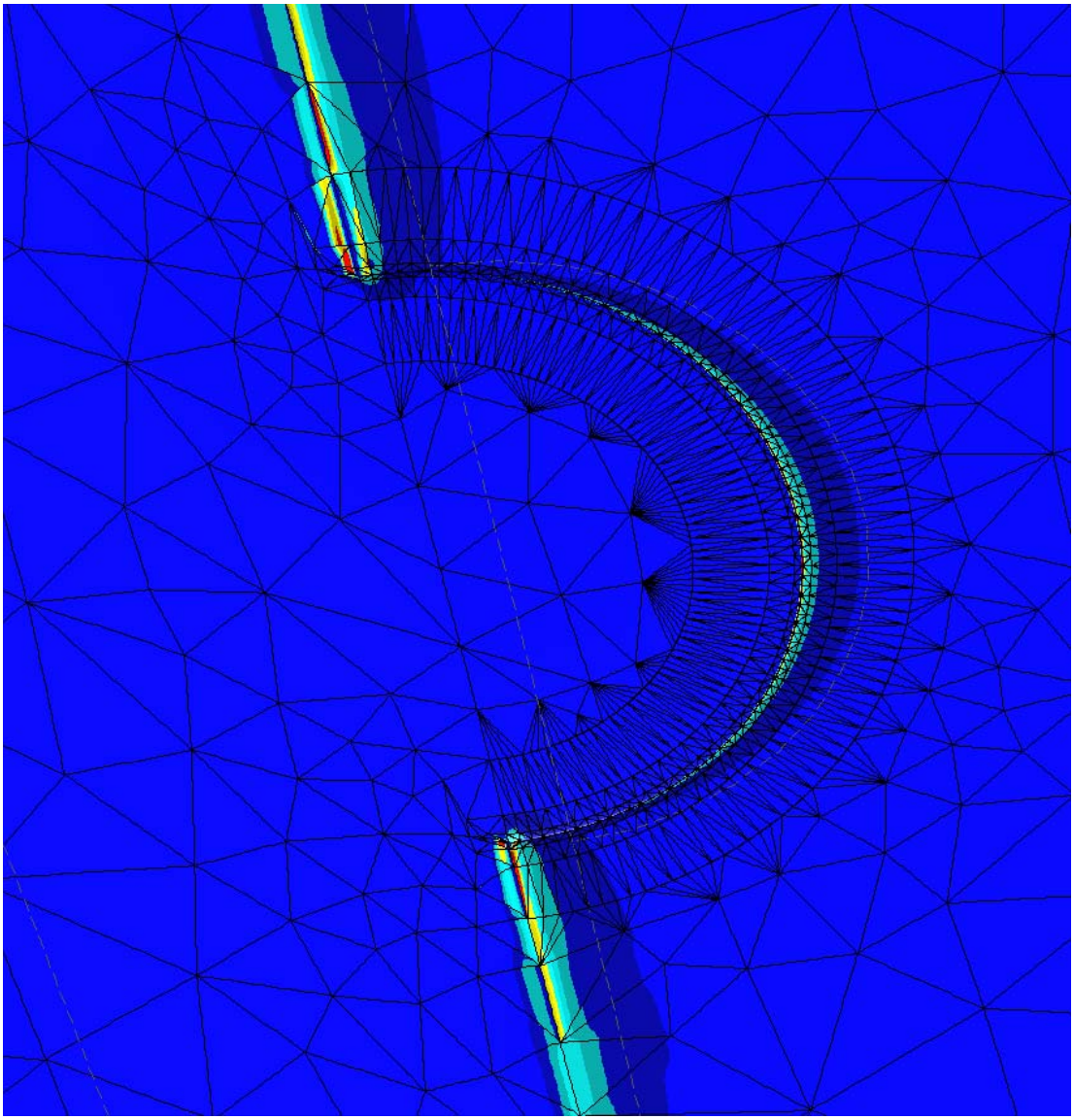

Figure 17. Detailed view of mesh and Y axis strain results (E_y) for a 1 mm circular crack at 50% through thickness subjected to fixed displacement ($7.8e^{-4}$ mm). The slender elements of this mesh are within the limit guidance provided by the software developer, ESRD.

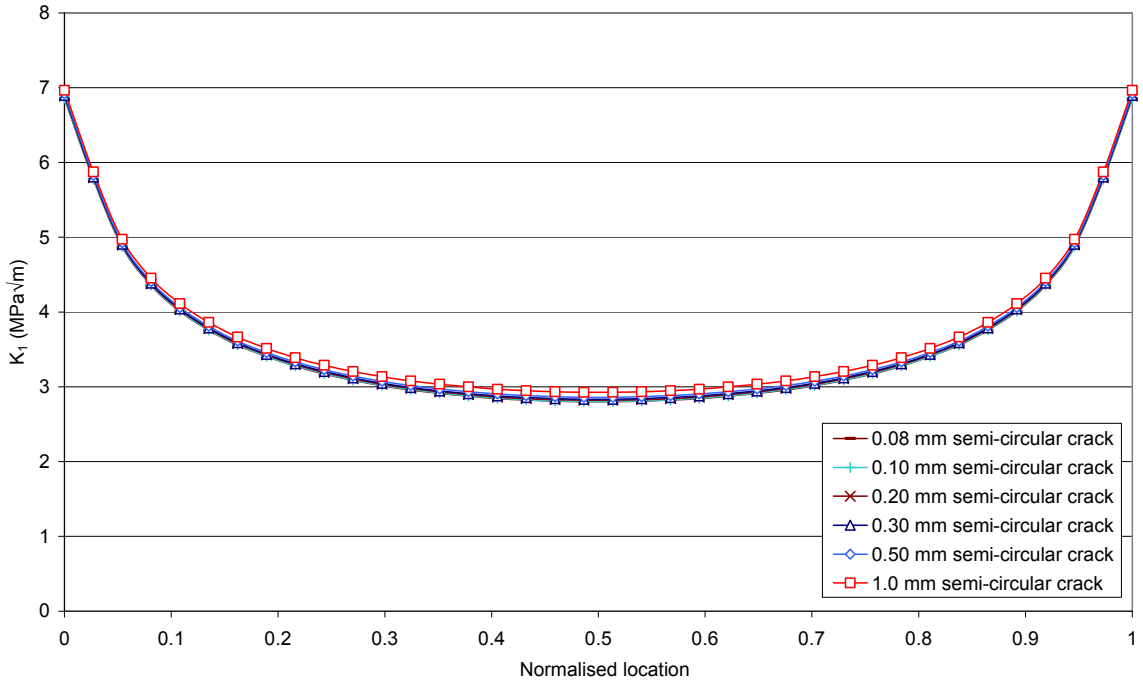

Figure 18. K_1 extraction around a semi-circular crack at the centre of the specimen thickness (50% of thickness)

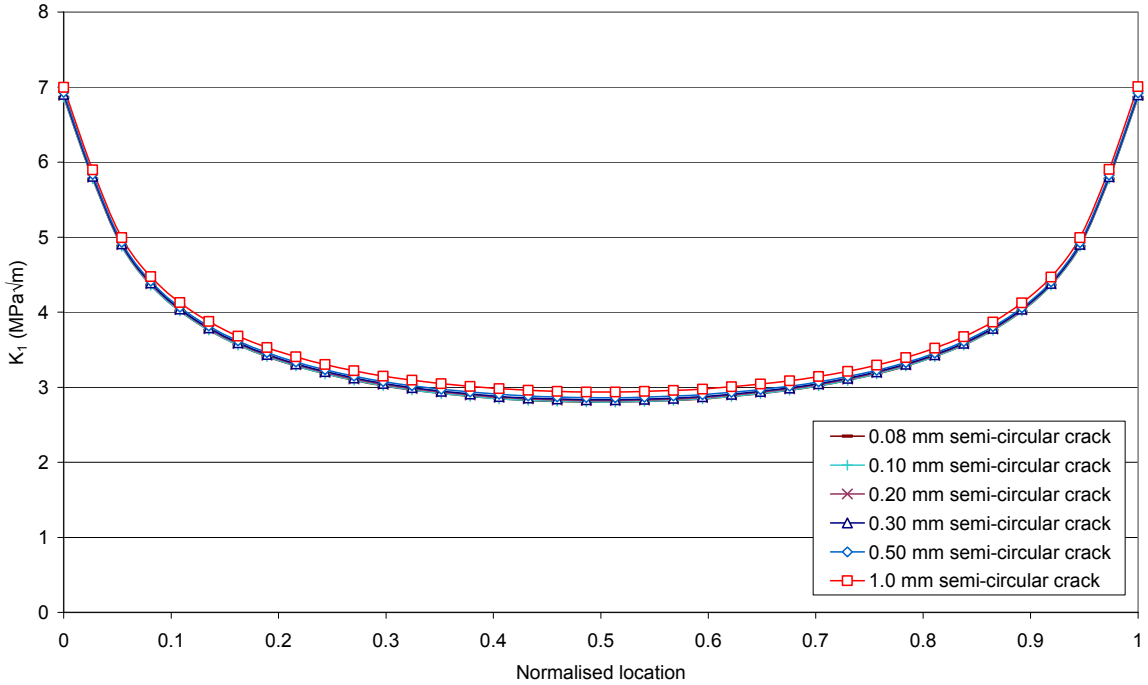

Figure 19. K_1 extraction around a semi-circular crack at the quarter of the specimen thickness (75% of thickness)

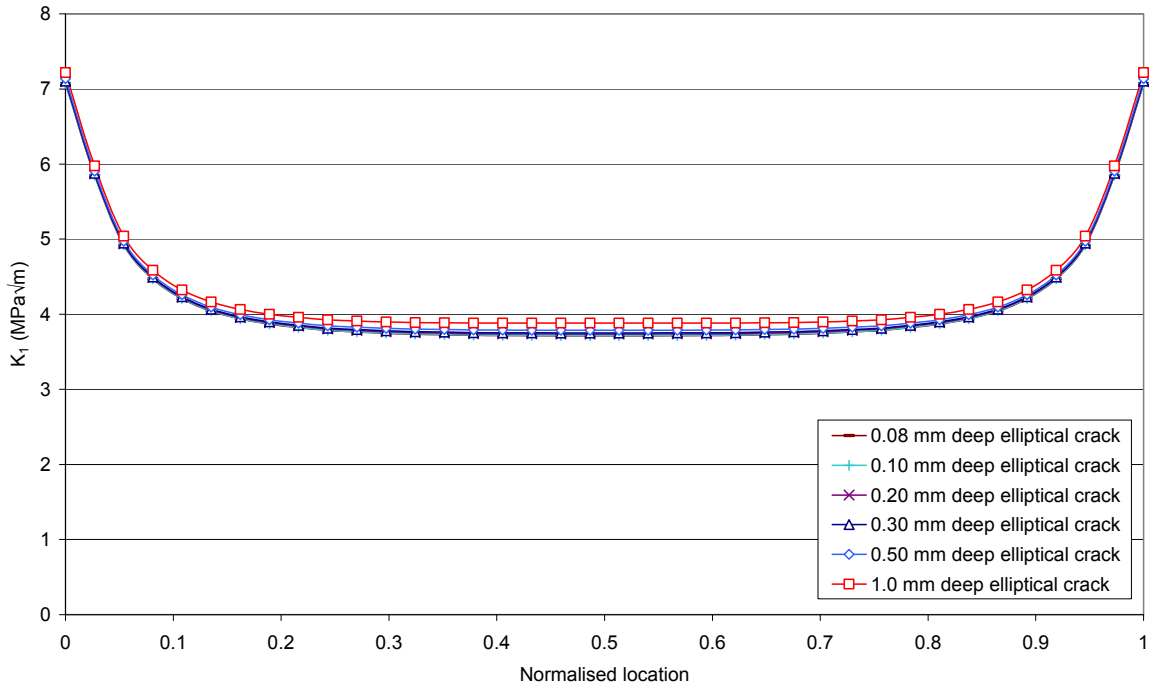

Figure 20. K_1 extraction around an elliptical crack with an aspect ration of 2

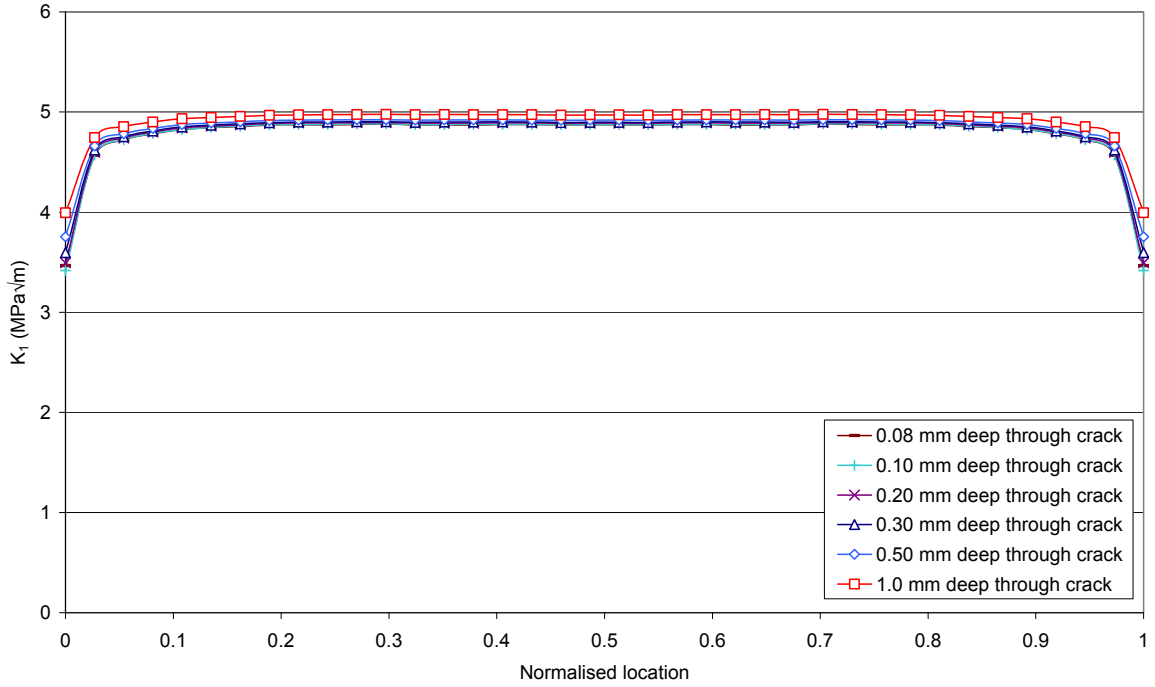

Figure 21. K_1 extraction across a through crack

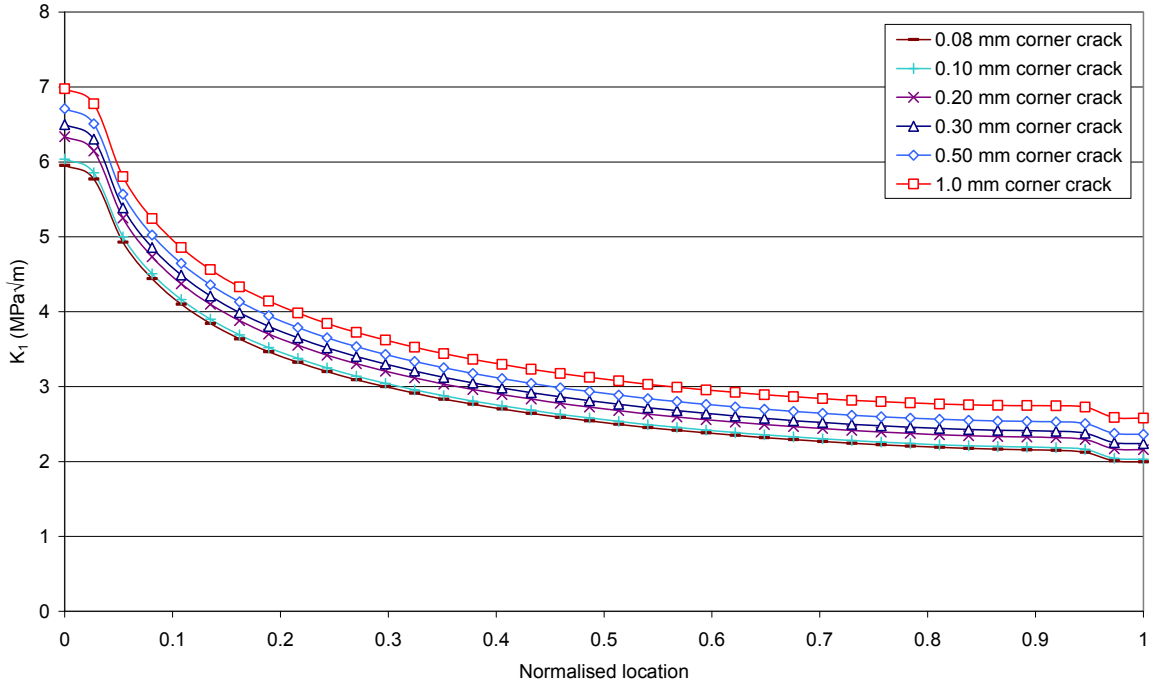

Figure 22. K_1 extraction around a quarter crack at surface of the specimen thickness (100% of thickness)

4.3 Variation of Crack Location

The runs were generally successful with only the centre extraction of the 0.08 mm near corner crack (0.4% and 99.6% of thickness) failing to compute. The judicious selection of near corner crack locations allowed for this high success rate. Detailed results are presented in Appendix D as both raw and processed data.

Crack location only played a small part in the variation of many of the K_1 results across the extraction limits. From Figure 23 we can see that there is little or no edge effect until the crack starts to vary its shape, covering less of the semicircular arc. If the comparison is made with crack front normalised to the length of the 180 arc, rather than their own length, we see that K_1 remains consistent with earlier 180 degree extractions and only varies near the local change in geometry. This effect is attributed to the influence of the stress raiser, or starter notch, in this geometry; it appears to dominate all other effects.

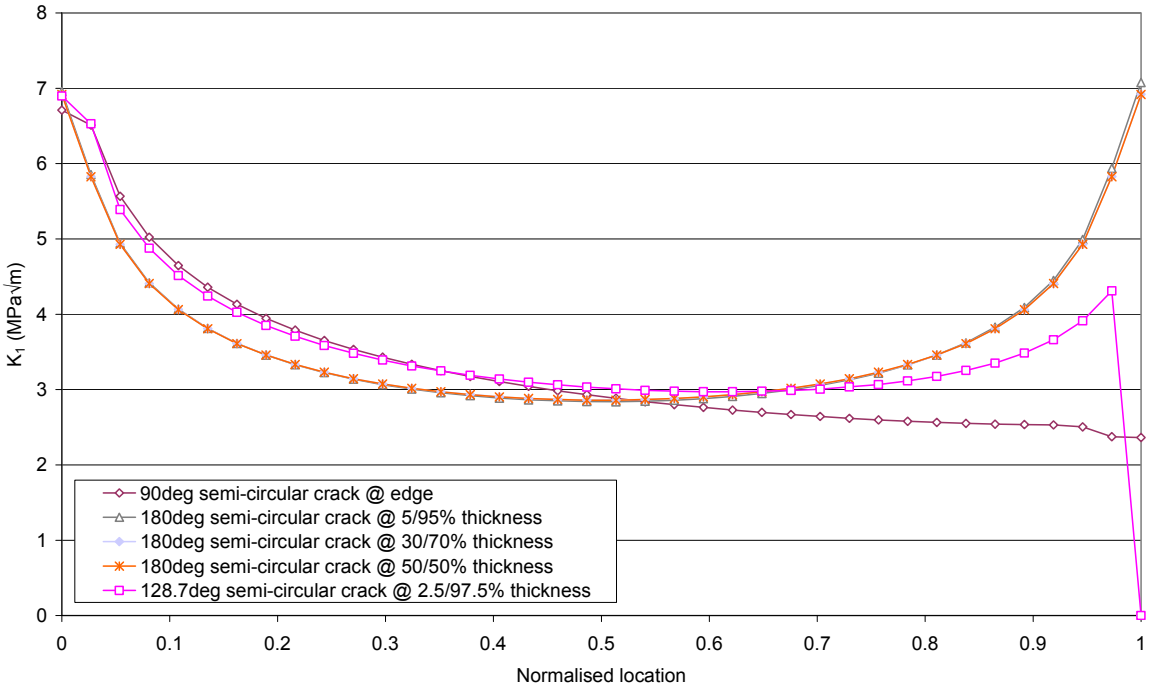

Figure 23. K_1 extractions for semi-circular cracks with various through thickness locations, varying from the centreline to a corner crack

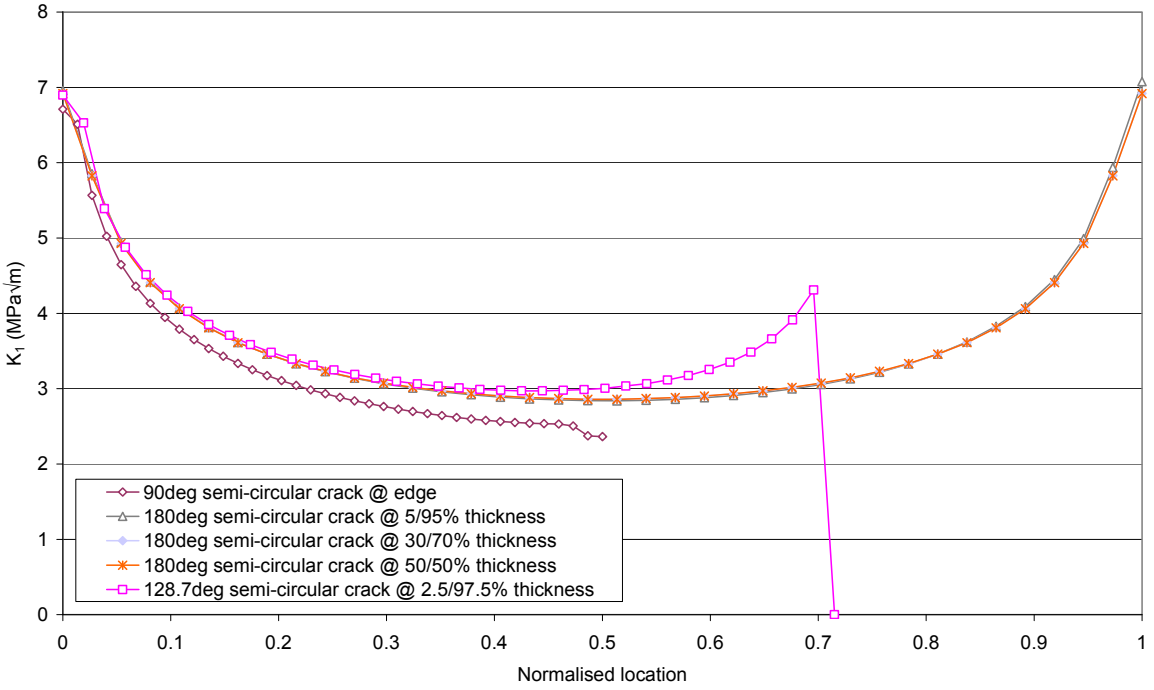

Figure 24. K_1 extractions for semi-circular cracks with various through thickness location, varying from the centreline to a corner crack. These extractions have all been normalised to the full 180 degree crack, hence some plots do not reach the normalised value of 1

Table 6. Cases that successfully meshed, ran and allowed for K_1 to be extracted

Aspect Ratio	Depth (mm)					
	1	0.5	0.3	0.2	0.1	0.08
1.0	OK	OK	OK	OK	OK	OK
2.0	OK	OK	OK	OK	OK	OK
3.0	OK	OK	OK	OK	OK	OK
4.0	OK	OK	OK	OK	OK	OK
5.0	OK	OK				
6.0	OK	OK				
6.1			OK			
7.0		Error				
7.5				Error		
8.0		Error				
8.22			Error			
9.0		Error				
10.0		Error				
10.33			Error			
11.0				Error		
11.67					Error	
12.44			OK			
13.75						OK
14.5				OK		
14.56			OK			
16.67			OK			
18.0				OK		
19.33					OK	
21.5				OK		
23.5						OK
25.0				OK		
27.0					OK	
33.25						Error
34.67					Error	
42.33					Error	
43.0						Error
50.0					Error	
52.75						Error
62.5						Error
Infinite (Through Crack)	OK	OK	OK	OK	OK	OK

4.4 Variation of Crack Shape

The results achieved for variations of crack shape were not as successful as for the semi-circular cracks. This is mainly because crack ratios where chosen that were based on geometric comparisons, not on meshing limits. As a result, the automesher had difficulty meshing some of the cases and results were not returned. These are denoted as 'error' in Table 6. In general, as the aspect ratio increased and the radius of curvature increased the automesher had more difficulty fitting elements, however, this was not always true.

Detailed results are presented in Appendix D as both raw and processed results.

Crack shape variations had a more pronounced influence on the extracted K_1 values. Figure 25 presents data for an elliptical crack of varying aspect ratios from one to infinity (a through crack) at a depth of 1 mm. From these results it can be seen that the peak K_1 values remain reasonably consistent, but the minima and distribution change considerably. Once the ellipse breaks away from the stress raiser, that is the crack end is no longer on the pre-notch, the peak drops sharply and the centre segment becomes the highest K_1.

As the aspect ratio of the ellipse increases the ability of StressCheck to mesh the geometry decreases and the veracity of the results also decreases. This is due to the increasing severity of the curvature at the end of the extremities of the ellipse, which the code has difficulty meshing. However, once the crack breaks the face of the specimen and the radius of curvature decreases the software can again mesh correctly and the results improve again, as with the through crack case.

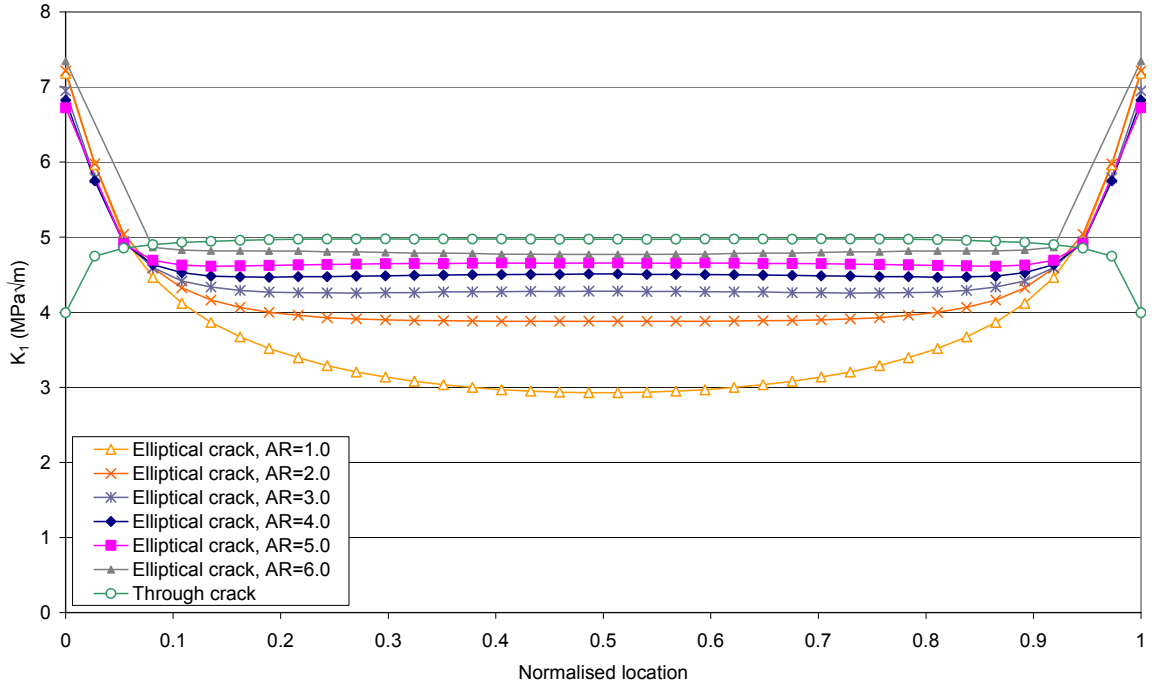

Figure 25. Changes in K_1 for elliptical cracks with changes in aspect ratio, all plotted for cracks with a depth of 1 mm

5. Discussion

5.1 Issues from the ASTM Standard

The ASTM example data set, provided in Figure 1, is assumed to be tested under the requirements of the ASTM standard [4]. For this, the pre-crack notch would be at least 20% of

the specimen width, or 20.32 mm (0.8 inches). Therefore, the minimum total crack length (a) would be half the precrack notch or 10.16 mm (0.4 inches). From Figure 1, it is clear that crack length data set is presented below 5 mm (0.2 inches). This suggests that either the initial pre-crack notch was much shorter or the measurements provided are the crack length beyond the pre-crack notch, sometimes called the natural crack. Neither of these options is in the spirit of the standard [4], however, for this work it is assumed that the second is true and that crack length of Figure 1 refers to only the natural crack, not considering the pre-crack notch.

The ASTM standard calls for specimens to be pre-cracked. This ensures that the initiation phase is completed and the results should only include the crack growth phase. This practice would mean most of the work undertaken herein is not applicable to the data of Figure 1, because the crack would already be established as a through crack. In this circumstance, there would not be the expected changes in stress intensity factor and the proposal that K_1 creates the non-exponential crack growth of stage 1 (in Figure 1) would not hold. However, as discussed earlier the full standard does not seem to have been applied to this data and as such it is also assumed that no pre-crack has occurred.

5.2 The Zone of K Dominance

K dominance, as described by Anderson [12], does not always hold and, in such cases, a K solution would become inappropriate and lead to erroneous results. However, for the cases presented here, the analysis is perfectly elastic and is not susceptible to the size of a plastic zone. Consequently, the zone of K dominance is not considered during the discussion of results.

5.3 Maximum and Minimum K_1

A common engineering practice is to select K_1, or geometry factors, away from a free edge, nominally five degrees in, a point amplified in communications with ESRD—the StressCheck developers [13]. This is to account for inaccuracies in computing the K_1 in the transition to a free edge or, in other words, from plane strain to plane stress conditions. The description previously given (Section 2.2) articulates how this is performed in the StressCheck code.

The predominantly consistent and continuous results near the free edges, for example show in Figure 19 and Figure 20, suggest the extractions are quite robust. Particularly, the semi-circular extractions—where both crack ends lie on the stress raising geometry (case (a) of Figure 14)—and the through-crack cases appear robust. However, some cases do appear to contain anomalies in the results. The two cases where results seem to degrade are the high aspect ratio ellipses and any crack that has breached a corner.

The errors in the high aspect ratio ellipses are most likely due to the StressCheck auto-mesher failing to accurately mesh the extreme curvature in the geometry. Similarly, where the semi-circular crack is in transition to a corner crack, the geometry can be more difficult to mesh. However, the full corner crack case is not difficult to mesh and the anomalies from these cases are most likely due to the edge effect. Interestingly, in the case of the corner crack, as seen in Figure 22, the anomaly appears at both ends—both at the edge with the stress raiser and the coupon's side. This seems to justify the common practice of selecting K_1 approximately 5 degrees in from a free edge [13].

The edge effects may stem from one of two explanations. The first is that the high stress gradient near this notch is having a positive influence on the accuracy of the K_1 solution. However, such an explanation is difficult to rationalise. The second and more favoured explanation is that when the path of the J-integral falls on a free surface the solution accuracy decreases. When the path of the J-integral lies within the material, as is the case near the notch, the solution is more robust. This geometric condition is depicted in Figure 26. This case would be related to the numerical stability of the contour integral method for the determination of the J-Integral on a free surface, where one side has zero stress and the other is a fully developed field.

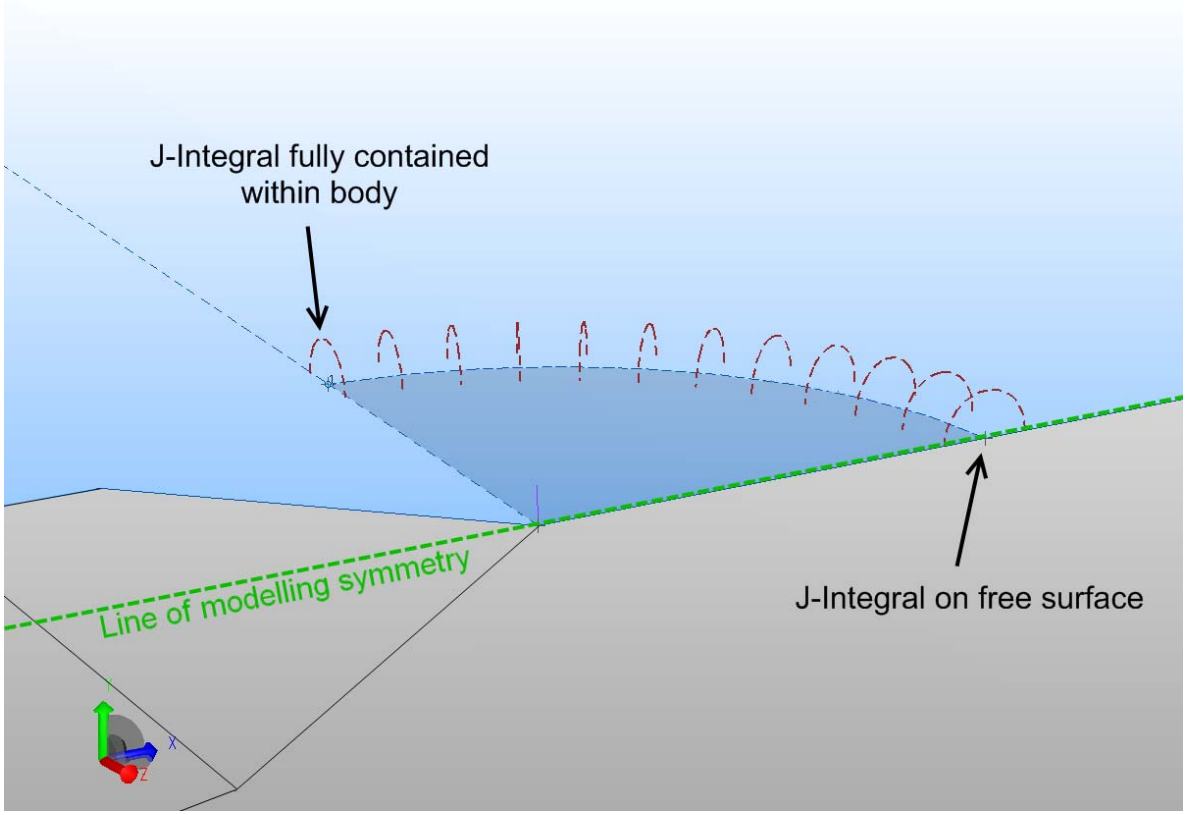

Figure 26. The J-Integral at the notch is contained within the body, whereas the other J-Integral lies on a free edge

Further, if the radius of integration is not tangential to a free surface, but instead passes through it, then the solution is likely to be less accurate. This is the case of the near corner cracks, case (b) of Figure 14.

Interestingly, for the cases where the edge solution is considered robust, selecting the five degree value would result in a K_1 that is more than 10% lower than the peak. Using this value may lead to non-conservative outcomes.

5.4 Likely Crack Path Due to K_1 Distribution

The plotted distributions of K_1 around the crack fronts for circular cracks indicate that such a crack is likely to grow faster at the free edges. This would lead the crack to grow into an ellipse before becoming a through crack. The data generated in this report indicates that the

peak K_1 varies very little through this process, but the K_1 distribution changes significantly as the crack elongates. This may lead to the crack growth distribution depicted in Figure 1. However, this is likely to be subjective and dependant on the measurements taken to determine the crack growth. For example, free surface length (via replicant or microscope) measurement would provide a different growth rate to fractographic results based solely on depth. If they are made as depth measurements it can be seen from Figure 25 that the K_1 varies at the crack centre, whereas the K_1 at the free edges appears more consistent. Therefore, the issue of how the growth rate is measured may have the largest bearing on the crack growth rates shown in the curve of Figure 1. Investigating this behaviour was beyond the scope of this report.

6. Conclusion

In conclusion, this modelling work set out to utilise advanced, high order finite element methods to assess whether there are changes in stress intensity factors for small cracks in the ASTM Middle Tension test specimen [4]. Several cases were considered; including corner initiated cracks, near corner initiated cracks, and centrally initiated cracks. The results apply to a geometric problem that is not in the open literature and are presented in a usable form of tabulated K_1 values.

The results show that K_1 and therefore the β factor may be influencing the non-exponential behaviour of the early portion of crack growth for an ASTM middle tension specimen, as shown in Figure 1. However, the method of crack length measurement of that early portion of crack growth is likely to significantly influence the experimental data for this region. As such, further consideration could be given to understand this aspect of the experimental data.

Finite element methods have the potential to produce inaccurate results and significant effort was expended to ensure accurate and robust solutions resulted from the chosen code. Many lessons were learnt and documented as part of this work.

7. Acknowledgements

The author would like to thank Dr Manfred Heller for his continued support and encouragement.

8. References

1. Molent, L., *The history of fatigue testing*, DSTO-TR-1773, 2005.
2. Molent, L., Jones, R., Barter, S. and Pitt, S. *Recent developments in fatigue crack growth assessment*, International Journal of Fatigue, Volume 28, Issue 12, December 2006, Pages 1759-1768.
3. Paris, P.C., Gomez, R.E., Anderson, W.E., *A rational analytic theory of fatigue*. Trend Eng 1961;13(1):9-14.
4. E 647-05, *Standard test method for measurement of fatigue crack growth rates*, ASTM International, 2005.
5. Murakami, Y., Axi, S., Hasebe, N., Itoh, Y., Miyata, H., Miyazaki, N., Terada, H., Tohgo, K., Toya, M., Yuuki, R., *Stress Intensity Factors Handbook*, Pergamon Press, 1987.
6. Broek, David, *The practical use of Fracture Mechanics*, Kluwer Academic Publishers, 1988.
7. RoXe, D.P., Cartwright, D.J., *Compendium of stress intensity factors*, Her Majesty's Stationary Office, 1976.
8. Sih, G.C. *Handbook of stress intensity factors*, Lehigh University Press, 1973.
9. Tada, H., Paris, P.C., Irwin, G.R., *The stress analysis of cracks handbook*, Del Research, 1973.
10. Engineering Software Research and Development Inc, *StressCheck – Getting started guide*, Release 7.1, October 2006.
11. Engineering Software Research and Development Inc, *StressCheck – Master guide*, Release 7.1, October 2007.
12. Anderson, T.L., *Fracture mechanics: fundamentals and applications*, 3rd Ed. CRC Press, 2005.
13. Personal communication, Callum Wright (DSTO) and ESRD, June 2008.

Appendix A Construction of Global Modal

A.1. Global Model Construction

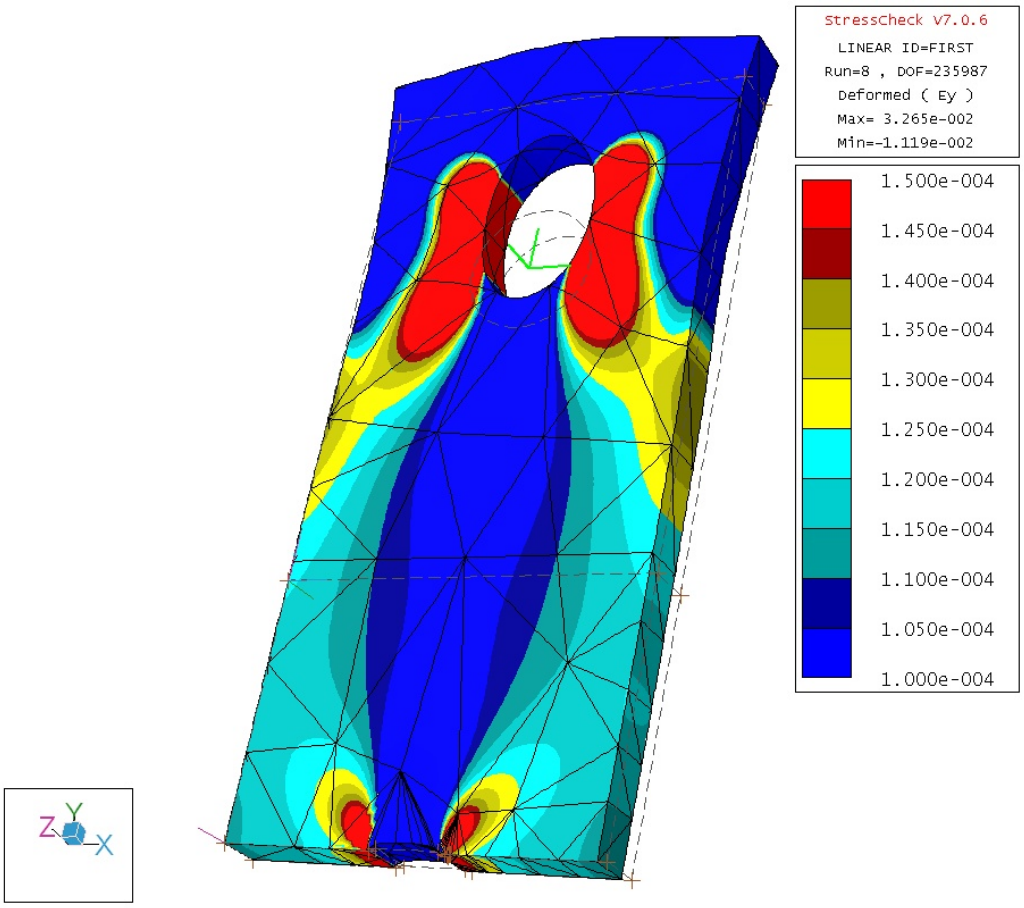

Figure 27. Early global model from StressCheck version 7.0.6. This plot shows y axis strain (E_y) with deformation

The global model was constructed initially in early versions of StressCheck, Figure 27, but was further developed until the method set out below proved successful.

A.2. Input Parameters

StressCheck is a parametric modelling tool that allows for multiple case studies through the variation of parameters built into the model. Table 7 presents the parameters of the global modal.

Table 7. Parameters used in global model

Parameters	Description	Formula	Value
A0	Crack Length	Bc/10	1.25
An	Notch Length		10
ANGn	Notch Tip Angle		75
At	Crack Position		0.5
Bc	Coupon Thickness		12.5
Lc	Coupon Length	Wc/2+1.5*Wc	200
Nx1		(Wc/2)-An	40
Nx2		(Wc/2)-An+(Wn/2)*Tan(ANGn*pi/180)	41.866
Nx3		(Wc/2)+An-(Wn/2)*Tan(ANGn*pi/180)	58.134
Nx4		(Wc/2)+An	60
Ny1		0	0
Ny2		Wn/2	0.5
Ny3		Wn/2	0.5
Ny4		0	0
RH			10
Wc	Coupon Width		100
Wn	Notch Width		1

A.3. Construction Methodology

This model was created with the following steps:

REFERENCE/THEORY TOOLBAR
Initiate a model with properties of “3d”, “Elasticity”, “Other”

HANDBOOK.
Set up the parameters (Table 7)

GEOMETRY (green plane setting)			
Create	box	locate	Solid (x,y,z)=(0,0,0) Width=Wc Height=Lc Depth=Bc Accept
Create	box	locate	Solid (x,y,z)=(0,-Lc/2,0) Width=Nx2-Nx3 Height=Wn Depth=Bc Accept

Create	body	Bool-Subtract	Select First box Select Second box Accept
Create	Blend Edge	Chamfer	Input R1: Wn/2 R2: Nx2-Nx1 Select first edge of cut out Accept
Create	Blend Edge	Chamfer	Input R1: Wn/2 R2: Nx2-Nx1 Select Second edge of cut out Accept
Create	Cylinder	Locate	(x,y,z) = (0,(Lc/2-Wc/2),0) Radius = Rh Height=Bc Rot=(0,0,0)
Create	body	Bool-Subtract	Select main geometry Select cylinder Accept
Create	System	Locate	Cartesian (x,y,z)= (0,Lc/2-Wc/2,Bc/2) Rot=(0,0,0)
Create	Plane	Locate	(x,y,z)=(0,-Lc/6,0) Width= Wc Height = Bc P1min=-0.5 P1max=0.5 P2min=0 P2max=1 Rot(x,y,z)=(90,0,0)
Create	body	Bool-Union	Select main geometry Select plane Accept

MESH			
Create	Mesh	Auto	Ratio = 0.2 D/H = 0.1 MinLen = 0.0005 Isopar = 0 Select main body Accept Automesh

MATERIAL			
Define	Linear	Selection	
		Define tab	Units = SI
			Browse – 7075-t6
			Accept
		Assign Tab	Select AllElement Selection
			ID = 7075-t6
			Colour = Aluminium
			Accept

LOAD	
	Select Any Surface Bearing
	ID = PinBear
	Dir = Mag/Dir
	System = SYS4 (centre of pin hole)
	Mag = 1000
	Ang = 90
	Z0 = 0
	Select pin hole surface
	ACCEPT

CONSTRAINT	
	Select Any Surface Symmetry
	ID = SymRest
	Click bottom two surfaces
	ACCEPT
	Select Point Rigid Body
	ID = SymRest
	Click 3 bottom corner points
	ACCEPT

SOLUTION ID
Trial2
SYMREST
PINBEAR

Appendix B Construction of Sub-Structured Model

B.1. Sub-structured Model Construction

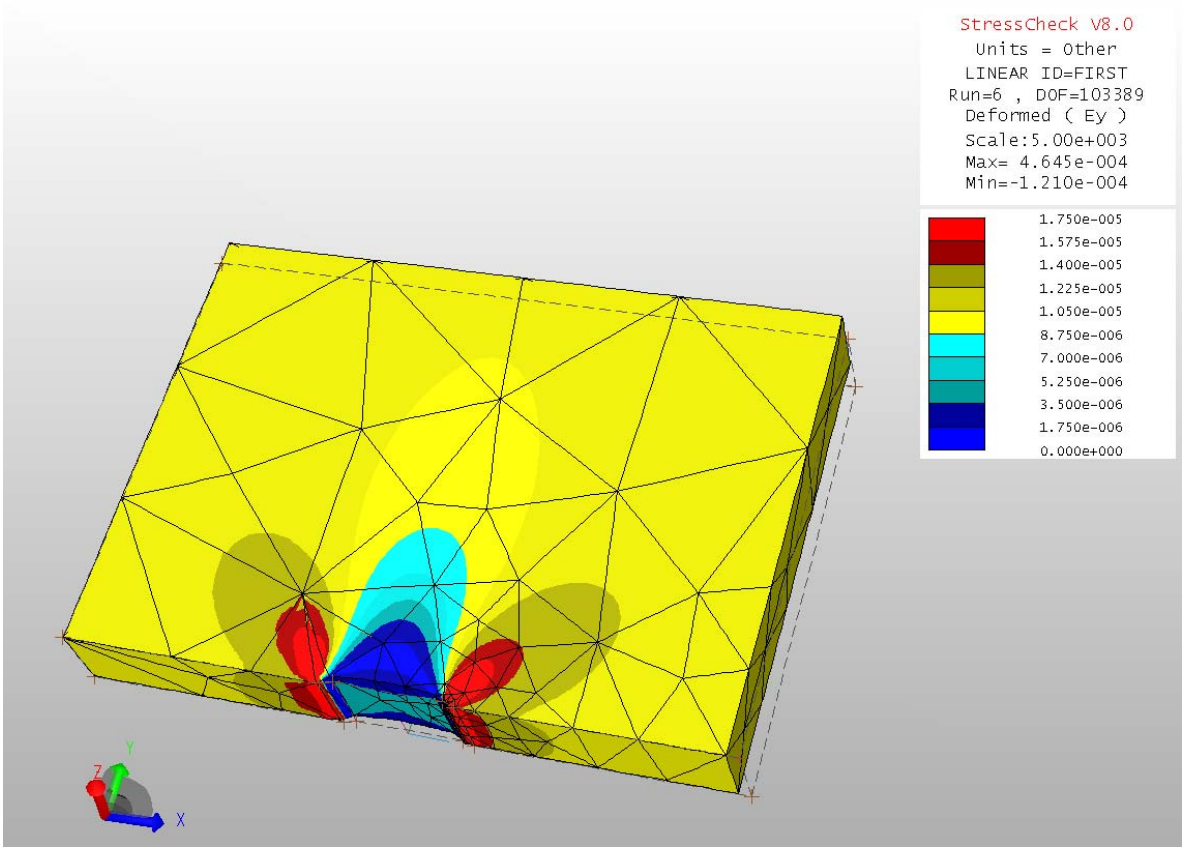

Figure 28. Substructured model from StressCheck version 8.0. Plotted y axis strain (E_y) under a fixed displacement load of 7.8e^{-4} mm

The global model was constructed initially in early versions of StressCheck, Figure 27, but was further developed until the method set out below proved successful.

B.2. Input Parameters

StressCheck is a parametric modelling tool that allows for multiple case studies through the variation of parameters built into the model. Table 7 presents the parameters of the global modal.

Table 8. Parameters used in sub-structured model

Parameters	Description	Formula	Value
A0	Crack Length	Bc/10	1.25
An	Notch Length		10
ANGn	Notch Tip Angle		75
At	Crack Position		0.5
Bc	Coupon Thickness		12.5
Lc	Coupon Length	Wc/2+1.5*Wc	200
Nx1		(Wc/2)-An	40
Nx2		(Wc/2)-An+(Wn/2)*Tan(ANGn*pi/180)	41.866
Nx3		(Wc/2)+An-(Wn/2)*Tan(ANGn*pi/180)	58.134
Nx4		(Wc/2)+An	60
Ny1		0	0
Ny2		Wn/2	0.5
Ny3		Wn/2	0.5
Ny4		0	0
RH			10
Wc	Coupon Width		100
Wn	Notch Width		1

B.3. Construction Methodology

This model was created with the following steps:

REFERENCE/THEORY TOOLBAR
Initiate a model with properties of "3d", "Elasticity", "Other"

HANDBOOK.
Set up the parameters (Table 8)

GEOMETRY (Green Plane Setting)			
Create	Box	Locate	Solid Width: wc Height: lc/3 Depth: bc Accept
Create	Box	Locate	Solid X: 0 Y:-lc/6 Z: 0 Width: nx2-nx3 Height: wn Depth: bc Accept

Create	Body	Bool-subtract	Input Select main box Select sub box Accept
Create	Blend edge	Chamfer	Input R1: wn/2 R2: nx2-nx1 Select left notch edge Accept
Create	Blend edge	Chamfer	Input R1: wn/2 R2: nx2-nx1 Select right notch edge Accept
Create	Circle	Locate	Input (this forms the path) X: nx4-wc/2 Y: -lc/6 Z: bc*at Radius: a0 Rot-x: 270 Accept
Create	Body	Bool-union	Select the main body, then select the circle and click 'accept'

MESH			
Create	Mesh	Auto	Ratio: 1 Minlen: 1.25e-5 Isopar: 0.0 Trans: 0.125 Select geometry Accept Automesh
Create		Bndry layer	Ratio: 0.02 Layers: 3 To: 0.0225*a0 T-total: 0.30*a0 Select the crack front boundary

MATERIAL (define tab)			
Define	Linear	Selection	Id: aluminium7075-t6 Material: linear Units: other Type: isotropic Shear: energy Comment: 7075-t6 forgings E: 7.17e4 V: 3e-1 Dens: 2.8e-9 A(th): 2.36e-5 Accept

MATERIAL (assign tab)			
Select	All elements	Selection	Id: aluminium7075-t6 System: global Color: aluminum Type: homogeneous Accept

CONSTRAINT			
Select	Any surface	General	Id: constdisp Direction: xyz System: global Y: 7.8e-4 Select top face Accept
Select		Symmetry	Id: constdisp Select bottom faces (not the notch or the open crack area) Accept
Select	Point	Rigid body	Id: constdisp Select three points on bottom edges (not at notch) Accept

SOLUTION ID			
Define	Name	Selection	Solution id: fixed Constraint id: constdisp Accept

STRESSCHECK SOLVER		
Linear	Extension:	upward-p
	P-limits:	1 to 7

Appendix C Lessons Learnt

Unfortunately, the development of the models for this project was not as simple as anticipated. Throughout the development, issues have arisen that have slowed the project and resulted in an adjustment of the goals. This section will outline some of these issues and provide lessons learnt were possible. It is worth noting that many issues were resolved with newer versions of StressCheck highlighting some issues of the earlier code releases, and the issues from earlier codes will only be touched briefly.

C.1. Stability

This project has used four versions of the chosen FEA code; StressCheck 7.0.6, StressCheck 7.1, and StressCheck 7.1.1 over a 24 month period. The general conclusion from the use of each of the versions is that they all appear to be unstable. There has been difficulty in proving the existence of any particular implementation anomalies because models that fail on one PC may run fine on another, or a model that runs fine once may fail if run a second time. These stability issues also often cause corruption to input data files or the operating code itself. Corrupted models need to be reconstructed from scratch. This was possible for this project because it used fairly simple geometry that was quick to build and this approach guaranteed that the anomaly did not stem from corrupt data in an earlier file. However, it did not assure the method of construction did not generate data corruption. As such when repeated models were still found to be unstable other methods of creating the same geometry were developed. Through a combination of version upgrades and revised geometry creation, the final models were stable enough to generate the results present herein.

Later versions of the code appear to be improvements on earlier versions, but sometimes these newer versions had new issues. For example, StressCheck 7.1 initially failed to run, despite a completely clean installation where the previous version had run. This was despite complete removal of the old versions, including a manual registry clean. ESRD had great difficulty sourcing the cause of this and eventually the anomaly was corrected locally.

Unfortunately system error messages and program crashes can still occur on StressCheck version 8.0.

C.2. Modelling Size Limits

Some preliminary models were attempted in StressCheck version 7.0.6 to assess whether the software could model the half specimen with a crack. At this early stage the models took a long time to run and were invariably corrupted upon completion, making result extraction difficult or pointless as the data set was shown to be invalid. It was felt that there may have been an issue when constructing a model with large element size variations, exceeding 1000:1. So this approach was abandoned in favour of sub-structured models.

The first sub-structured models were created in the 3D space using the units “mm/N/sec/C” and employed geometric features embedded in the solid to force the creation of a refined mesh. StressCheck behaved erratically when attempting to generate semi-circular cracks with

a radius less than 0.5 mm. This issue was traced by ESRD to the Parasoild kernel employed for geometry creation in StressCheck models. It was caused because the kernel is limited to dimensions smaller no smaller than 0.1 mm in the 3-D space using the units "mm/N/sec/C", and this lead to instability.

As a result, the modelling units were switched to "other" and an attempt was made to model the sub-structured model where 1 unit was equivalent to one tenth of a millimetre. Again issues were encountered, this time the model appeared to change from a solid to a wire-frame and further geometric or Boolean operations failed. These issues were again traced by ESRD to the Parasoild kernel. This time it was because the kernel has a maximum dimension limit of a sphere of 500 units (radius) about the origin (0, 0, 0) when using the "Other" units. This is because it considers these to be metres, despite the "other" tag, and going outside this spheres causes the modeller to fail.

As a work around the "other units" was used and 1 unit was set equivalent to 1 mm, thereby staying with the maximum limit and potentially permitting small geometries, down to 0.0001 mm.

C.3. K_1 Determination Concerns

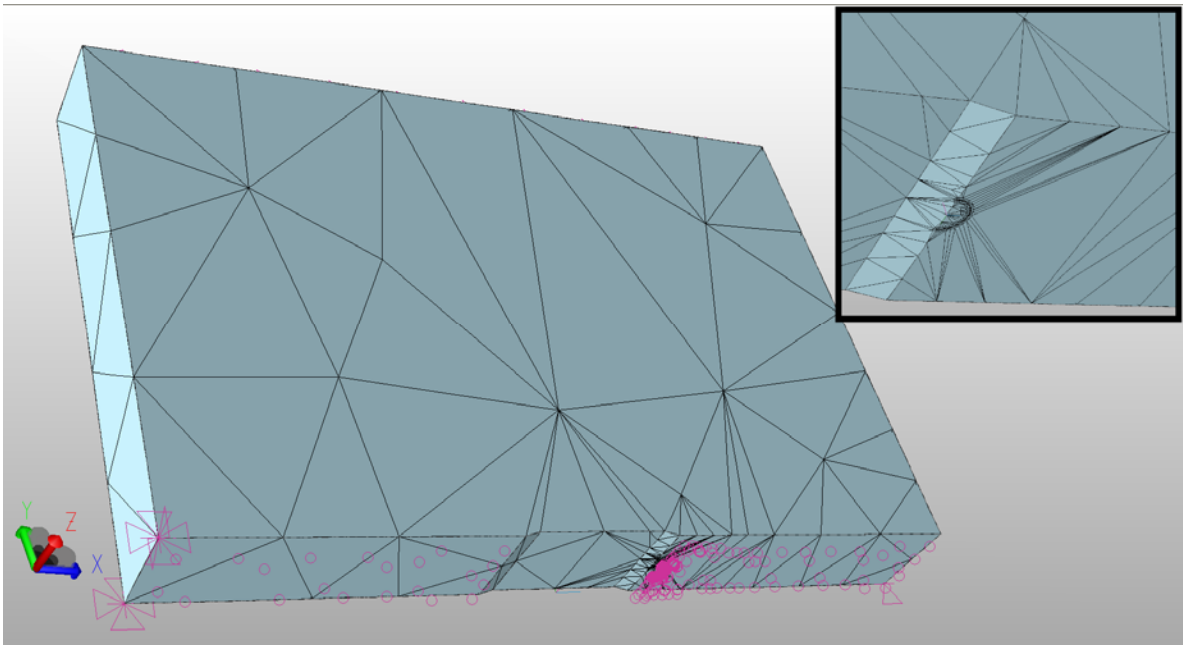

Figure 29. Initial sub-structured model and mesh with 1 mm semicircular crack and local mesh detail shown in the insert

Two anomalies with the result for K_1 were found when performing the first set of extractions from the sub-structured model with an initial semicircular crack in the centre of the thickness, under StressCheck 7.1.1. The extractions were performed under the "points" tab of the results menu. Ten extraction points were selected (giving 12 results) around the semicircular crack front with a radius of 1 mm, see Figure 29. This model configuration was symmetrical, so the

extraction was expected to yield symmetrical results. Secondly, an attempt was made to verify the stability of the result by checking the influence of the radius of integration on the K_1. Both of these checks returned results that were worse than expected, leading to a small investigation. The results of this first extraction are presented in Table 9. The initial model had 1229 Tetra elements and 2129 nodes. It is worth noting that the mesh for this model is not ideal, it has distended elements. However, the refinement near the crack tip was within the guidance of ESRD. This approach was taken with these early models to ensure successful runs by keeping the models small. This approach was taken due to instability found in early versions of StressCheck.

The variance of the symmetry check for the initial model was up to 5.3%. The extractions taken only from within the crack tip's second mesh refinement were typically in the range 3.4%-5.3%. When considering the issue of stability of K_1 with changes to the radius of integration two percentage measures were calculated. The first is for the radius variations from the outer edge of the second refinement to the middle of the inner refinement. The second is from three points inside the second refinement. In this initial model the variations were 40%-42% and 17.5%-19%, respectively. The percentage calculations are based on the 8^{th} order polynomial result.

It should be mentioned that these early developmental meshes appear less than ideal, but they passed the system checks within the code. However, the work that follows considers the mesh refinement issue so as to ascertain its influence, by comparing models with differing mesh refinement.

C.3.1 Constraints

The model presented in Figure 29 was over constrained in the global "Y" axis. To ensure this over restraint was not interfering in the results, it was rectified and the revised model (see Figure 30) was re-run. As suspected, removing the over-constraint had no influence on the results. The extracted K1 values were identical to the original model as reported in Table 9.

Table 9. K1 extractions for varying radii of integration on 1 mm semicircular crack using initial sub-structured model and mesh

			K1 (MPa √m)							
Radius Of Integration	N	Z	Run #1	Run #2	Run #3	Run #4	Run #5	Run #6	Run #7	Run #8
0.15 * A_0	1	7.25	1.52	3.30	4.54	5.23	5.50	5.54	5.53	5.54
	6	6.39	1.43	2.48	2.81	2.93	2.99	3.02	3.04	3.05
	7	6.11	1.67	2.80	3.09	3.10	3.07	3.05	3.04	3.04
	12	5.25	1.41	2.73	3.61	4.30	4.81	5.15	5.34	5.42
0.1125 * A_0	1	7.25	1.74	3.09	4.18	4.93	5.43	5.74	5.90	5.96
	6	6.39	1.92	2.42	2.62	2.81	2.86	2.90	2.94	2.96
	7	6.11	1.72	2.33	2.60	2.83	2.85	2.91	2.94	2.96
	12	5.25	2.15	2.75	3.62	4.15	4.65	5.06	5.41	5.66
0.15 * $A_0/2$	1	7.25	3.30	5.69	5.91	6.74	6.59	6.86	6.78	6.77
	6	6.39	1.52	2.49	2.65	2.74	2.83	2.88	2.91	2.93
	7	6.11	1.39	2.55	2.63	2.73	2.83	2.88	2.91	2.93
	12	5.25	3.94	5.65	6.16	6.19	6.45	6.45	6.53	6.52
0.04875 * A_0	1	7.25	3.12	5.87	6.45	6.94	7.01	7.20	7.18	7.23
	6	6.39	1.21	2.37	2.72	2.78	2.81	2.85	2.89	2.91
	7	6.11	1.11	2.42	2.71	2.76	2.80	2.85	2.89	2.91
	12	5.25	3.87	5.64	6.43	6.51	6.82	6.82	6.98	6.99
0.15* 0.15* A_0	1	7.25	4.91	5.54	7.17	7.52	7.84	8.01	8.14	8.16
	6	6.39	1.47	1.84	2.46	2.67	2.77	2.83	2.86	2.88
	7	6.11	0.837	1.84	2.35	2.60	2.74	2.82	2.86	2.88
	12	5.25	4.62	6.48	7.10	7.45	7.72	7.94	7.87	8.14
0.15* 0.15* $A_0/2$	1	7.25	5.42	7.67	8.28	8.69	9.44	9.26	9.23	9.28
	6	6.39	1.35	2.46	2.56	2.58	2.76	2.90	2.87	2.82
	7	6.11	1.54	2.76	2.36	2.60	2.90	2.87	2.77	2.82
	12	5.25	4.16	6.12	6.88	8.30	8.95	9.02	9.05	9.40

C.3.2 Mesh refinement

After removing any doubt from the set up of constraints, the influence of mesh refinement was considered. With the initial model the global mesh was kept course with quick transition to keep this size of the model down, improve run time and maintain stability. This meant that meshing away from the area of interest was less than ideal. Many of the Automesher parameters were adjusted in an attempt to improve the mesh without it becoming overly large. In the end, the best solution was to embed a sphere in the region near the crack to create local refinement. The radius of the sphere was set at 3 times the crack radius. Figure 31 shows the resultant model which contained substantially improved meshing near the crack for only 1749 Tetra element and 2848 nodes.

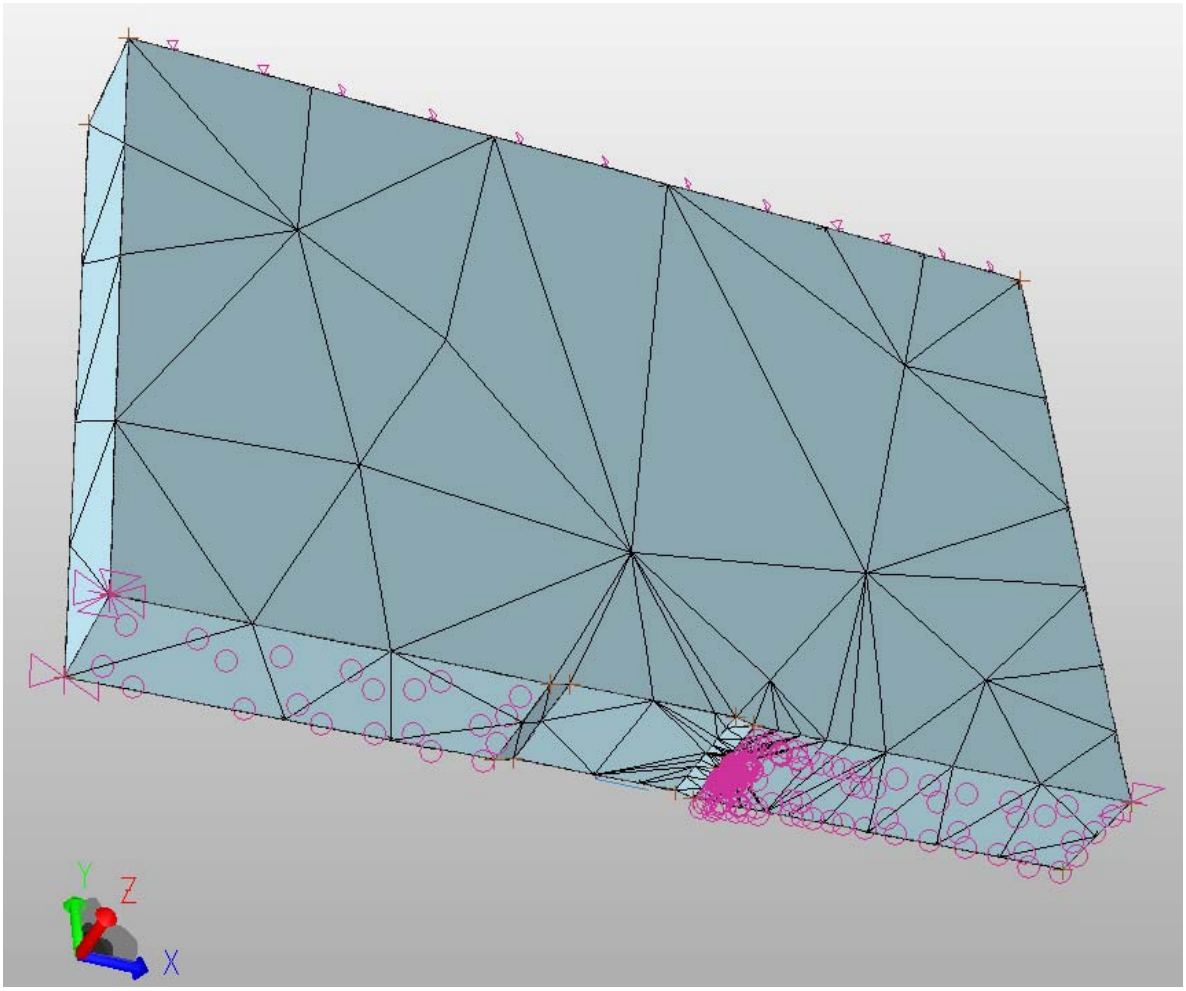

Figure 30. Sub-structured model and mesh with 1 mm semicircular crack and revised boundary conditions

The results for the revised mesh showed an improvement, but were still beyond what was expected for the variation of K_1 with changes to the radius of integration, with 39%-42.5%. The improvement was more pronounced when considering the extractions from the inside the second refinement with results of 13.8%-15.6%. The symmetric K_1 result was better, however, despite having an almost symmetrical mesh the result still showed a variation of up to 4%. These percentage variation calculations are based on the 8th order polynomial result. A summary of these results is presented in Table 10.

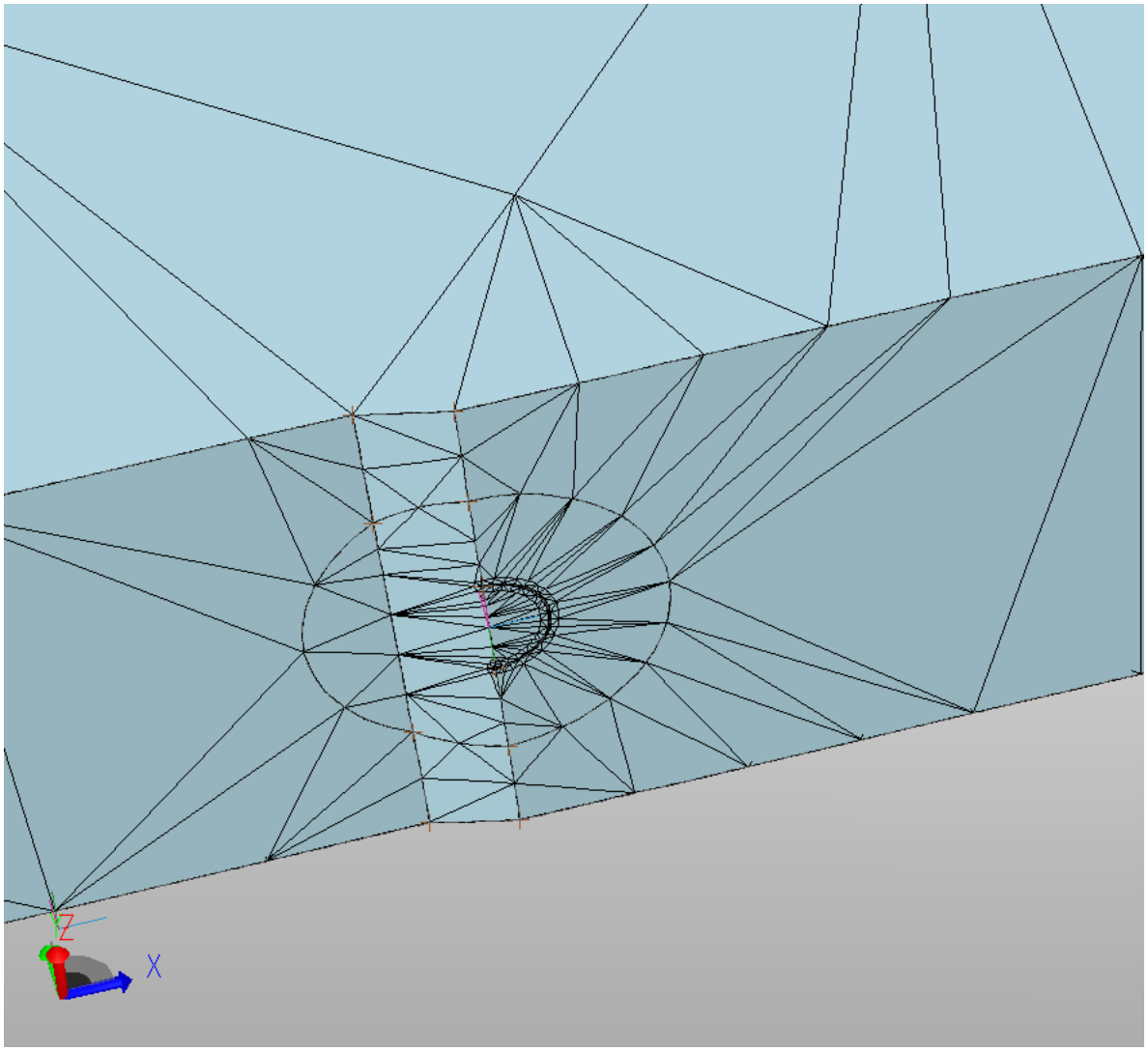

Figure 31. Sub-structured model with 1 mm semicircular crack revised mesh and boundary conditions

C.3.3 Validation of a StressCheck Handbook example

As part of the research program, it was decided that it would have been instructive to compare the results with a handbook example that uses a crack on a plane of symmetry. As such, the ESRD Channel with a crack example was chosen and run straight from the handbook without revision, Figure 32. This example is not symmetrical so it only provides a reference for the variation of K_1 with the radius of integration. The results were better than for the sub-structured model, but still quite high at 15.6% - %19.3% and 7.8% - 11.7% respectively. A more detailed summary is provided in Table 11 and these percentage calculations are based on the 8th order polynomial result.

Table 10. K1 extractions for varying radii of integration on 1mm semicircular crack using the sub-structured model with revised mesh and boundary conditions

			K1 (MPa √m)							
Radius Of Integration (mm)	N	Z	Run #1	Run #2	Run #3	Run #4	Run #5	Run #6	Run #7	Run #8
0.15 * A_0	1	7.25	2.269	4.119	5.375	5.769	5.851	5.763	5.689	5.646
	6	6.392	1.38	2.218	2.624	2.815	2.934	2.99	3.016	3.028
	7	6.108	1.209	2.124	2.582	2.78	2.899	2.961	2.994	3.013
	12	5.25	1.901	3.87	4.83	5.285	5.497	5.538	5.552	5.562
0.1125 * A_0	1	7.25	2.335	4.074	5.368	5.938	6.216	6.252	6.233	6.163
	6	6.392	1.819	2.437	2.7	2.898	2.938	2.955	2.974	2.982
	7	6.108	1.501	2.344	2.75	2.874	2.935	2.955	2.97	2.981
	12	5.25	2.662	3.762	4.762	5.263	5.609	5.864	6.005	6.069
0.15 * $A_0/2$	1	7.25	2.792	5.599	5.902	6.622	6.472	6.708	6.61	6.627
	6	6.392	1.299	2.482	2.764	2.831	2.899	2.932	2.944	2.952
	7	6.108	1.307	2.374	2.717	2.856	2.904	2.924	2.941	2.952
	12	5.25	4.286	6.417	6.906	6.79	6.897	6.815	6.789	6.717
0.04875 * A_0	1	7.25	2.673	5.822	6.471	6.885	6.948	7.104	7.09	7.151
	6	6.392	1.151	2.342	2.753	2.841	2.882	2.907	2.922	2.93
	7	6.108	1.155	2.298	2.668	2.821	2.886	2.91	2.923	2.928
	12	5.25	3.914	6.303	7.133	7.084	7.265	7.181	7.249	7.192
0.15* 0.15* A_0	1	7.25	4.493	5.533	7.266	7.566	7.806	7.988	8.098	8.134
	6	6.392	1.483	2.062	2.696	2.816	2.863	2.889	2.9	2.902
	7	6.108	1.188	2.34	2.801	2.859	2.904	2.892	2.906	2.897
	12	5.25	4.118	7.304	7.923	8.111	8.223	8.355	8.171	8.38
0.15* 0.15* $A_0/2$	1	7.25	5.095	7.928	8.465	8.786	9.45	9.267	9.211	9.276
	6	6.392	1.037	2.429	2.623	2.641	2.824	2.947	2.909	2.847
	7	6.108	1.23	2.595	2.411	2.673	2.968	2.923	2.802	2.846
	12	5.25	3.789	6.906	7.724	9.024	9.545	9.49	9.403	9.674

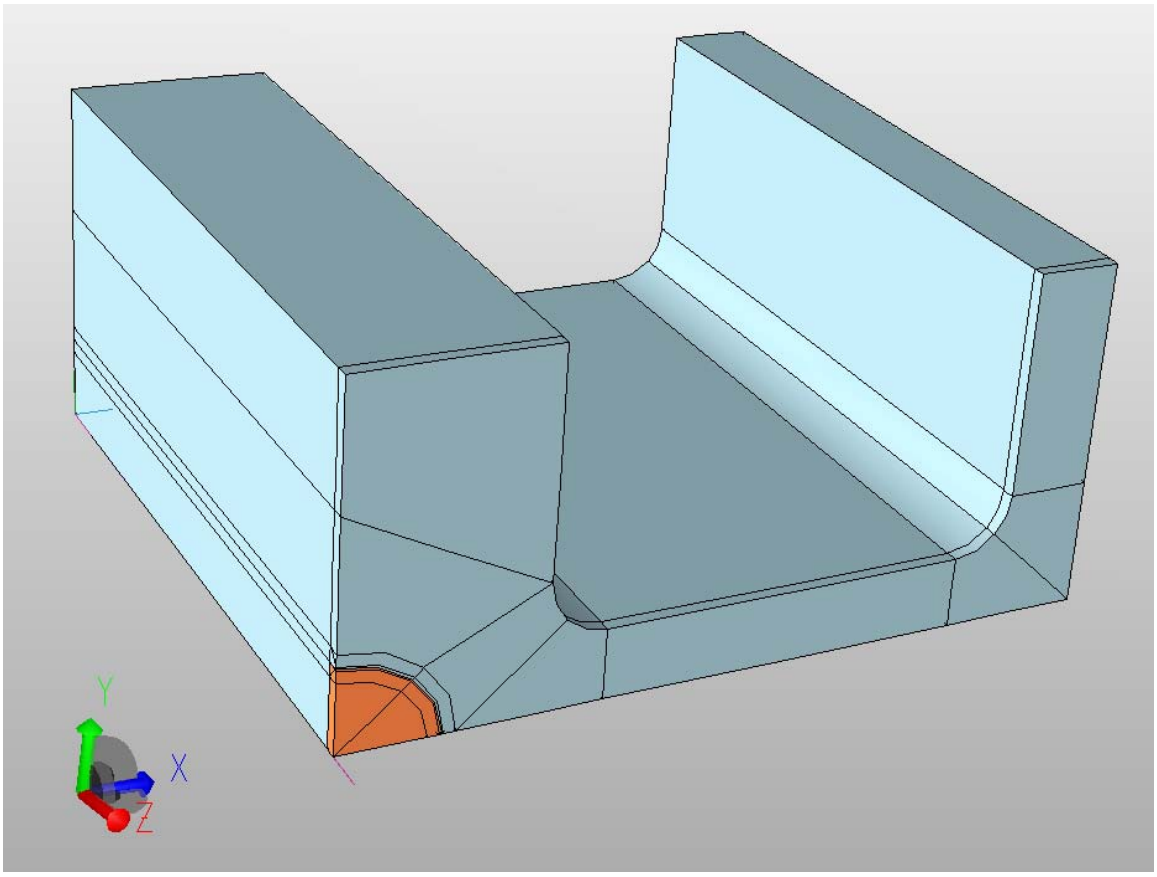

Figure 32. ESRD's handbook channel crack example

C.3.4 Validation against an Abaqus Handbook example

After obtaining another disappointing result for the ESRD handbook channel crack example, consideration was given to the accuracy of other codes. A worked example with matched handbook solutions was found in another code licensed to DSTO, Abaqus. This model was recreated in StressCheck with the aim of comparing the StressCheck result with that from the Abaqus handbook solution. The model is a simple elliptical crack in the centre of a plate, as shown in Figure 33. In this example it is modelled utilising the symmetry about its centreline and as such it is not possible to compare K_1 symmetry anomalies. To speed up result generation these models were only run to polynomial order 6.

Table 11. K_1 extractions for varying radii of integration on ESRD's handbook channel crack example

			K1 (MPa √m)							
Radius Of Integration (mm)	N	Z	Run #1	Run #2	Run #3	Run #4	Run #5	Run #6	Run #7	Run #8
0.15 * A_0	1	2.5	6099	6381	7519	7657	7782	7763	7894	7980
	6	2.5	6014	6389	7438	7828	7991	8110	8214	8225
	7	2.5	5944	6425	7455	7798	8016	8153	8272	8282
	12	2.5	6360	6841	7889	7758	8025	8184	8320	8408
0.1125 * A_0	1	2.5	5501	6740	6592	7142	7416	7576	7686	8100
	6	2.5	5443	6822	7269	7774	7952	8085	8125	8171
	7	2.5	5374	6866	7305	7795	8008	8149	8180	8240
	12	2.5	5756	7323	7361	7608	7868	7997	8104	8177
0.15 * A_0/2	1	2.5	4680	6599	6565	6886	7147	7322	7418	7570
	6	2.5	4631	6747	7372	7647	7806	8028	8027	8090
	7	2.5	4561	6802	7424	7697	7866	8099	8080	8163
	12	2.5	4900	7233	7573	7368	7576	7730	7821	7889
0.04875 * A_0	1	2.5	3675	5908	6393	6781	6966	7020	7098	7155
	6	2.5	3634	6117	7298	7665	7769	7927	7922	7991
	7	2.5	3565	6183	7357	7734	7825	7998	7979	8064
	12	2.5	3859	6528	7765	7301	7396	7423	7486	7534
0.15* 0.15* A_0	1	2.5	6116	5535	6353	7156	6809	6245	6651	6771
	6	2.5	6070	5782	6645	7559	7961	7528	7888	7963
	7	2.5	6021	5887	6648	7610	7990	7582	7958	8032
	12	2.5	6594	6067	6854	7570	8026	6806	6939	7090
0.15* 0.15* A_0/2	1	2.5	6283	6813	7355	7155	6821	6779	6482	6533
	6	2.5	6182	7008	7567	7411	7321	7643	7942	7939
	7	2.5	6159	7118	7587	7463	7346	7705	8012	8012
	12	2.5	6723	7467	7969	7683	7273	7377	7659	7411

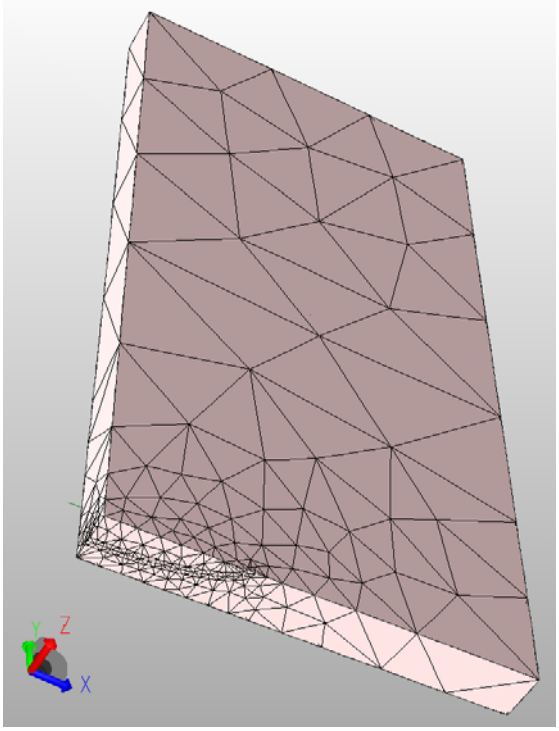

Figure 33. Elliptical crack in plate with handbook solutions and comparisons from Abaqus handbook example (Model V1)

Table 12. K_1 extractions for varying radii of integration on verifiable model (presented in the Abaqus Handbook) of elliptical crack in a plate

			K_1 (MPa √m)							
Radius Of Integration (mm)	N	Z	Run #1	Run #2	Run #3	Run #4	Run #5	Run #6	Run #7	Run #8
0.15 * A_0	1	0.6667	1663	2507	2643	2678	2696	2702		
	12	1.667	1221	1723	1727	1736	1737	1742		
0.1125 * A_0	1	0.6667	2650	2569	2611	2734	2668	2703		
	12	1.667	1506	1612	1791	1702	1709	1722		
0.15 * $A_0/2$	1	0.6667	2341	2823	2596	2649	2697	2695		
	12	1.667	1337	1661	1657	1717	1683	1689		
0.04875 * A_0	1	0.6667	1894	2772	2752	2678	2666	2683		
	12	1.667	1156	1620	1620	1651	1667	1667		
0.15* 0.15* A_0	1	0.6667	1130	2080	2352	2568	2623	2684		
	12	1.667	1057	1657	1676	1663	1646	1639		
0.15* 0.15* $A_0/2$	1	0.6667	2483	3034	2401	2579	2770	2736		
	12	1.667	1114	1782	1371	1517	1632	1614		

This model showed excellent results with the K_1 variation down to 2%-7% and 0.7-3.2%. With this successful result an attempted was made to perturb the model by varying the mesh, crack shape and crack size. This would then indicate what was causing the earlier inaccuracies.

This first model (V1, Figure 33) had 3363 tetra elements and 5047 nodes. The second model (V2, Figure 34) looked at reducing the element numbers. The third model (V3, Figure 35) reduced these as much as possible, but still ensuring no meshing errors were generated. The first set of results showed that this model layout did not suffer from mesh sensitivity.

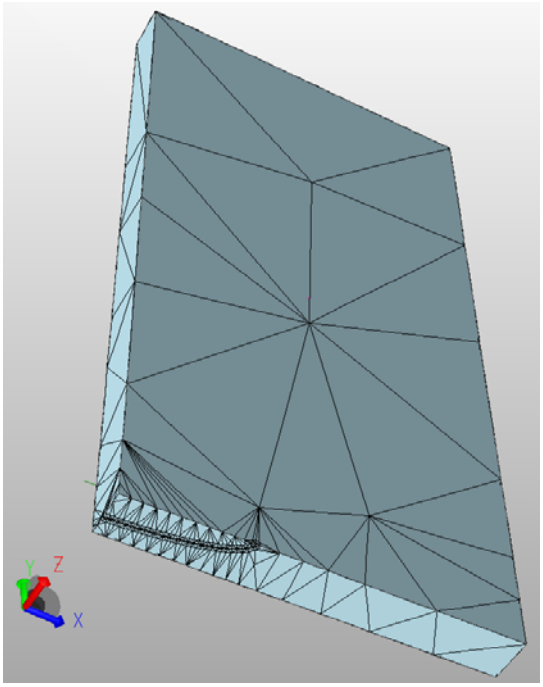

Figure 34. Elliptical crack in plate with handbook solutions and comparisons from other FEA code, reduced mesh example (Model V2)

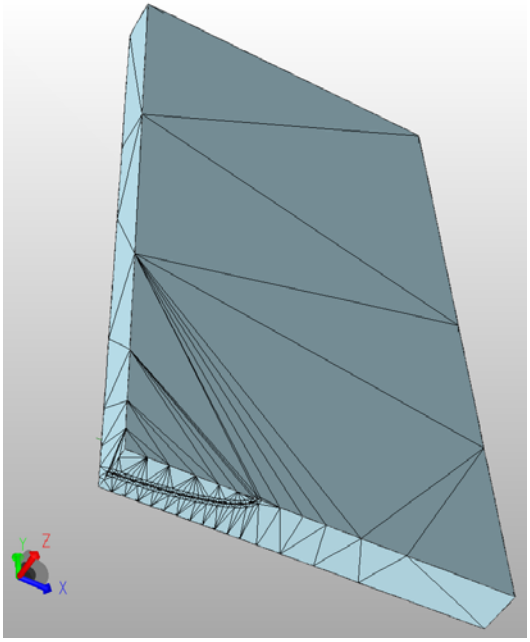

Figure 35. Elliptical crack in plate with handbook solutions and comparisons from other FEA code, second reduced mesh example (Model V3)

Table 13. Summary of results from verifiable model of symmetric crack in a plate

Model #	Description	Smallest Radius	Elements	Nodes	Global Variance	Confined Variance
V1	Elliptical Crack baseline	1 inch / 25.4 mm	3363	5047	2%-7%	0.7-3.2%
V2	Elliptical Crack – Revised Mesh	1 inch / 25.4 mm	1728	2893	1.9%-8.2%	0.7%-3.2%
V3	Elliptical Crack – Revised Mesh 2	1 inch / 25.4 mm	1471	2447	2%-18%	0.7%-4.15%
V4	Circular Crack (1 inch/25.4 mm)	1 inch / 25.4 mm	1584	2555	2.3%-7.2%	1.6%-1.8%
V5	Circular Crack (0.0394 inch/1 mm)	0.0394 inch/1 mm	1184	2094	4.3%-7%	2.1%-2.8%
V6	Circular Crack (0.0394 inch/1 mm) Revised Mesh	0.0394 inch/1 mm	493	977	5.3%-8.6%	2-2.3%

The results of this study showed that consistently good results with little mesh dependence within the confined zone and performance better than the channel example for the global variance, as presented in Table 13.

Following this work, shape influences were considered by reducing the elliptical crack to a circular crack with sizes varying from 1 inch (25.4 mm) to 0.0394 inch (1 mm) and various levels of mesh refinement. Figure 36 (Model V4), Figure 37 (Model V5), and Figure 38 (Model V6) graphically present these variations while Table 13 again presents the results.

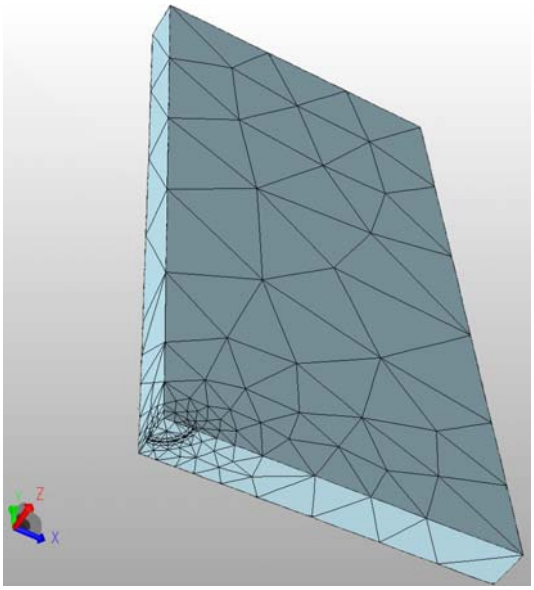

Figure 36. One inch circular crack in plate variation to comparison model (Model V4)

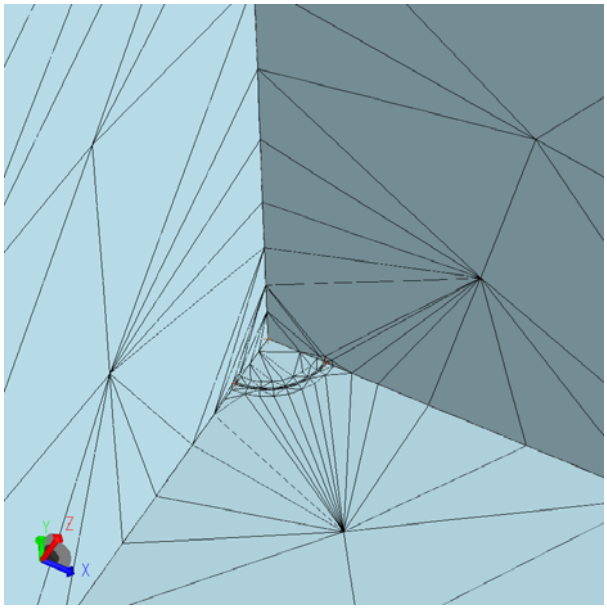

Figure 37. One millimetre circular crack in plate variation to comparison model (Model V5)

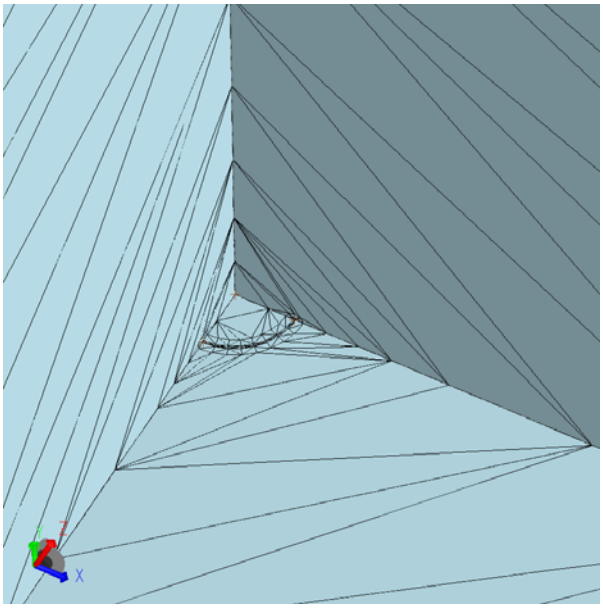

Figure 38. One millimetre circular crack in plate variation to comparison model, reduced mesh (Model V6)

Again all these models showed exceptional results and did not identify a source of the large variations seen in the substructure models of a middle tension specimen or the ESRD handbook channel crack example. This is despite a range of geometries, element sizes and mesh refinement.

C.3.5 Conclusion

In the end, no confirmed source of these anomalies was identified. Switching to StressCheck version 8.0 and quadrupling the number of elements into the range of 15,000 to 20,000 reduced the impact of the anomalies. Additionally, averaging solutions with symmetrical geometry and non-symmetrical meshing further improved the results and consequently the solutions presented in the main report appear robust and consistent.

However, these issues show that the increased solution efficiency, through the requirement for reduced numbers of elements, claimed by the developer is not as great as implied. This statement is supported by the poor performance of their test case, Figure 32, in this investigation. Additionally, it leaves other doubts because the solutions did not appear to provide consistent results across a range of models, and re-amplifies the importance of model and results validation.

This page is intentionally blank

Appendix D Results for Circular Crack

Table 14. Raw extraction results for K_1 (MPa √m) about a circular crack of radius 0.08 mm

Through thickness location		0.5/0.5		0.55/0.45		0.6/0.4		0.65/0.35		0.7/0.3		0.75/0.25		0.8/0.2		0.85/0.15		0.9/0.1		0.95/0.05		0.992/0.008		0.996/0.004		1/0	
Extraction Number	Normalized Location	Normal (0.5)	Mirror (0.5)	Normal (0.55)	Mirror (0.45)	Normal (0.6)	Mirror (0.4)	Normal (0.65)	Mirror (0.35)	Normal (0.7)	Mirror (0.3)	Normal (0.75)	Mirror (0.25)	Normal (0.8)	Mirror (0.2)	Normal (0.85)	Mirror (0.15)	Normal (0.9)	Mirror (0.1)	Normal (0.95)	Mirror (0.05)	Normal (0.992)	Mirror (0.008)	Normal (0.996)	Mirror (0.004)	Normal (1)	Mirror (0)
0	0.000	6.814	6.895	6.807	6.889	6.814	6.891	6.803	6.899	6.809	6.893	6.825	6.900	6.806	6.882	6.784	6.856	6.719	6.802	6.547	6.614	6.190	6.304	6.441	6.454	1.996	1.996
1	0.027	5.757	5.783	5.750	5.778	5.756	5.780	5.747	5.786	5.752	5.781	5.766	5.787	5.750	5.772	5.731	5.750	5.675	5.704	5.529	5.545	5.223	5.244	3.709	3.705	2.009	2.007
2	0.054	4.863	4.886	4.857	4.881	4.862	4.883	4.855	4.884	4.859	4.884	4.868	4.889	4.856	4.876	4.840	4.857	4.793	4.818	4.668	4.683	4.384	4.403	3.364	3.368	2.124	2.123
3	0.081	4.347	4.362	4.342	4.358	4.346	4.360	4.340	4.364	4.343	4.361	4.353	4.365	4.340	4.353	4.326	4.336	4.282	4.301	4.171	4.179	3.904	3.916	3.152	3.151	2.151	2.148
4	0.108	4.005	4.014	4.001	4.010	4.004	4.012	3.999	4.016	4.002	4.013	4.011	4.017	3.999	4.005	3.986	3.993	3.946	3.957	3.842	3.845	3.586	3.592	3.001	3.000	2.156	2.158
5	0.135	3.753	3.760	3.749	3.756	3.752	3.758	3.747	3.761	3.750	3.758	3.758	3.762	3.747	3.751	3.734	3.737	3.697	3.705	3.600	3.600	3.351	3.356	2.888	2.887	2.165	2.163
6	0.162	3.555	3.560	3.552	3.556	3.554	3.558	3.550	3.561	3.552	3.558	3.560	3.562	3.549	3.551	3.537	3.541	3.502	3.508	3.410	3.409	3.168	3.170	2.804	2.803	2.175	2.175
7	0.189	3.403	3.405	3.400	3.402	3.402	3.403	3.398	3.406	3.401	3.404	3.407	3.407	3.397	3.397	3.386	3.384	3.352	3.355	3.264	3.261	3.026	3.026	2.742	2.734	2.190	2.187
8	0.216	3.276	3.278	3.273	3.275	3.275	3.276	3.274	3.279	3.274	3.277	3.280	3.280	3.270	3.270	3.259	3.258	3.227	3.230	3.142	3.145	2.908	2.908	2.689	2.687	2.205	2.205
9	0.243	3.173	3.174	3.170	3.170	3.172	3.172	3.169	3.174	3.171	3.172	3.177	3.175	3.168	3.165	3.157	3.154	3.130	3.128	3.044	3.040	2.813	2.811	2.650	2.649	2.223	2.223
10	0.270	3.084	3.091	3.081	3.088	3.083	3.090	3.080	3.092	3.082	3.090	3.087	3.093	3.078	3.084	3.068	3.073	3.038	3.047	2.961	2.962	2.731	2.736	2.623	2.623	2.244	2.242
11	0.297	3.015	3.016	3.012	3.013	3.014	3.014	3.011	3.016	3.013	3.015	3.018	3.018	3.010	3.006	3.000	2.998	2.971	2.973	2.894	2.891	2.669	2.668	2.602	2.600	2.266	2.269
12	0.324	2.957	2.959	2.954	2.956	2.956	2.958	2.953	2.960	2.955	2.958	2.960	2.961	2.952	2.953	2.942	2.942	2.914	2.918	2.840	2.838	2.617	2.617	2.588	2.586	2.295	2.290
13	0.351	2.911	2.912	2.908	2.909	2.909	2.910	2.907	2.913	2.909	2.911	2.914	2.914	2.906	2.905	2.897	2.895	2.869	2.872	2.796	2.794	2.577	2.576	2.583	2.580	2.319	2.319
14	0.378	2.873	2.874	2.871	2.871	2.872	2.873	2.870	2.875	2.872	2.874	2.877	2.876	2.869	2.868	2.860	2.858	2.833	2.836	2.762	2.759	2.546	2.544	2.579	2.577	2.350	2.347
15	0.405	2.840	2.844	2.838	2.841	2.839	2.845	2.837	2.844	2.839	2.843	2.836	2.846	2.836	2.838	2.827	2.828	2.801	2.805	2.732	2.731	2.519	2.519	2.582	2.581	2.383	2.381
16	0.432	2.820	2.824	2.818	2.819	2.822	2.820	2.817	2.822	2.819	2.822	2.824	2.824	2.817	2.816	2.808	2.807	2.782	2.784	2.714	2.711	2.504	2.502	2.588	2.590	2.416	2.417
17	0.459	2.808	2.807	2.806	2.804	2.807	2.808	2.804	2.808	2.807	2.807	2.812	2.809	2.805	2.802	2.796	2.792	2.770	2.770	2.703	2.698	2.495	2.492	0.000	2.603	2.454	2.454
18	0.486	2.800	2.798	2.798	2.795	2.800	2.795	2.797	2.799	2.800	2.798	2.804	2.800	2.797	2.793	2.789	2.782	2.766	2.762	2.697	2.691	2.492	2.488	2.624	2.621	2.496	2.498
19	0.514	2.798	2.800	2.796	2.797	2.795	2.799	2.794	2.801	2.795	2.801	2.802	2.803	2.795	2.796	2.786	2.787	2.762	2.765	2.696	2.695	2.492	2.493	2.646	2.645	2.544	2.539
20	0.541	2.807	2.808	2.805	2.805	2.806	2.807	2.803	2.809	2.806	2.808	2.811	2.810	2.804	2.804	2.796	2.794	2.771	2.773	2.708	2.703	2.505	2.503	2.676	0.000	2.590	2.587
21	0.568	2.824	2.820	2.820	2.818	2.821	2.822	2.818	2.822	2.821	2.824	2.826	2.823	2.819	2.819	2.811	2.807	2.786	2.786	2.721	2.719	2.522	2.519	2.711	2.705	2.645	2.641
22	0.595	2.844	2.840	2.842	2.837	2.846	2.839	2.843	2.842	2.843	2.841	2.848	2.843	2.841	2.828	2.833	2.827	2.808	2.805	2.743	2.736	2.548	2.540	2.750	2.747	2.702	2.700
23	0.622	2.874	2.873	2.872	2.871	2.874	2.873	2.871	2.875	2.874	2.875	2.879	2.877	2.872	2.869	2.863	2.860	2.838	2.838	2.773	2.769	2.576	2.573	2.797	2.795	2.764	2.763
24	0.649	2.912	2.911	2.910	2.908	2.912	2.910	2.909	2.916	2.912	2.912	2.917	2.914	2.909	2.907	2.901	2.897	2.876	2.875	2.810	2.805	2.614	2.610	2.853	2.852	2.836	2.830
25	0.676	2.959	2.957	2.958	2.954	2.960	2.956	2.956	2.959	2.959	2.958	2.964	2.960	2.957	2.953	2.948	2.944	2.923	2.921	2.857	2.850	2.661	2.656	2.914	2.911	2.911	2.912
26	0.703	3.016	3.015	3.014	3.012	3.016	3.014	3.012	3.017	3.016	3.016	3.021	3.018	3.013	3.011	3.004	3.002	2.979	2.979	2.910	2.907	2.716	2.712	2.986	2.983	3.002	2.994
27	0.730	3.091	3.084	3.090	3.081	3.091	3.083	3.087	3.086	3.091	3.085	3.097	3.087	3.089	3.080	3.079	3.070	3.053	3.047	2.985	2.974	2.788	2.780	3.073	3.067	3.093	3.091
28	0.757	3.174	3.173	3.172	3.170	3.173	3.176	3.170	3.175	3.173	3.174	3.179	3.176	3.171	3.169	3.161	3.159	3.134	3.135	3.065	3.060	2.866	2.863	3.166	3.161	3.205	3.197
29	0.784	3.278	3.276	3.277	3.273	3.278	3.275	3.274	3.278	3.277	3.277	3.284	3.279	3.275	3.272	3.265	3.262	3.238	3.239	3.167	3.163	2.965	2.960	3.279	3.274	3.329	3.321
30	0.811	3.405	3.403	3.404	3.400	3.405	3.402	3.401	3.405	3.404	3.404	3.411	3.406	3.402	3.398	3.391	3.387	3.363	3.362	3.290	3.283	3.085	3.080	3.409	3.410	3.470	3.464
31	0.838	3.560	3.555	3.559	3.552	3.560	3.558	3.555	3.557	3.562	3.557	3.566	3.559	3.556	3.550	3.549	3.539	3.516	3.512	3.441	3.431	3.231	3.223	3.576	3.565	3.641	3.631
32	0.865	3.760	3.753	3.759	3.749	3.759	3.752	3.755	3.755	3.758	3.754	3.766	3.756	3.756	3.747	3.744	3.736	3.713	3.707	3.635	3.622	3.418	3.407	3.773	3.760	3.846	3.840
33	0.892	4.014	4.005	4.013	4.001	4.014	4.004	4.009	4.008	4.013	4.007	4.021	4.009	4.010	4.000	3.998	3.987	3.965	3.957	3.882	3.867	3.656	3.643	4.025	4.008	4.112	4.088
34	0.919	4.362	4.347	4.362	4.342	4.362	4.345	4.356	4.349	4.365	4.348	4.369	4.350	4.358	4.341	4.344	4.327	4.309	4.294	4.221	4.198	3.981	3.961	4.360	4.336	4.450	4.429
35	0.946	4.886	4.863	4.885	4.857	4.885	4.860	4.879	4.865	4.883	4.864	4.893	4.866	4.881	4.856	4.866	4.841	4.826	4.804	4.729	4.698	4.467	4.439	4.836	4.787	4.945	4.910
36	0.973	5.783	5.757	5.783	5.750	5.783	5.754	5.775	5.760	5.780	5.758	5.793	5.761	5.778	5.749	5.760	5.732	5.713	5.688	5.601	5.564	5.300	5.267	5.873	5.807	5.803	5.738
37	1.000	6.895	6.814	6.895	6.807	6.895	6.811	6.885	6.819	6.891	6.817	6.906	6.820	6.889	6.805	6.868	6.786	6.813	6.734	6.682	6.590	6.334	6.249	6.224	6.126	5.953	5.949

Table 15. Raw extraction results for K_1 (MPa √m) about a circular crack of radius 0.10 mm

Through thickness location		0.5/0.5		0.55/0.45		0.6/0.4		0.65/0.35		0.7/0.3		0.75/0.25		0.8/0.2		0.85/0.15		0.9/0.1		0.95/0.05		0.99/0.01		0.995/0.005		1/0	
Extraction Number	Normalized Location	Normal (0.5)	Mirror (0.5)	Normal (0.55)	Mirror (0.45)	Normal (0.6)	Mirror (0.4)	Normal (0.65)	Mirror (0.35)	Normal (0.7)	Mirror (0.3)	Normal (0.75)	Mirror (0.25)	Normal (0.8)	Mirror (0.2)	Normal (0.85)	Mirror (0.15)	Normal (0.9)	Mirror (0.1)	Normal (0.95)	Mirror (0.05)	Normal (0.99)	Mirror (0.01)	Normal (0.995)	Mirror (0.005)	Normal (1)	Mirror (0)
0	0.000	6.819	6.904	6.817	6.899	6.822	6.900	6.815	6.900	6.823	6.905	6.821	6.910	6.812	6.893	6.790	6.864	6.723	6.808	6.545	6.626	6.289	6.402	0.000	0.000	2.026	2.033
1	0.027	5.761	5.791	5.759	5.787	5.763	5.788	5.757	5.787	5.764	5.792	5.763	5.795	5.754	5.781	5.735	5.757	5.678	5.709	5.527	5.555	5.305	5.328	3.772	3.766	2.039	2.044
2	0.054	4.866	4.892	4.865	4.889	4.868	4.889	4.863	4.889	4.868	4.893	4.868	4.895	4.860	4.884	4.844	4.863	4.795	4.822	4.666	4.690	4.454	4.473	3.421	3.423	2.156	2.167
3	0.081	4.350	4.368	4.349	4.365	4.351	4.366	4.347	4.365	4.352	4.368	4.351	4.370	4.344	4.361	4.330	4.342	4.285	4.305	4.169	4.186	3.966	3.978	3.205	3.202	2.182	2.187
4	0.108	4.009	4.020	4.007	4.017	4.010	4.017	4.006	4.017	4.010	4.020	4.009	4.021	4.003	4.012	3.989	3.995	3.948	3.963	3.840	3.850	3.643	3.649	3.051	3.048	2.187	2.197
5	0.135	3.756	3.765	3.755	3.762	3.762	3.763	3.753	3.762	3.757	3.765	3.757	3.766	3.751	3.758	3.743	3.741	3.699	3.709	3.598	3.605	3.405	3.409	2.937	2.934	2.196	2.203
6	0.162	3.559	3.565	3.557	3.565	3.559	3.563	3.556	3.562	3.559	3.565	3.559	3.566	3.553	3.562	3.541	3.543	3.504	3.512	3.408	3.413	3.218	3.220	2.851	2.849	2.207	2.214
7	0.189	3.407	3.410	3.405	3.407	3.406	3.408	3.403	3.407	3.407	3.410	3.407	3.411	3.401	3.403	3.389	3.395	3.354	3.359	3.262	3.265	3.074	3.074	2.788	2.778	2.220	2.227
8	0.216	3.280	3.283	3.278	3.280	3.280	3.287	3.277	3.280	3.280	3.283	3.280	3.283	3.274	3.277	3.263	3.263	3.229	3.234	3.141	3.144	2.955	2.960	2.734	2.730	2.237	2.245
9	0.243	3.177	3.178	3.175	3.176	3.177	3.176	3.174	3.176	3.181	3.178	3.177	3.179	3.176	3.172	3.161	3.159	3.128	3.131	3.043	3.044	2.858	2.856	2.694	2.691	2.254	2.263
10	0.270	3.088	3.096	3.086	3.093	3.087	3.094	3.085	3.093	3.087	3.096	3.088	3.097	3.082	3.090	3.072	3.077	3.040	3.051	2.959	2.966	2.775	2.780	2.667	2.665	2.276	2.283
11	0.297	3.019	3.020	3.017	3.018	3.018	3.019	3.016	3.018	3.018	3.020	3.019	3.021	3.014	3.015	3.004	3.003	2.973	2.977	2.894	2.895	2.712	2.711	2.644	2.642	2.298	2.308
12	0.324	2.961	2.963	2.959	2.961	2.960	2.962	2.958	2.962	2.960	2.964	2.961	2.964	2.956	2.959	2.947	2.947	2.917	2.921	2.840	2.842	2.659	2.659	2.630	2.627	2.326	2.331
13	0.351	2.914	2.916	2.913	2.914	2.914	2.915	2.912	2.915	2.914	2.917	2.915	2.917	2.910	2.912	2.901	2.900	2.871	2.876	2.797	2.799	2.618	2.617	2.625	2.621	2.352	2.360
14	0.378	2.877	2.879	2.876	2.876	2.877	2.877	2.875	2.877	2.877	2.879	2.878	2.880	2.873	2.874	2.864	2.863	2.836	2.839	2.763	2.764	2.586	2.585	2.621	2.618	2.383	2.389
15	0.405	2.844	2.848	2.842	2.846	2.844	2.847	2.842	2.846	2.844	2.849	2.845	2.849	2.840	2.844	2.823	2.833	2.804	2.810	2.733	2.736	2.559	2.559	2.624	2.621	2.416	2.423
16	0.432	2.825	2.826	2.823	2.824	2.824	2.825	2.822	2.825	2.825	2.827	2.825	2.827	2.821	2.823	2.812	2.812	2.785	2.789	2.716	2.717	2.543	2.542	2.630	2.631	2.450	2.460
17	0.459	2.812	2.811	2.810	2.809	2.811	2.810	2.809	2.810	2.812	2.812	2.812	2.813	2.809	2.808	2.800	2.798	2.773	2.775	2.705	2.704	2.535	2.532	0.000	2.643	2.488	2.497
18	0.486	2.804	2.802	2.803	2.798	2.804	2.801	2.802	2.801	2.805	2.803	2.805	2.802	2.804	2.799	2.793	2.789	2.766	2.767	2.700	2.697	2.531	2.527	2.666	2.661	2.530	2.541
19	0.514	2.802	2.804	2.800	2.803	2.802	2.804	2.800	2.804	2.802	2.806	2.803	2.807	2.797	2.802	2.791	2.792	2.765	2.773	2.699	2.701	2.532	2.532	2.688	2.686	2.579	2.583
20	0.541	2.811	2.812	2.809	2.810	2.811	2.812	2.809	2.812	2.811	2.814	2.812	2.814	2.808	2.810	2.802	2.800	2.774	2.778	2.709	2.709	2.544	2.543	2.718	0.000	2.626	2.632
21	0.568	2.826	2.825	2.824	2.823	2.826	2.826	2.824	2.824	2.826	2.826	2.827	2.827	2.823	2.823	2.815	2.813	2.789	2.791	2.724	2.723	2.561	2.558	2.754	2.746	2.681	2.687
22	0.595	2.848	2.844	2.846	2.843	2.848	2.844	2.848	2.844	2.848	2.838	2.852	2.839	2.846	2.843	2.837	2.833	2.811	2.811	2.746	2.743	2.585	2.580	2.793	2.789	2.739	2.747
23	0.622	2.879	2.877	2.876	2.876	2.878	2.877	2.876	2.877	2.879	2.880	2.880	2.880	2.876	2.876	2.868	2.866	2.842	2.844	2.777	2.776	2.616	2.613	2.841	2.837	2.802	2.811
24	0.649	2.916	2.914	2.914	2.913	2.916	2.914	2.914	2.914	2.917	2.917	2.918	2.917	2.914	2.913	2.906	2.903	2.879	2.881	2.814	2.813	2.655	2.651	2.897	2.895	2.874	2.881
25	0.676	2.963	2.961	2.961	2.959	2.963	2.961	2.961	2.960	2.964	2.963	2.965	2.964	2.961	2.959	2.953	2.949	2.926	2.927	2.861	2.858	2.701	2.697	2.959	2.954	2.950	2.962
26	0.703	3.020	3.019	3.018	3.017	3.020	3.019	3.018	3.019	3.021	3.021	3.022	3.022	3.018	3.018	3.009	3.007	2.982	2.985	2.916	2.915	2.757	2.754	3.032	3.027	3.042	3.045
27	0.730	3.096	3.088	3.094	3.086	3.095	3.090	3.093	3.088	3.095	3.090	3.097	3.091	3.093	3.086	3.084	3.076	3.057	3.053	2.990	2.983	2.830	2.821	3.120	3.113	3.134	3.144
28	0.757	3.178	3.177	3.176	3.176	3.178	3.177	3.175	3.181	3.178	3.180	3.179	3.180	3.176	3.176	3.166	3.165	3.138	3.141	3.070	3.070	2.909	2.906	3.214	3.208	3.247	3.252
29	0.784	3.283	3.280	3.280	3.279	3.282	3.280	3.280	3.280	3.282	3.283	3.284	3.283	3.280	3.279	3.270	3.268	3.242	3.243	3.172	3.170	3.009	3.005	3.329	3.322	3.372	3.378
30	0.811	3.410	3.407	3.407	3.406	3.409	3.407	3.406	3.406	3.409	3.410	3.411	3.410	3.407	3.406	3.397	3.394	3.373	3.369	3.296	3.294	3.131	3.126	3.460	3.460	3.515	3.523
31	0.838	3.565	3.559	3.562	3.558	3.564	3.559	3.561	3.559	3.564	3.562	3.565	3.562	3.561	3.557	3.551	3.546	3.520	3.520	3.447	3.445	3.278	3.271	3.629	3.617	3.689	3.693
32	0.865	3.765	3.756	3.761	3.755	3.764	3.757	3.761	3.757	3.763	3.765	3.765	3.760	3.761	3.760	3.750	3.743	3.718	3.715	3.642	3.634	3.468	3.458	3.828	3.815	3.896	3.900
33	0.892	4.020	4.009	4.016	4.008	4.019	4.009	4.015	4.009	4.018	4.012	4.020	4.012	4.015	4.007	4.003	3.994	3.970	3.965	3.890	3.880	3.709	3.697	4.084	4.066	4.165	4.162
34	0.919	4.368	4.350	4.364	4.349	4.367	4.351	4.363	4.351	4.366	4.354	4.368	4.354	4.363	4.349	4.350	4.335	4.315	4.304	4.229	4.212	4.037	4.020	4.424	4.398	4.507	4.505
35	0.946	4.892	4.866	4.887	4.865	4.891	4.867	4.886	4.867	4.889	4.870	4.892	4.870	4.886	4.865	4.872	4.850	4.833	4.815	4.739	4.714	4.531	4.505	4.906	4.855	5.008	4.992
36	0.973	5.791	5.761	5.784	5.760	5.789	5.762	5.783	5.761	5.786	5.766	5.790	5.766	5.784	5.759	5.767	5.742	5.722	5.702	5.613	5.584	5.374	5.345	5.957	5.890	5.877	5.834
37	1.000	6.904	6.819	6.896	6.818	6.903	6.821	6.894	6.820	6.898	6.825	6.903	6.825	6.896	6.818	6.877	6.797	6.824	6.751	6.697	6.613	6.422	6.341	6.313	6.213	6.028	6.049

Table 16. Raw extraction results for K_1 (MPa √m) about a circular crack of radius 0.20 mm

Through thickness location		0.5/0.5		0.55/0.45		0.6/0.4		0.65/0.35		0.7/0.3		0.75/0.25		0.8/0.2		0.85/0.15		0.9/0.1		0.95/0.05		0.98/0.02		0.99/0.01		1/0	
Extraction Number	Normalized Location	Normal (0.5)	Mirror (0.5)	Normal (0.55)	Mirror (0.45)	Normal (0.6)	Mirror (0.4)	Normal (0.65)	Mirror (0.35)	Normal (0.7)	Mirror (0.3)	Normal (0.75)	Mirror (0.25)	Normal (0.8)	Mirror (0.2)	Normal (0.85)	Mirror (0.15)	Normal (0.9)	Mirror (0.1)	Normal (0.95)	Mirror (0.05)	Normal (0.98)	Mirror (0.02)	Normal (0.99)	Mirror (0.01)	Normal (1)	Mirror (0)
0	0.000	6.845	6.927	6.836	6.912	6.847	6.926	6.841	6.927	9.653	6.931	6.850	6.927	6.831	6.909	6.804	6.890	6.727	6.819	6.537	6.631	6.597	6.717	0.000	0.000	2.158	2.157
1	0.027	5.783	5.810	5.776	5.798	5.784	5.809	5.780	5.810	5.321	5.813	5.787	5.810	5.771	5.794	5.747	5.778	5.682	5.718	5.518	5.556	5.567	5.592	3.986	3.978	2.171	2.169
2	0.054	4.886	4.909	4.880	4.899	4.887	4.908	4.883	4.909	4.884	4.912	4.889	4.909	4.875	4.895	4.854	4.881	4.799	4.829	4.657	4.689	4.675	4.697	3.616	3.616	2.294	2.293
3	0.081	4.369	4.385	4.364	4.376	4.369	4.383	4.366	4.384	4.367	4.386	4.371	4.383	4.358	4.372	4.339	4.358	4.289	4.311	4.162	4.183	4.165	4.179	3.387	3.382	2.321	2.317
4	0.108	4.027	4.036	4.022	4.028	4.027	4.035	4.024	4.035	4.025	4.037	4.028	4.034	4.016	4.023	3.998	4.010	3.952	3.966	3.833	3.851	3.827	3.835	3.224	3.219	2.325	2.327
5	0.135	3.774	3.781	3.770	3.774	3.774	3.779	3.771	3.780	3.772	3.781	3.775	3.779	3.763	3.769	3.747	3.756	3.704	3.715	3.591	3.603	3.579	3.584	3.103	3.098	2.334	2.332
6	0.162	3.576	3.581	3.572	3.574	3.576	3.579	3.573	3.580	3.574	3.581	3.577	3.579	3.566	3.569	3.550	3.557	3.509	3.518	3.403	3.411	3.383	3.386	3.011	3.007	2.345	2.343
7	0.189	3.424	3.426	3.420	3.419	3.424	3.424	3.421	3.425	3.422	3.426	3.424	3.424	3.414	3.415	3.399	3.403	3.360	3.365	3.258	3.264	3.233	3.233	2.944	2.932	2.359	2.356
8	0.216	3.297	3.299	3.293	3.293	3.296	3.297	3.294	3.298	3.295	3.299	3.297	3.297	3.287	3.288	3.273	3.277	3.236	3.241	3.141	3.144	3.107	3.107	2.887	2.881	2.375	2.375
9	0.243	3.194	3.194	3.190	3.188	3.193	3.193	3.191	3.193	3.192	3.194	3.194	3.192	3.184	3.184	3.171	3.173	3.135	3.139	3.042	3.046	3.006	3.005	2.845	2.840	2.393	2.393
10	0.270	3.105	3.112	3.101	3.106	3.104	3.111	3.102	3.111	3.103	3.112	3.105	3.110	3.096	3.102	3.083	3.092	3.049	3.059	2.959	2.969	2.919	2.924	2.815	2.811	2.415	2.413
11	0.297	3.036	3.037	3.034	3.031	3.035	3.035	3.033	3.036	3.034	3.034	3.036	3.035	3.027	3.027	3.015	3.018	2.982	2.986	2.896	2.900	2.852	2.852	2.791	2.786	2.438	2.440
12	0.324	2.978	2.980	2.974	2.975	2.977	2.979	2.975	2.979	2.976	2.981	2.978	2.979	2.970	2.971	2.957	2.964	2.926	2.931	2.843	2.848	2.797	2.797	2.775	2.770	2.467	2.462
13	0.351	2.932	2.933	2.929	2.928	2.931	2.932	2.929	2.932	2.931	2.933	2.932	2.932	2.924	2.925	2.912	2.916	2.886	2.886	2.802	2.806	2.754	2.753	2.770	2.763	2.493	2.492
14	0.378	2.895	2.895	2.893	2.890	2.894	2.894	2.893	2.894	2.894	2.896	2.895	2.894	2.888	2.887	2.876	2.879	2.847	2.850	2.770	2.773	2.721	2.718	2.765	2.759	2.525	2.522
15	0.405	2.861	2.865	2.858	2.860	2.861	2.864	2.860	2.864	2.861	2.865	2.862	2.864	2.855	2.858	2.844	2.849	2.815	2.821	2.741	2.747	2.690	2.691	2.767	2.761	2.559	2.558
16	0.432	2.842	2.843	2.839	2.838	2.841	2.842	2.840	2.842	2.841	2.844	2.843	2.842	2.836	2.836	2.825	2.828	2.798	2.801	2.725	2.728	2.676	2.673	2.772	2.771	2.594	2.595
17	0.459	2.829	2.828	2.826	2.823	2.828	2.827	2.828	2.827	2.829	2.829	2.830	2.828	2.823	2.822	2.813	2.814	2.787	2.787	2.716	2.717	2.664	2.661	0.000	2.783	2.634	2.631
18	0.486	2.822	2.819	2.819	2.814	2.821	2.818	2.820	2.818	2.822	2.820	2.823	2.819	2.817	2.813	2.807	2.806	2.780	2.780	2.712	2.711	2.659	2.655	2.809	2.802	2.678	2.679
19	0.514	2.819	2.822	2.816	2.817	2.818	2.824	2.818	2.821	2.819	2.823	2.819	2.822	2.814	2.816	2.805	2.809	2.779	2.783	2.712	2.716	2.660	2.660	2.832	2.827	2.728	2.723
20	0.541	2.828	2.829	2.825	2.824	2.827	2.828	2.827	2.828	2.829	2.831	2.830	2.829	2.824	2.824	2.814	2.817	2.789	2.792	2.723	2.726	2.671	2.670	2.862	0.000	2.775	2.774
21	0.568	2.843	2.842	2.840	2.837	2.842	2.841	2.842	2.841	2.844	2.844	2.845	2.843	2.839	2.837	2.830	2.830	2.804	2.805	2.740	2.741	2.689	2.686	2.890	2.888	2.834	2.832
22	0.595	2.865	2.861	2.862	2.856	2.864	2.861	2.864	2.861	2.866	2.863	2.868	2.862	2.861	2.849	2.852	2.850	2.827	2.826	2.763	2.762	2.712	2.707	2.944	2.932	2.895	2.893
23	0.622	2.895	2.895	2.892	2.890	2.895	2.894	2.894	2.894	2.896	2.897	2.898	2.896	2.892	2.891	2.883	2.884	2.858	2.859	2.795	2.796	2.745	2.742	2.989	2.982	2.960	2.959
24	0.649	2.933	2.932	2.930	2.926	2.932	2.931	2.932	2.931	2.934	2.934	2.936	2.937	2.929	2.928	2.920	2.921	2.896	2.896	2.833	2.834	2.784	2.780	3.047	3.041	3.035	3.032
25	0.676	2.980	2.978	2.977	2.972	2.979	2.977	2.981	2.977	2.981	2.980	2.983	2.979	2.977	2.974	2.968	2.967	2.943	2.943	2.881	2.880	2.832	2.828	3.111	3.102	3.115	3.116
26	0.703	3.037	3.036	3.034	3.030	3.036	3.035	3.036	3.035	3.038	3.038	3.040	3.037	3.033	3.032	3.024	3.025	2.999	3.001	2.937	2.939	2.889	2.886	3.187	3.178	3.211	3.202
27	0.730	3.112	3.105	3.109	3.099	3.111	3.104	3.111	3.104	3.114	3.107	3.115	3.106	3.109	3.101	3.100	3.094	3.074	3.069	3.012	3.007	2.964	2.955	3.278	3.266	3.307	3.304
28	0.757	3.194	3.194	3.191	3.188	3.193	3.194	3.193	3.193	3.196	3.196	3.198	3.195	3.191	3.190	3.181	3.183	3.156	3.158	3.094	3.096	3.046	3.044	3.376	3.364	3.424	3.417
29	0.784	3.299	3.297	3.295	3.291	3.297	3.297	3.298	3.296	3.300	3.299	3.302	3.298	3.295	3.293	3.285	3.286	3.259	3.260	3.197	3.197	3.150	3.146	3.495	3.483	3.556	3.548
30	0.811	3.426	3.424	3.422	3.417	3.430	3.424	3.424	3.423	3.427	3.426	3.429	3.425	3.421	3.419	3.412	3.412	3.386	3.386	3.322	3.323	3.275	3.271	3.632	3.625	3.705	3.699
31	0.838	3.581	3.576	3.577	3.569	3.578	3.576	3.579	3.575	3.582	3.579	3.584	3.577	3.576	3.575	3.566	3.564	3.539	3.538	3.474	3.473	3.427	3.421	3.807	3.788	3.886	3.876
32	0.865	3.781	3.774	3.776	3.766	3.778	3.773	3.779	3.773	3.782	3.776	3.784	3.774	3.775	3.769	3.766	3.761	3.737	3.734	3.671	3.668	3.624	3.615	4.015	3.992	4.103	4.093
33	0.892	4.036	4.027	4.034	4.018	4.032	4.026	4.033	4.025	4.037	4.029	4.039	4.027	4.030	4.021	4.020	4.013	3.990	3.985	3.922	3.916	3.873	3.863	4.281	4.253	4.384	4.361
34	0.919	4.385	4.369	4.379	4.359	4.379	4.368	4.381	4.367	4.386	4.371	4.387	4.369	4.378	4.363	4.368	4.355	4.336	4.325	4.264	4.253	4.214	4.197	4.635	4.597	4.742	4.722
35	0.946	4.909	4.886	4.903	4.874	4.902	4.885	4.905	4.884	4.911	4.889	4.912	4.886	4.901	4.879	4.891	4.870	4.857	4.838	4.778	4.761	4.726	4.701	5.138	5.072	5.268	5.232
36	0.973	5.810	5.783	5.803	5.768	5.800	5.782	5.805	5.780	5.812	5.786	5.813	5.783	5.800	5.776	5.789	5.765	5.750	5.729	5.661	5.641	5.603	5.575	6.236	6.148	6.178	6.112
37	1.000	6.927	6.845	6.918	6.826	6.914	6.844	6.920	6.842	6.929	6.850	6.931	6.846	6.915	6.837	6.904	6.825	6.858	6.785	6.756	6.684	6.691	6.610	6.607	6.484	6.337	6.336

Table 17. Raw extraction results for K_1 (MPa √m) about a circular crack of radius 0.30 mm

Through thickness location		0.5/0.5		0.55/0.45		0.6/0.4		0.65/0.35		0.7/0.3		0.75/0.25		0.8/0.2		0.85/0.15		0.9/0.1		0.95/0.05		0.97/0.03		0.985/0.015		1/0	
Extraction Number	Normalized Location	Normal (0.5)	Mirror (0.5)	Normal (0.55)	Mirror (0.45)	Normal (0.6)	Mirror (0.4)	Normal (0.65)	Mirror (0.35)	Normal (0.7)	Mirror (0.3)	Normal (0.75)	Mirror (0.25)	Normal (0.8)	Mirror (0.2)	Normal (0.85)	Mirror (0.15)	Normal (0.9)	Mirror (0.1)	Normal (0.95)	Mirror (0.05)	Normal (0.97)	Mirror (0.03)	Normal (0.985)	Mirror (0.015)	Normal (1)	Mirror (0)
0	0.000	6.856	6.938	6.854	6.939	6.855	6.932	6.846	6.934	6.859	6.937	6.859	6.937	6.844	6.931	6.806	6.902	6.753	6.833	6.606	6.683	6.780	6.909	0.000	0.000	2.241	2.238
1	0.027	5.793	5.820	5.791	5.821	5.792	5.815	5.785	5.818	5.795	5.819	5.795	5.819	5.782	5.813	5.749	5.788	5.703	5.729	5.570	5.595	5.723	5.753	4.120	4.117	2.254	2.250
2	0.054	4.896	4.919	4.894	4.920	4.895	4.915	4.890	4.917	4.896	4.918	4.897	4.918	4.884	4.912	4.858	4.890	4.815	4.838	4.696	4.718	4.808	4.834	3.737	3.741	2.381	2.377
3	0.081	4.379	4.395	4.377	4.395	4.378	4.390	4.374	4.393	4.379	4.393	4.379	4.393	4.367	4.387	4.344	4.366	4.304	4.319	4.193	4.207	4.286	4.302	3.499	3.499	2.407	2.401
4	0.108	4.037	4.046	4.035	4.046	4.036	4.042	4.033	4.044	4.036	4.044	4.036	4.044	4.025	4.038	4.004	4.019	3.965	3.974	3.860	3.868	3.939	3.949	3.331	3.330	2.410	2.410
5	0.135	3.785	3.792	3.783	3.791	3.783	3.787	3.781	3.790	3.783	3.789	3.783	3.789	3.772	3.783	3.758	3.765	3.716	3.723	3.615	3.621	3.684	3.692	3.205	3.204	2.419	2.415
6	0.162	3.587	3.592	3.585	3.591	3.585	3.588	3.584	3.590	3.586	3.589	3.586	3.589	3.575	3.583	3.557	3.566	3.521	3.526	3.425	3.429	3.484	3.489	3.110	3.110	2.429	2.426
7	0.189	3.436	3.437	3.433	3.437	3.434	3.433	3.432	3.435	3.434	3.435	3.434	3.434	3.423	3.429	3.406	3.412	3.372	3.374	3.280	3.281	3.330	3.332	3.041	3.033	2.443	2.442
8	0.216	3.309	3.311	3.307	3.310	3.307	3.307	3.306	3.309	3.307	3.308	3.307	3.308	3.297	3.302	3.281	3.286	3.248	3.250	3.161	3.161	3.201	3.203	2.981	2.979	2.459	2.456
9	0.243	3.206	3.207	3.204	3.206	3.204	3.203	3.204	3.205	3.204	3.204	3.204	3.204	3.195	3.198	3.179	3.183	3.147	3.148	3.065	3.064	3.097	3.098	2.937	2.936	2.477	2.475
10	0.270	3.117	3.125	3.115	3.124	3.115	3.121	3.115	3.123	3.115	3.123	3.115	3.122	3.106	3.117	3.092	3.102	3.061	3.069	2.982	2.988	3.008	3.015	2.906	2.906	2.499	2.494
11	0.297	3.049	3.050	3.046	3.049	3.047	3.046	3.046	3.048	3.047	3.048	3.047	3.047	3.038	3.042	3.024	3.028	2.995	2.996	2.920	2.919	2.939	2.940	2.880	2.879	2.522	2.522
12	0.324	2.991	2.993	2.988	2.992	2.989	2.989	2.989	2.992	2.989	2.991	2.989	2.991	2.981	2.986	2.968	2.973	2.940	2.943	2.868	2.869	2.882	2.884	2.863	2.862	2.551	2.540
13	0.351	2.945	2.946	2.943	2.945	2.943	2.943	2.943	2.945	2.943	2.945	2.944	2.944	2.935	2.940	2.923	2.927	2.896	2.898	2.827	2.827	2.837	2.838	2.857	2.854	2.577	2.574
14	0.378	2.908	2.908	2.906	2.908	2.906	2.905	2.906	2.907	2.907	2.907	2.907	2.907	2.899	2.903	2.888	2.891	2.862	2.863	2.795	2.795	2.802	2.802	2.851	2.849	2.610	2.604
15	0.405	2.875	2.878	2.873	2.877	2.873	2.875	2.873	2.877	2.874	2.877	2.875	2.877	2.867	2.873	2.856	2.861	2.831	2.835	2.767	2.769	2.771	2.774	2.852	2.851	2.644	2.640
16	0.432	2.855	2.856	2.853	2.856	2.854	2.853	2.854	2.856	2.855	2.856	2.855	2.856	2.848	2.852	2.837	2.841	2.813	2.815	2.752	2.752	2.753	2.754	2.857	2.860	2.680	2.678
17	0.459	2.842	2.842	2.840	2.841	2.841	2.839	2.841	2.841	2.842	2.841	2.843	2.842	2.836	2.840	2.825	2.827	2.802	2.802	2.743	2.741	2.743	2.741	0.000	2.873	2.720	2.717
18	0.486	2.835	2.833	2.833	2.832	2.834	2.830	2.834	2.832	2.835	2.833	2.836	2.833	2.829	2.829	2.819	2.819	2.797	2.795	2.740	2.736	2.738	2.735	2.893	2.891	2.764	2.764
19	0.514	2.833	2.835	2.831	2.835	2.831	2.832	2.832	2.835	2.833	2.835	2.834	2.836	2.827	2.832	2.818	2.822	2.796	2.799	2.741	2.742	2.738	2.740	2.916	2.916	2.816	2.808
20	0.541	2.842	2.842	2.842	2.842	2.840	2.840	2.841	2.842	2.842	2.843	2.843	2.844	2.836	2.840	2.827	2.830	2.806	2.807	2.753	2.752	2.749	2.749	2.947	0.000	2.865	2.859
21	0.568	2.856	2.855	2.855	2.855	2.855	2.853	2.856	2.855	2.857	2.856	2.858	2.857	2.851	2.853	2.843	2.844	2.822	2.821	2.770	2.768	2.766	2.764	2.983	2.977	2.923	2.916
22	0.595	2.878	2.875	2.876	2.874	2.877	2.872	2.881	2.875	2.879	2.876	2.880	2.877	2.874	2.873	2.865	2.864	2.845	2.842	2.794	2.790	2.789	2.786	3.025	3.022	2.985	2.980
23	0.622	2.908	2.908	2.907	2.908	2.908	2.905	2.908	2.908	2.909	2.909	2.912	2.910	2.904	2.907	2.896	2.897	2.876	2.876	2.827	2.825	2.821	2.820	3.074	3.073	3.051	3.048
24	0.649	2.946	2.945	2.944	2.944	2.945	2.946	2.946	2.945	2.947	2.946	2.949	2.947	2.942	2.944	2.934	2.934	2.914	2.913	2.866	2.863	2.861	2.859	3.133	3.133	3.127	3.121
25	0.676	2.993	2.991	2.991	2.990	2.992	2.988	2.993	2.991	2.994	2.992	2.996	2.994	2.989	2.990	2.981	2.981	2.962	2.959	2.915	2.911	2.909	2.906	3.197	3.195	3.208	3.207
26	0.703	3.050	3.049	3.048	3.048	3.049	3.046	3.050	3.049	3.051	3.050	3.052	3.051	3.045	3.048	3.037	3.039	3.019	3.017	2.972	2.970	2.967	2.965	3.275	3.272	3.306	3.295
27	0.730	3.125	3.117	3.123	3.117	3.124	3.115	3.125	3.118	3.126	3.119	3.128	3.120	3.121	3.117	3.113	3.107	3.094	3.086	3.048	3.039	3.043	3.035	3.367	3.362	3.404	3.399
28	0.757	3.207	3.206	3.205	3.206	3.205	3.203	3.207	3.207	3.208	3.208	3.210	3.209	3.202	3.206	3.194	3.196	3.176	3.175	3.131	3.129	3.126	3.125	3.466	3.462	3.523	3.513
29	0.784	3.311	3.309	3.309	3.309	3.310	3.306	3.311	3.309	3.312	3.310	3.314	3.312	3.306	3.308	3.298	3.299	3.280	3.277	3.235	3.232	3.230	3.228	3.587	3.583	3.657	3.647
30	0.811	3.437	3.436	3.435	3.435	3.436	3.433	3.437	3.436	3.439	3.437	3.440	3.438	3.433	3.435	3.425	3.426	3.406	3.404	3.362	3.359	3.358	3.355	3.726	3.728	3.809	3.801
31	0.838	3.592	3.587	3.590	3.587	3.590	3.584	3.592	3.588	3.593	3.589	3.595	3.590	3.587	3.587	3.579	3.577	3.561	3.555	3.516	3.510	3.512	3.506	3.905	3.894	3.994	3.981
32	0.865	3.792	3.785	3.789	3.785	3.790	3.781	3.791	3.785	3.793	3.786	3.795	3.788	3.787	3.785	3.778	3.775	3.760	3.751	3.715	3.707	3.711	3.703	4.116	4.103	4.216	4.202
33	0.892	4.046	4.037	4.044	4.037	4.044	4.033	4.046	4.037	4.047	4.039	4.049	4.040	4.041	4.043	4.033	4.027	4.014	4.002	3.968	3.958	3.965	3.954	4.387	4.370	4.503	4.476
34	0.919	4.395	4.379	4.392	4.379	4.392	4.375	4.394	4.379	4.396	4.381	4.398	4.382	4.389	4.379	4.381	4.369	4.361	4.342	4.315	4.297	4.312	4.293	4.748	4.722	4.869	4.845
35	0.946	4.919	4.896	4.917	4.896	4.916	4.891	4.919	4.896	4.921	4.898	4.923	4.900	4.913	4.896	4.901	4.886	4.884	4.855	4.835	4.810	4.833	4.806	5.261	5.209	5.406	5.367
36	0.973	5.820	5.793	5.817	5.793	5.816	5.788	5.819	5.793	5.822	5.796	5.825	5.799	5.814	5.795	5.804	5.783	5.782	5.747	5.727	5.699	5.726	5.694	6.383	6.313	6.338	6.267
37	1.000	6.938	6.856	6.934	6.856	6.932	6.850	6.937	6.856	6.940	6.859	6.943	6.863	6.931	6.859	6.920	6.847	6.897	6.804	6.836	6.753	6.835	6.747	6.766	6.655	6.500	6.496

Table 18. Raw extraction results for K_1 (MPa √m) about a circular crack of radius 0.50 mm

Through thickness location		0.5/0.5		0.55/0.45		0.6/0.4		0.65/0.35		0.7/0.3		0.75/0.25		0.8/0.2		0.85/0.15		0.9/0.1		0.95/0.05		0.975/0.025		1/0	
Extraction Number	Normalized Location	Normal (0.5)	Mirror (0.5)	Normal (0.55)	Mirror (0.45)	Normal (0.6)	Mirror (0.4)	Normal (0.65)	Mirror (0.35)	Normal (0.7)	Mirror (0.3)	Normal (0.75)	Mirror (0.25)	Normal (0.8)	Mirror (0.2)	Normal (0.85)	Mirror (0.15)	Normal (0.9)	Mirror (0.1)	Normal (0.95)	Mirror (0.05)	Normal (0.975)	Mirror (0.025)	Normal (1)	Mirror (0)
0	0.000	6.880	6.958	6.874	6.962	6.878	6.959	6.880	6.967	6.881	6.962	6.883	6.961	6.874	6.957	6.850	6.939	6.808	6.885	7.009	7.148	0.000	0.000	2.364	2.362
1	0.027	5.815	5.839	5.810	5.842	5.814	5.840	5.815	5.846	5.815	5.842	5.816	5.840	5.807	5.836	5.786	5.819	5.747	5.769	5.919	5.956	4.314	4.308	2.377	2.372
2	0.054	4.916	4.938	4.913	4.940	4.915	4.938	4.916	4.943	4.915	4.939	4.916	4.937	4.907	4.932	4.888	4.916	4.851	4.871	4.977	5.008	3.912	3.915	2.508	2.504
3	0.081	4.399	4.414	4.396	4.415	4.398	4.413	4.399	4.417	4.398	4.414	4.398	4.412	4.389	4.406	4.371	4.391	4.335	4.348	4.439	4.460	3.663	3.660	2.533	2.527
4	0.108	4.058	4.066	4.055	4.067	4.056	4.065	4.057	4.068	4.056	4.066	4.056	4.063	4.047	4.057	4.029	4.042	3.995	4.001	4.084	4.097	3.486	3.483	2.535	2.535
5	0.135	3.806	3.812	3.803	3.813	3.804	3.811	3.805	3.814	3.803	3.811	3.803	3.809	3.795	3.802	3.777	3.788	3.744	3.748	3.822	3.833	3.354	3.351	2.543	2.539
6	0.162	3.609	3.613	3.606	3.614	3.608	3.612	3.608	3.615	3.606	3.612	3.606	3.609	3.598	3.603	3.581	3.589	3.549	3.551	3.616	3.624	3.254	3.252	2.552	2.549
7	0.189	3.458	3.459	3.455	3.460	3.456	3.458	3.457	3.460	3.455	3.458	3.455	3.455	3.446	3.449	3.431	3.436	3.400	3.399	3.457	3.462	3.180	3.170	2.566	2.560
8	0.216	3.332	3.333	3.329	3.333	3.330	3.332	3.333	3.334	3.329	3.332	3.328	3.329	3.321	3.323	3.305	3.310	3.277	3.276	3.325	3.330	3.117	3.113	2.581	2.578
9	0.243	3.230	3.230	3.227	3.230	3.228	3.228	3.228	3.230	3.227	3.229	3.227	3.226	3.219	3.220	3.205	3.208	3.177	3.175	3.217	3.221	3.069	3.066	2.598	2.596
10	0.270	3.141	3.148	3.139	3.149	3.140	3.147	3.140	3.149	3.138	3.147	3.138	3.145	3.131	3.140	3.118	3.128	3.092	3.097	3.125	3.135	3.036	3.034	2.620	2.615
11	0.297	3.073	3.074	3.071	3.074	3.072	3.072	3.072	3.075	3.071	3.073	3.070	3.071	3.064	3.066	3.051	3.055	3.027	3.025	3.053	3.057	3.008	3.005	2.643	2.643
12	0.324	3.016	3.018	3.013	3.018	3.014	3.017	3.015	3.019	3.014	3.017	3.013	3.015	3.007	3.010	2.995	3.000	2.973	2.973	2.994	2.999	2.989	2.986	2.672	2.665
13	0.351	2.970	2.971	2.968	2.971	2.969	2.970	2.969	2.972	2.968	2.971	2.968	2.969	2.962	2.965	2.951	2.955	2.930	2.929	2.947	2.951	2.981	2.976	2.698	2.695
14	0.378	2.934	2.934	2.931	2.934	2.932	2.933	2.933	2.935	2.932	2.934	2.932	2.933	2.927	2.929	2.916	2.920	2.896	2.895	2.910	2.913	2.973	2.970	2.731	2.725
15	0.405	2.901	2.907	2.898	2.904	2.900	2.903	2.900	2.905	2.899	2.907	2.900	2.903	2.895	2.899	2.885	2.891	2.867	2.867	2.877	2.883	2.974	2.971	2.765	2.761
16	0.432	2.881	2.882	2.879	2.882	2.880	2.881	2.881	2.884	2.880	2.883	2.881	2.882	2.876	2.878	2.867	2.871	2.850	2.848	2.858	2.861	2.977	2.979	2.801	2.799
17	0.459	2.869	2.868	2.867	2.868	2.868	2.867	2.869	2.869	2.868	2.869	2.869	2.868	2.864	2.864	2.856	2.858	2.839	2.836	2.846	2.847	0.000	2.990	2.841	2.838
18	0.486	2.861	2.859	2.859	2.859	2.861	2.858	2.862	2.861	2.861	2.860	2.862	2.860	2.858	2.856	2.853	2.848	2.835	2.830	2.840	2.839	3.012	3.008	2.886	2.886
19	0.514	2.859	2.861	2.857	2.862	2.858	2.861	2.860	2.863	2.859	2.863	2.860	2.863	2.856	2.859	2.849	2.854	2.834	2.834	2.838	2.843	3.034	3.033	2.939	2.929
20	0.541	2.868	2.869	2.866	2.869	2.867	2.868	2.869	2.871	2.868	2.871	2.870	2.870	2.866	2.867	2.859	2.862	2.845	2.843	2.849	2.852	3.064	0.000	2.988	2.982
21	0.568	2.882	2.881	2.880	2.882	2.882	2.881	2.883	2.884	2.883	2.883	2.885	2.883	2.881	2.880	2.874	2.876	2.861	2.858	2.865	2.866	3.101	3.093	3.047	3.039
22	0.595	2.907	2.901	2.902	2.901	2.904	2.900	2.905	2.903	2.905	2.903	2.907	2.903	2.903	2.900	2.897	2.896	2.885	2.879	2.888	2.887	3.142	3.138	3.110	3.104
23	0.622	2.934	2.934	2.932	2.934	2.934	2.933	2.935	2.936	2.935	2.936	2.937	2.936	2.934	2.934	2.928	2.930	2.916	2.913	2.919	2.921	3.192	3.189	3.177	3.172
24	0.649	2.971	2.970	2.969	2.970	2.971	2.970	2.973	2.973	2.972	2.973	2.974	2.973	2.971	2.971	2.966	2.967	2.955	2.951	2.958	2.959	3.251	3.249	3.255	3.247
25	0.676	3.018	3.016	3.016	3.016	3.018	3.015	3.020	3.018	3.019	3.018	3.021	3.019	3.018	3.016	3.013	3.013	3.003	2.998	3.007	3.006	3.315	3.312	3.337	3.334
26	0.703	3.074	3.073	3.072	3.073	3.074	3.073	3.076	3.076	3.075	3.076	3.077	3.076	3.074	3.074	3.069	3.071	3.060	3.056	3.064	3.066	3.393	3.389	3.437	3.423
27	0.730	3.148	3.141	3.146	3.142	3.148	3.141	3.150	3.144	3.150	3.144	3.152	3.145	3.149	3.143	3.145	3.140	3.135	3.126	3.141	3.136	3.486	3.480	3.536	3.530
28	0.757	3.230	3.230	3.228	3.230	3.230	3.229	3.232	3.233	3.231	3.233	3.234	3.233	3.231	3.231	3.226	3.229	3.218	3.215	3.224	3.226	3.587	3.581	3.658	3.646
29	0.784	3.333	3.332	3.331	3.332	3.333	3.331	3.335	3.335	3.334	3.335	3.337	3.336	3.335	3.333	3.330	3.332	3.323	3.318	3.329	3.330	3.709	3.704	3.795	3.783
30	0.811	3.459	3.458	3.457	3.458	3.459	3.457	3.461	3.461	3.460	3.461	3.464	3.462	3.461	3.460	3.457	3.458	3.450	3.445	3.458	3.458	3.851	3.851	3.950	3.940
31	0.838	3.613	3.609	3.611	3.609	3.613	3.608	3.615	3.612	3.614	3.612	3.618	3.613	3.615	3.611	3.611	3.610	3.605	3.597	3.614	3.612	4.032	4.020	4.140	4.124
32	0.865	3.812	3.806	3.809	3.806	3.811	3.804	3.814	3.809	3.812	3.809	3.817	3.810	3.814	3.808	3.811	3.808	3.805	3.795	3.815	3.811	4.246	4.234	4.367	4.350
33	0.892	4.066	4.058	4.063	4.058	4.065	4.056	4.068	4.061	4.066	4.061	4.071	4.062	4.068	4.060	4.066	4.060	4.061	4.048	4.073	4.067	4.523	4.505	4.661	4.631
34	0.919	4.414	4.399	4.410	4.399	4.412	4.397	4.416	4.402	4.414	4.402	4.419	4.404	4.417	4.402	4.415	4.403	4.410	4.390	4.425	4.412	4.890	4.865	5.037	5.010
35	0.946	4.938	4.916	4.934	4.916	4.936	4.913	4.940	4.919	4.938	4.919	4.944	4.921	4.942	4.920	4.940	4.922	4.937	4.909	4.954	4.935	5.414	5.363	5.590	5.545
36	0.973	5.839	5.815	5.835	5.814	5.837	5.811	5.842	5.818	5.839	5.818	5.847	5.821	5.845	5.819	5.844	5.823	5.842	5.809	5.864	5.842	6.563	6.494	6.549	6.471
37	1.000	6.958	6.880	6.953	6.879	6.955	6.874	6.961	6.883	6.958	6.884	6.969	6.888	6.967	6.886	6.967	6.892	6.967	6.878	6.996	6.919	6.953	6.844	6.714	6.705

Table 19. Raw extraction results for K_1 (MPa √m) about a circular crack of radius 1.00 mm

Through thickness location		0.5/0.5		0.55/0.45		0.6/0.4		0.65/0.35		0.7/0.3		0.75/0.25		0.8/0.2		0.85/0.15		0.9/0.1		0.95/0.05		1/0	
Extraction Number	Normalized Location	Normal (0.5)	Mirror (0.5)	Normal (0.55)	Mirror (0.45)	Normal (0.6)	Mirror (0.4)	Normal (0.65)	Mirror (0.35)	Normal (0.7)	Mirror (0.3)	Normal (0.75)	Mirror (0.25)	Normal (0.8)	Mirror (0.2)	Normal (0.85)	Mirror (0.15)	Normal (0.9)	Mirror (0.1)	Normal (0.95)	Mirror (0.05)	Normal (1)	Mirror (0)
0	0.000	6.927	7.009	6.924	7.009	6.932	7.016	6.940	7.027	6.957	7.035	6.967	7.046	6.984	7.057	7.022	7.104	7.332	7.473	0.000	0.000	2.578	2.578
1	0.027	5.860	5.887	5.858	5.887	5.864	5.893	5.870	5.901	5.884	5.907	5.891	5.915	5.902	5.921	5.929	5.955	6.201	6.236	4.634	4.625	2.587	2.585
2	0.054	4.962	4.985	4.959	4.985	4.964	4.986	4.968	4.995	4.978	4.999	4.983	5.004	4.990	5.008	5.008	5.031	5.223	5.253	4.201	4.204	2.726	2.724
3	0.081	4.446	4.462	4.444	4.462	4.448	4.465	4.451	4.475	4.459	4.473	4.462	4.476	4.467	4.477	4.479	4.494	4.667	4.687	3.931	3.929	2.747	2.743
4	0.108	4.107	4.116	4.105	4.115	4.108	4.118	4.110	4.122	4.117	4.124	4.119	4.127	4.122	4.127	4.132	4.140	4.300	4.312	3.740	3.737	2.746	2.749
5	0.135	3.857	3.864	3.861	3.863	3.857	3.865	3.859	3.869	3.865	3.870	3.867	3.872	3.869	3.872	3.877	3.883	4.029	4.039	3.596	3.593	2.752	2.749
6	0.162	3.662	3.667	3.660	3.666	3.662	3.668	3.664	3.671	3.669	3.672	3.670	3.674	3.672	3.673	3.679	3.683	3.817	3.824	3.487	3.485	2.758	2.757
7	0.189	3.513	3.515	3.511	3.514	3.513	3.516	3.514	3.518	3.519	3.520	3.520	3.521	3.522	3.520	3.528	3.529	3.653	3.657	3.406	3.395	2.769	2.766
8	0.216	3.389	3.391	3.387	3.390	3.389	3.391	3.390	3.394	3.394	3.395	3.395	3.396	3.397	3.396	3.404	3.405	3.515	3.519	3.337	3.332	2.782	2.782
9	0.243	3.289	3.289	3.287	3.288	3.288	3.289	3.290	3.292	3.293	3.293	3.295	3.294	3.297	3.294	3.303	3.303	3.404	3.406	3.283	3.280	2.798	2.798
10	0.270	3.202	3.209	3.200	3.209	3.201	3.210	3.203	3.212	3.206	3.213	3.208	3.215	3.210	3.215	3.217	3.224	3.307	3.316	3.245	3.243	2.818	2.816
11	0.297	3.135	3.136	3.133	3.135	3.135	3.136	3.136	3.139	3.140	3.140	3.142	3.142	3.144	3.143	3.151	3.151	3.232	3.235	3.213	3.209	2.839	2.842
12	0.324	3.079	3.081	3.077	3.081	3.078	3.082	3.080	3.084	3.084	3.086	3.086	3.088	3.089	3.089	3.096	3.097	3.169	3.173	3.190	3.186	2.867	2.862
13	0.351	3.034	3.036	3.033	3.035	3.034	3.036	3.036	3.039	3.040	3.040	3.042	3.043	3.045	3.044	3.052	3.053	3.119	3.122	3.179	3.173	2.892	2.891
14	0.378	2.999	2.999	2.997	2.999	2.999	3.000	3.000	3.002	3.004	3.004	3.007	3.007	3.010	3.009	3.018	3.017	3.079	3.081	3.168	3.164	2.923	2.920
15	0.405	2.967	2.970	2.965	2.970	2.967	2.971	2.968	2.973	2.972	2.975	2.975	2.978	2.979	2.980	2.986	2.989	3.043	3.048	3.165	3.162	2.957	2.955
16	0.432	2.948	2.949	2.947	2.949	2.948	2.950	2.950	2.952	2.954	2.955	2.957	2.957	2.961	2.960	2.969	2.969	3.022	3.024	3.166	3.167	2.991	2.992
17	0.459	2.935	2.935	2.934	2.934	2.936	2.936	2.938	2.938	2.942	2.941	2.945	2.944	2.949	2.947	2.957	2.956	3.007	3.007	0.000	3.176	3.031	3.030
18	0.486	2.928	2.926	2.928	2.926	2.929	2.927	2.931	2.930	2.935	2.932	2.939	2.935	2.943	2.939	2.951	2.948	2.998	2.996	3.196	3.191	3.075	3.077
19	0.514	2.926	2.928	2.925	2.928	2.926	2.930	2.928	2.932	2.933	2.935	2.937	2.939	2.941	2.942	2.950	2.952	2.994	2.998	3.216	3.214	3.127	3.120
20	0.541	2.935	2.935	2.934	2.935	2.935	2.937	2.937	2.939	2.942	2.942	2.946	2.946	2.951	2.950	2.959	2.960	3.002	3.004	3.244	0.000	3.176	3.172
21	0.568	2.949	2.948	2.948	2.948	2.949	2.949	2.952	2.952	2.956	2.955	2.961	2.959	2.966	2.963	2.975	2.973	3.016	3.016	3.278	3.270	3.234	3.229
22	0.595	2.970	2.967	2.969	2.967	2.971	2.968	2.973	2.971	2.978	2.974	2.982	2.978	2.987	2.982	2.997	2.993	3.037	3.034	3.318	3.314	3.297	3.294
23	0.622	2.999	2.999	2.999	2.999	3.000	3.000	3.002	3.003	3.007	3.006	3.012	3.011	3.018	3.015	3.027	3.026	3.067	3.067	3.366	3.362	3.363	3.362
24	0.649	3.036	3.034	3.035	3.034	3.036	3.036	3.039	3.039	3.044	3.042	3.049	3.046	3.055	3.052	3.065	3.062	3.103	3.103	3.424	3.422	3.442	3.437
25	0.676	3.081	3.079	3.081	3.079	3.082	3.080	3.085	3.083	3.089	3.087	3.095	3.091	3.101	3.097	3.111	3.108	3.150	3.148	3.487	3.483	3.524	3.525
26	0.703	3.136	3.135	3.135	3.135	3.137	3.136	3.139	3.140	3.144	3.143	3.150	3.148	3.156	3.154	3.167	3.165	3.206	3.205	3.565	3.559	3.625	3.615
27	0.730	3.209	3.202	3.209	3.202	3.210	3.203	3.213	3.206	3.218	3.210	3.224	3.215	3.231	3.221	3.242	3.234	3.281	3.273	3.657	3.650	3.725	3.722
28	0.757	3.289	3.289	3.288	3.288	3.289	3.290	3.292	3.293	3.298	3.297	3.303	3.303	3.311	3.309	3.323	3.322	3.362	3.362	3.757	3.750	3.848	3.839
29	0.784	3.391	3.389	3.390	3.389	3.391	3.390	3.394	3.394	3.400	3.397	3.406	3.403	3.414	3.410	3.426	3.424	3.466	3.465	3.879	3.873	3.987	3.978
30	0.811	3.515	3.513	3.514	3.513	3.515	3.514	3.518	3.518	3.524	3.522	3.531	3.528	3.539	3.535	3.552	3.550	3.593	3.592	4.021	4.021	4.144	4.138
31	0.838	3.667	3.662	3.666	3.662	3.667	3.663	3.670	3.667	3.676	3.671	3.684	3.678	3.692	3.686	3.706	3.701	3.749	3.744	4.203	4.190	4.337	4.325
32	0.865	3.864	3.857	3.863	3.856	3.864	3.858	3.867	3.862	3.873	3.866	3.881	3.873	3.891	3.882	3.906	3.898	3.950	3.943	4.420	4.405	4.568	4.556
33	0.892	4.116	4.107	4.115	4.106	4.115	4.107	4.119	4.112	4.125	4.116	4.134	4.124	4.144	4.133	4.161	4.151	4.207	4.199	4.700	4.680	4.870	4.843
34	0.919	4.462	4.446	4.460	4.445	4.461	4.446	4.464	4.451	4.471	4.455	4.482	4.464	4.493	4.474	4.511	4.495	4.561	4.546	5.073	5.045	5.255	5.232
35	0.946	4.985	4.962	4.983	4.959	4.983	4.960	4.987	4.966	4.994	4.970	5.007	4.981	5.019	4.993	5.040	5.016	5.096	5.073	5.607	5.551	5.823	5.782
36	0.973	5.887	5.860	5.884	5.857	5.894	5.858	5.888	5.865	5.897	5.869	5.912	5.883	5.927	5.897	5.953	5.926	6.018	5.991	6.784	6.709	6.812	6.739
37	1.000	7.009	6.927	7.005	6.922	7.001	6.923	7.009	6.932	7.020	6.937	7.039	6.954	7.057	6.971	7.089	7.006	7.166	7.083	7.179	7.061	6.978	6.975

Table 20. Processed extraction results for K_1 (MPa √m) about a circular crack of radius 0.08 mm

Through thickness location		0.5/0.5	0.55/0.45	0.6/0.4	0.65/0.35	0.7/0.3	0.75/0.25	0.8/0.2	0.85/0.15	0.9/0.1	0.95/0.05	0.992/0.008	0.996/0.004	1/0
Extraction Number	Normalized Location	Average	Average	Average	Average	Average	Average	Average	Average	Average	Average	Average	Average	Average
0	0.000	6.854	6.848	6.852	6.851	6.851	6.863	6.844	6.820	6.761	6.581	6.247	6.448	1.996
1	0.027	5.770	5.764	5.768	5.767	5.767	5.777	5.761	5.740	5.690	5.537	5.233	3.707	2.008
2	0.054	4.874	4.869	4.872	4.870	4.871	4.878	4.866	4.848	4.805	4.675	4.393	3.366	2.124
3	0.081	4.355	4.350	4.353	4.352	4.352	4.359	4.347	4.331	4.291	4.175	3.910	3.151	2.149
4	0.108	4.010	4.006	4.008	4.008	4.007	4.014	4.002	3.989	3.952	3.844	3.589	3.000	2.157
5	0.135	3.756	3.752	3.755	3.754	3.754	3.760	3.749	3.735	3.701	3.600	3.353	2.888	2.164
6	0.162	3.558	3.554	3.556	3.555	3.555	3.561	3.550	3.539	3.505	3.409	3.169	2.804	2.175
7	0.189	3.404	3.401	3.403	3.402	3.402	3.407	3.397	3.385	3.354	3.262	3.026	2.738	2.188
8	0.216	3.277	3.274	3.276	3.276	3.275	3.280	3.270	3.258	3.229	3.144	2.908	2.688	2.205
9	0.243	3.173	3.170	3.172	3.171	3.172	3.176	3.166	3.155	3.129	3.042	2.812	2.650	2.223
10	0.270	3.088	3.085	3.086	3.086	3.086	3.090	3.081	3.070	3.043	2.962	2.734	2.623	2.243
11	0.297	3.015	3.012	3.014	3.014	3.014	3.018	3.008	2.999	2.972	2.893	2.668	2.601	2.267
12	0.324	2.958	2.955	2.957	2.956	2.957	2.961	2.952	2.942	2.916	2.839	2.617	2.587	2.292
13	0.351	2.911	2.909	2.910	2.910	2.910	2.914	2.906	2.896	2.870	2.795	2.577	2.582	2.319
14	0.378	2.874	2.871	2.873	2.872	2.873	2.877	2.869	2.859	2.834	2.761	2.545	2.578	2.349
15	0.405	2.842	2.839	2.842	2.840	2.841	2.841	2.837	2.828	2.803	2.731	2.519	2.581	2.382
16	0.432	2.822	2.818	2.821	2.820	2.821	2.824	2.817	2.807	2.783	2.713	2.503	2.589	2.417
17	0.459	2.807	2.805	2.807	2.806	2.807	2.810	2.803	2.794	2.770	2.701	2.494	2.603	2.454
18	0.486	2.799	2.797	2.797	2.798	2.799	2.802	2.795	2.785	2.764	2.694	2.490	2.622	2.497
19	0.514	2.799	2.797	2.797	2.798	2.798	2.803	2.795	2.787	2.763	2.695	2.492	2.646	2.542
20	0.541	2.807	2.805	2.806	2.806	2.807	2.811	2.804	2.795	2.772	2.705	2.504	2.676	2.589
21	0.568	2.822	2.819	2.822	2.820	2.823	2.825	2.819	2.809	2.786	2.720	2.520	2.708	2.643
22	0.595	2.842	2.840	2.843	2.842	2.842	2.846	2.835	2.830	2.807	2.740	2.544	2.749	2.701
23	0.622	2.874	2.872	2.873	2.873	2.874	2.878	2.870	2.862	2.838	2.771	2.575	2.796	2.764
24	0.649	2.911	2.909	2.911	2.912	2.912	2.915	2.908	2.899	2.876	2.808	2.612	2.852	2.833
25	0.676	2.958	2.956	2.958	2.957	2.958	2.962	2.955	2.946	2.922	2.854	2.658	2.912	2.912
26	0.703	3.015	3.013	3.015	3.014	3.016	3.020	3.012	3.003	2.979	2.908	2.714	2.985	2.998
27	0.730	3.088	3.085	3.087	3.086	3.088	3.092	3.084	3.075	3.050	2.980	2.784	3.070	3.092
28	0.757	3.173	3.171	3.175	3.172	3.174	3.178	3.170	3.160	3.135	3.063	2.865	3.164	3.201
29	0.784	3.277	3.275	3.276	3.276	3.277	3.281	3.273	3.263	3.238	3.165	2.963	3.277	3.325
30	0.811	3.404	3.402	3.403	3.403	3.404	3.409	3.400	3.389	3.363	3.287	3.082	3.410	3.467
31	0.838	3.558	3.555	3.559	3.556	3.559	3.562	3.553	3.544	3.514	3.436	3.227	3.571	3.636
32	0.865	3.756	3.754	3.755	3.755	3.756	3.761	3.752	3.740	3.710	3.629	3.413	3.766	3.843
33	0.892	4.010	4.007	4.009	4.008	4.010	4.015	4.005	3.993	3.961	3.875	3.649	4.017	4.100
34	0.919	4.355	4.352	4.353	4.353	4.357	4.360	4.349	4.336	4.301	4.209	3.971	4.348	4.440
35	0.946	4.874	4.871	4.873	4.872	4.873	4.880	4.868	4.853	4.815	4.713	4.453	4.811	4.928
36	0.973	5.770	5.767	5.768	5.768	5.769	5.777	5.763	5.746	5.701	5.583	5.284	5.840	5.771
37	1.000	6.854	6.851	6.853	6.852	6.854	6.863	6.847	6.827	6.774	6.636	6.291	6.175	5.951

Table 21. Processed extraction results for K_1 (MPa √m) about a circular crack of radius 0.10 mm

Through thickness location		0.5/0.5	0.55/0.45	0.6/0.4	0.65/0.35	0.7/0.3	0.75/0.25	0.8/0.2	0.85/0.15	0.9/0.1	0.95/0.05	0.99/0.01	0.995/0.005	1/0
Extraction Number	Normalized Location	Average	Average	Average	Average	Average	Average	Average	Average	Average	Average	Average	Average	Average
0	0.000	6.861	6.858	6.861	6.857	6.864	6.865	6.852	6.827	6.766	6.585	6.346	#N/A	2.029
1	0.027	5.776	5.773	5.775	5.772	5.778	5.779	5.768	5.746	5.694	5.541	5.316	3.769	2.042
2	0.054	4.879	4.877	4.878	4.876	4.880	4.881	4.872	4.853	4.808	4.678	4.463	3.422	2.162
3	0.081	4.359	4.357	4.358	4.356	4.360	4.361	4.353	4.336	4.295	4.177	3.972	3.203	2.185
4	0.108	4.014	4.012	4.014	4.011	4.015	4.015	4.008	3.992	3.956	3.845	3.646	3.050	2.192
5	0.135	3.761	3.759	3.762	3.758	3.761	3.761	3.754	3.742	3.704	3.601	3.407	2.935	2.199
6	0.162	3.562	3.561	3.561	3.559	3.562	3.562	3.557	3.542	3.508	3.411	3.219	2.850	2.210
7	0.189	3.408	3.406	3.407	3.405	3.408	3.409	3.402	3.392	3.356	3.264	3.074	2.783	2.224
8	0.216	3.281	3.279	3.283	3.278	3.281	3.282	3.275	3.263	3.231	3.142	2.957	2.732	2.241
9	0.243	3.177	3.176	3.177	3.175	3.180	3.178	3.174	3.160	3.129	3.044	2.857	2.693	2.259
10	0.270	3.092	3.089	3.091	3.089	3.092	3.092	3.086	3.075	3.045	2.963	2.777	2.666	2.279
11	0.297	3.019	3.018	3.019	3.017	3.019	3.020	3.014	3.003	2.975	2.895	2.711	2.643	2.303
12	0.324	2.962	2.960	2.961	2.960	2.962	2.963	2.957	2.947	2.919	2.841	2.659	2.628	2.328
13	0.351	2.915	2.913	2.914	2.913	2.915	2.916	2.911	2.900	2.873	2.798	2.618	2.623	2.356
14	0.378	2.878	2.876	2.877	2.876	2.878	2.879	2.874	2.864	2.837	2.764	2.586	2.620	2.386
15	0.405	2.846	2.844	2.845	2.844	2.846	2.847	2.842	2.828	2.807	2.735	2.559	2.622	2.420
16	0.432	2.825	2.823	2.824	2.823	2.826	2.826	2.822	2.812	2.787	2.716	2.543	2.630	2.455
17	0.459	2.811	2.809	2.811	2.809	2.812	2.813	2.808	2.799	2.774	2.705	2.533	2.643	2.492
18	0.486	2.803	2.800	2.803	2.801	2.804	2.804	2.802	2.791	2.767	2.698	2.529	2.664	2.536
19	0.514	2.803	2.801	2.803	2.802	2.804	2.805	2.800	2.792	2.769	2.700	2.532	2.687	2.581
20	0.541	2.811	2.810	2.811	2.810	2.813	2.813	2.809	2.801	2.776	2.709	2.543	2.718	2.629
21	0.568	2.825	2.823	2.826	2.824	2.826	2.827	2.823	2.814	2.790	2.724	2.560	2.750	2.684
22	0.595	2.846	2.844	2.846	2.846	2.843	2.845	2.844	2.835	2.811	2.745	2.582	2.791	2.743
23	0.622	2.878	2.876	2.878	2.877	2.879	2.880	2.876	2.867	2.843	2.776	2.615	2.839	2.806
24	0.649	2.915	2.914	2.915	2.914	2.917	2.917	2.914	2.904	2.880	2.814	2.653	2.896	2.877
25	0.676	2.962	2.960	2.962	2.961	2.963	2.964	2.960	2.951	2.927	2.860	2.699	2.956	2.956
26	0.703	3.019	3.018	3.019	3.018	3.021	3.022	3.018	3.008	2.983	2.916	2.755	3.030	3.044
27	0.730	3.092	3.090	3.092	3.090	3.093	3.094	3.090	3.080	3.055	2.986	2.825	3.116	3.139
28	0.757	3.177	3.176	3.177	3.178	3.179	3.180	3.176	3.166	3.140	3.070	2.908	3.211	3.249
29	0.784	3.281	3.279	3.281	3.280	3.282	3.283	3.279	3.269	3.242	3.171	3.007	3.326	3.375
30	0.811	3.408	3.406	3.408	3.406	3.409	3.410	3.406	3.395	3.371	3.295	3.128	3.460	3.519
31	0.838	3.562	3.560	3.562	3.560	3.563	3.564	3.559	3.548	3.520	3.446	3.275	3.623	3.691
32	0.865	3.761	3.758	3.760	3.759	3.764	3.762	3.761	3.746	3.717	3.638	3.463	3.821	3.898
33	0.892	4.014	4.012	4.014	4.012	4.015	4.016	4.011	3.999	3.968	3.885	3.703	4.075	4.163
34	0.919	4.359	4.356	4.359	4.357	4.360	4.361	4.356	4.343	4.309	4.220	4.029	4.411	4.506
35	0.946	4.879	4.876	4.879	4.876	4.880	4.881	4.875	4.861	4.824	4.726	4.518	4.881	5.000
36	0.973	5.776	5.772	5.776	5.772	5.776	5.778	5.771	5.755	5.712	5.598	5.360	5.923	5.855
37	1.000	6.861	6.857	6.862	6.857	6.862	6.864	6.857	6.837	6.788	6.655	6.381	6.263	6.039

Table 22. Processed extraction results for K_1 (MPa √m) about a circular crack of radius 0.20 mm

Through thickness location		0.5/0.5	0.55/0.45	0.6/0.4	0.65/0.35	0.7/0.3	0.75/0.25	0.8/0.2	0.85/0.15	0.9/0.1	0.95/0.05	0.98/0.02	0.99/0.01	1/0
Extraction Number	Normalized Location	Average	Average	Average	Average	Average	Average	Average	Average	Average	Average	Average	Average	Average
0	0.000	6.886	6.874	6.886	6.884	8.292	6.889	6.870	6.847	6.773	6.584	6.657	#N/A	2.158
1	0.027	5.797	5.787	5.797	5.795	5.567	5.799	5.783	5.763	5.700	5.537	5.580	3.982	2.170
2	0.054	4.898	4.890	4.898	4.896	4.898	4.899	4.885	4.868	4.814	4.673	4.686	3.616	2.293
3	0.081	4.377	4.370	4.376	4.375	4.377	4.377	4.365	4.349	4.300	4.172	4.172	3.384	2.319
4	0.108	4.031	4.025	4.031	4.030	4.031	4.031	4.020	4.004	3.959	3.842	3.831	3.222	2.326
5	0.135	3.777	3.772	3.777	3.776	3.777	3.777	3.766	3.752	3.709	3.597	3.581	3.100	2.333
6	0.162	3.579	3.573	3.578	3.577	3.578	3.578	3.567	3.554	3.514	3.407	3.385	3.009	2.344
7	0.189	3.425	3.420	3.424	3.423	3.424	3.424	3.414	3.401	3.363	3.261	3.233	2.938	2.358
8	0.216	3.298	3.293	3.297	3.296	3.297	3.297	3.287	3.275	3.238	3.142	3.107	2.884	2.375
9	0.243	3.194	3.189	3.193	3.192	3.193	3.193	3.184	3.172	3.137	3.044	3.005	2.842	2.393
10	0.270	3.109	3.104	3.107	3.107	3.108	3.108	3.099	3.087	3.054	2.964	2.921	2.813	2.414
11	0.297	3.036	3.033	3.035	3.034	3.034	3.035	3.027	3.016	2.984	2.898	2.852	2.788	2.439
12	0.324	2.979	2.975	2.978	2.977	2.978	2.978	2.970	2.961	2.928	2.846	2.797	2.772	2.465
13	0.351	2.932	2.928	2.931	2.931	2.932	2.932	2.924	2.914	2.886	2.804	2.753	2.766	2.493
14	0.378	2.895	2.892	2.894	2.893	2.895	2.895	2.888	2.878	2.848	2.771	2.720	2.762	2.524
15	0.405	2.863	2.859	2.862	2.862	2.863	2.863	2.856	2.847	2.818	2.744	2.691	2.764	2.558
16	0.432	2.842	2.838	2.841	2.841	2.843	2.843	2.836	2.827	2.799	2.727	2.674	2.772	2.595
17	0.459	2.828	2.824	2.828	2.828	2.829	2.829	2.823	2.814	2.787	2.716	2.662	2.783	2.633
18	0.486	2.820	2.816	2.820	2.819	2.821	2.821	2.815	2.806	2.780	2.711	2.657	2.805	2.679
19	0.514	2.820	2.816	2.821	2.819	2.821	2.821	2.815	2.807	2.781	2.714	2.660	2.829	2.726
20	0.541	2.828	2.824	2.828	2.828	2.830	2.830	2.824	2.816	2.790	2.724	2.671	2.862	2.774
21	0.568	2.842	2.838	2.842	2.842	2.844	2.844	2.838	2.830	2.805	2.740	2.687	2.889	2.833
22	0.595	2.863	2.859	2.862	2.862	2.865	2.865	2.855	2.851	2.826	2.762	2.710	2.938	2.894
23	0.622	2.895	2.891	2.894	2.894	2.897	2.897	2.891	2.883	2.858	2.795	2.743	2.986	2.960
24	0.649	2.932	2.928	2.932	2.932	2.934	2.936	2.929	2.921	2.896	2.833	2.782	3.044	3.033
25	0.676	2.979	2.975	2.978	2.979	2.981	2.981	2.975	2.967	2.943	2.881	2.830	3.107	3.115
26	0.703	3.036	3.032	3.036	3.036	3.038	3.039	3.033	3.025	3.000	2.938	2.888	3.182	3.207
27	0.730	3.109	3.104	3.108	3.108	3.110	3.111	3.105	3.097	3.072	3.010	2.960	3.272	3.306
28	0.757	3.194	3.189	3.193	3.193	3.196	3.196	3.190	3.182	3.157	3.095	3.045	3.370	3.421
29	0.784	3.298	3.293	3.297	3.297	3.300	3.300	3.294	3.286	3.260	3.197	3.148	3.489	3.552
30	0.811	3.425	3.420	3.427	3.424	3.427	3.427	3.420	3.412	3.386	3.322	3.273	3.628	3.702
31	0.838	3.579	3.573	3.577	3.577	3.580	3.580	3.575	3.565	3.538	3.474	3.424	3.797	3.881
32	0.865	3.777	3.771	3.775	3.776	3.779	3.779	3.772	3.763	3.736	3.669	3.619	4.003	4.098
33	0.892	4.031	4.026	4.029	4.029	4.033	4.033	4.025	4.017	3.988	3.919	3.868	4.267	4.372
34	0.919	4.377	4.369	4.374	4.374	4.379	4.378	4.370	4.361	4.331	4.258	4.206	4.616	4.732
35	0.946	4.898	4.889	4.894	4.895	4.900	4.899	4.890	4.881	4.848	4.770	4.714	5.105	5.250
36	0.973	5.797	5.785	5.791	5.792	5.799	5.798	5.788	5.777	5.740	5.651	5.589	6.192	6.145
37	1.000	6.886	6.872	6.879	6.881	6.890	6.888	6.876	6.865	6.821	6.720	6.651	6.546	6.337

Table 23. Processed extraction results for K_1 (MPa √m) about a circular crack of radius 0.30 mm

Through thickness location		0.5/0.5	0.55/0.45	0.6/0.4	0.65/0.35	0.7/0.3	0.75/0.25	0.8/0.2	0.85/0.15	0.9/0.1	0.95/0.05	0.97/0.03	0.985/0.015	1/0
Extraction Number	Normalized Location	Average	Average	Average	Average	Average	Average	Average	Average	Average	Average	Average	Average	Average
0	0.000	6.897	6.897	6.894	6.890	6.898	6.898	6.887	6.854	6.793	6.644	6.844	#N/A	2.240
1	0.027	5.807	5.806	5.804	5.801	5.807	5.807	5.797	5.769	5.716	5.582	5.738	4.118	2.252
2	0.054	4.908	4.907	4.905	4.903	4.907	4.907	4.898	4.874	4.827	4.707	4.821	3.739	2.379
3	0.081	4.387	4.386	4.384	4.383	4.386	4.386	4.377	4.355	4.311	4.200	4.294	3.499	2.404
4	0.108	4.042	4.041	4.039	4.039	4.040	4.040	4.031	4.011	3.970	3.864	3.944	3.331	2.410
5	0.135	3.788	3.787	3.785	3.785	3.786	3.786	3.778	3.762	3.719	3.618	3.688	3.205	2.417
6	0.162	3.590	3.588	3.587	3.587	3.588	3.587	3.579	3.561	3.523	3.427	3.487	3.110	2.427
7	0.189	3.436	3.435	3.433	3.434	3.434	3.434	3.426	3.409	3.373	3.281	3.331	3.037	2.442
8	0.216	3.310	3.308	3.307	3.307	3.308	3.307	3.299	3.283	3.249	3.161	3.202	2.980	2.457
9	0.243	3.206	3.205	3.203	3.204	3.204	3.204	3.196	3.181	3.148	3.064	3.098	2.936	2.476
10	0.270	3.121	3.119	3.118	3.119	3.119	3.119	3.111	3.097	3.065	2.985	3.012	2.906	2.497
11	0.297	3.049	3.047	3.046	3.047	3.047	3.047	3.040	3.026	2.996	2.919	2.940	2.879	2.522
12	0.324	2.992	2.990	2.989	2.990	2.990	2.990	2.983	2.970	2.941	2.868	2.883	2.862	2.546
13	0.351	2.945	2.944	2.943	2.944	2.944	2.944	2.938	2.925	2.897	2.827	2.838	2.855	2.576
14	0.378	2.908	2.907	2.906	2.907	2.907	2.907	2.901	2.889	2.862	2.795	2.802	2.850	2.607
15	0.405	2.876	2.875	2.874	2.875	2.876	2.876	2.870	2.859	2.833	2.768	2.772	2.852	2.642
16	0.432	2.856	2.854	2.853	2.855	2.855	2.856	2.850	2.839	2.814	2.752	2.754	2.859	2.679
17	0.459	2.842	2.841	2.840	2.841	2.842	2.842	2.838	2.826	2.802	2.742	2.742	2.873	2.719
18	0.486	2.834	2.833	2.832	2.833	2.834	2.835	2.829	2.819	2.796	2.738	2.736	2.892	2.764
19	0.514	2.834	2.833	2.832	2.834	2.834	2.835	2.830	2.820	2.797	2.741	2.739	2.916	2.812
20	0.541	2.842	2.842	2.840	2.842	2.842	2.843	2.838	2.829	2.807	2.753	2.749	2.947	2.862
21	0.568	2.856	2.855	2.854	2.856	2.856	2.857	2.852	2.843	2.822	2.769	2.765	2.980	2.920
22	0.595	2.876	2.875	2.875	2.878	2.877	2.878	2.873	2.864	2.843	2.792	2.787	3.023	2.982
23	0.622	2.908	2.907	2.906	2.908	2.909	2.911	2.905	2.897	2.876	2.826	2.821	3.074	3.049
24	0.649	2.945	2.944	2.946	2.946	2.946	2.948	2.943	2.934	2.914	2.865	2.860	3.133	3.124
25	0.676	2.992	2.991	2.990	2.992	2.993	2.995	2.989	2.981	2.961	2.913	2.908	3.196	3.208
26	0.703	3.049	3.048	3.047	3.049	3.050	3.052	3.047	3.038	3.018	2.971	2.966	3.273	3.300
27	0.730	3.121	3.120	3.119	3.121	3.122	3.124	3.119	3.110	3.090	3.044	3.039	3.364	3.401
28	0.757	3.206	3.205	3.204	3.207	3.208	3.209	3.204	3.195	3.175	3.130	3.125	3.464	3.518
29	0.784	3.310	3.309	3.308	3.310	3.311	3.313	3.307	3.299	3.279	3.234	3.229	3.585	3.652
30	0.811	3.436	3.435	3.434	3.437	3.438	3.439	3.434	3.425	3.405	3.360	3.356	3.727	3.805
31	0.838	3.590	3.589	3.587	3.590	3.591	3.593	3.587	3.578	3.558	3.513	3.509	3.899	3.988
32	0.865	3.788	3.787	3.786	3.788	3.789	3.791	3.786	3.777	3.756	3.711	3.707	4.109	4.209
33	0.892	4.042	4.041	4.039	4.041	4.043	4.045	4.042	4.030	4.008	3.963	3.960	4.378	4.489
34	0.919	4.387	4.386	4.383	4.386	4.388	4.390	4.384	4.375	4.351	4.306	4.303	4.735	4.857
35	0.946	4.908	4.906	4.903	4.907	4.909	4.911	4.905	4.893	4.870	4.822	4.819	5.235	5.387
36	0.973	5.807	5.805	5.802	5.806	5.809	5.812	5.804	5.793	5.764	5.713	5.710	6.348	6.302
37	1.000	6.897	6.895	6.891	6.896	6.900	6.903	6.895	6.883	6.850	6.795	6.791	6.710	6.498

Table 24. Processed extraction results for K_1 (MPa √m) about a circular crack of radius 0.50 mm

Through thickness location		0.5/0.5	0.55/0.45	0.6/0.4	0.65/0.35	0.7/0.3	0.75/0.25	0.8/0.2	0.85/0.15	0.9/0.1	0.95/0.05	0.975/0.025	1/0
Extraction Number	Normalized Location	Average	Average	Average	Average	Average	Average	Average	Average	Average	Average	Average	Average
0	0.000	6.919	6.918	6.919	6.923	6.921	6.922	6.915	6.894	6.847	7.078	#N/A	2.363
1	0.027	5.827	5.826	5.827	5.831	5.828	5.828	5.821	5.802	5.758	5.937	4.311	2.374
2	0.054	4.927	4.926	4.926	4.929	4.927	4.927	4.920	4.902	4.861	4.993	3.914	2.506
3	0.081	4.406	4.405	4.406	4.408	4.406	4.405	4.398	4.381	4.341	4.450	3.662	2.530
4	0.108	4.062	4.061	4.061	4.063	4.061	4.059	4.052	4.036	3.998	4.090	3.485	2.535
5	0.135	3.809	3.808	3.808	3.809	3.807	3.806	3.798	3.782	3.746	3.827	3.352	2.541
6	0.162	3.611	3.610	3.610	3.611	3.609	3.608	3.600	3.585	3.550	3.620	3.253	2.550
7	0.189	3.459	3.457	3.457	3.458	3.457	3.455	3.448	3.433	3.400	3.460	3.175	2.563
8	0.216	3.332	3.331	3.331	3.333	3.330	3.329	3.322	3.308	3.276	3.327	3.115	2.579
9	0.243	3.230	3.228	3.228	3.229	3.228	3.226	3.220	3.206	3.176	3.219	3.068	2.597
10	0.270	3.145	3.144	3.143	3.145	3.143	3.142	3.135	3.123	3.095	3.130	3.035	2.618
11	0.297	3.073	3.072	3.072	3.073	3.072	3.071	3.065	3.053	3.026	3.055	3.006	2.643
12	0.324	3.017	3.016	3.015	3.017	3.016	3.014	3.009	2.998	2.973	2.996	2.987	2.668
13	0.351	2.971	2.969	2.969	2.971	2.970	2.969	2.964	2.953	2.930	2.949	2.979	2.696
14	0.378	2.934	2.933	2.933	2.934	2.933	2.933	2.928	2.918	2.896	2.911	2.972	2.728
15	0.405	2.904	2.901	2.901	2.903	2.903	2.902	2.897	2.888	2.867	2.880	2.972	2.763
16	0.432	2.882	2.881	2.881	2.883	2.882	2.882	2.877	2.869	2.849	2.860	2.978	2.800
17	0.459	2.868	2.867	2.867	2.869	2.868	2.868	2.864	2.857	2.838	2.847	2.990	2.840
18	0.486	2.860	2.859	2.859	2.861	2.861	2.861	2.857	2.850	2.832	2.840	3.010	2.886
19	0.514	2.860	2.859	2.860	2.861	2.861	2.861	2.858	2.851	2.834	2.841	3.033	2.934
20	0.541	2.868	2.867	2.868	2.870	2.869	2.870	2.866	2.860	2.844	2.850	3.064	2.985
21	0.568	2.882	2.881	2.881	2.884	2.883	2.884	2.881	2.875	2.860	2.865	3.097	3.043
22	0.595	2.904	2.902	2.902	2.904	2.904	2.905	2.902	2.896	2.882	2.887	3.140	3.107
23	0.622	2.934	2.933	2.934	2.936	2.935	2.937	2.934	2.929	2.915	2.920	3.190	3.175
24	0.649	2.971	2.970	2.970	2.973	2.972	2.974	2.971	2.966	2.953	2.959	3.250	3.251
25	0.676	3.017	3.016	3.017	3.019	3.019	3.020	3.017	3.013	3.000	3.007	3.313	3.336
26	0.703	3.073	3.073	3.073	3.076	3.075	3.077	3.074	3.070	3.058	3.065	3.391	3.430
27	0.730	3.145	3.144	3.145	3.147	3.147	3.149	3.146	3.142	3.130	3.138	3.483	3.533
28	0.757	3.230	3.229	3.229	3.232	3.232	3.234	3.231	3.228	3.217	3.225	3.584	3.652
29	0.784	3.332	3.332	3.332	3.335	3.335	3.336	3.334	3.331	3.320	3.330	3.707	3.789
30	0.811	3.459	3.458	3.458	3.461	3.461	3.463	3.460	3.458	3.447	3.458	3.851	3.945
31	0.838	3.611	3.610	3.610	3.614	3.613	3.615	3.613	3.611	3.601	3.613	4.026	4.132
32	0.865	3.809	3.808	3.808	3.811	3.811	3.813	3.811	3.809	3.800	3.813	4.240	4.359
33	0.892	4.062	4.060	4.060	4.064	4.063	4.067	4.064	4.063	4.054	4.070	4.514	4.646
34	0.919	4.406	4.405	4.405	4.409	4.408	4.412	4.409	4.409	4.400	4.418	4.878	5.024
35	0.946	4.927	4.925	4.925	4.929	4.929	4.933	4.931	4.931	4.923	4.944	5.389	5.567
36	0.973	5.827	5.825	5.824	5.830	5.829	5.834	5.832	5.834	5.826	5.853	6.529	6.510
37	1.000	6.919	6.916	6.915	6.922	6.921	6.928	6.926	6.929	6.923	6.957	6.898	6.710

Table 25. Processed extraction results for K_1 (MPa √m) about a circular crack of radius 1.00 mm

Through thickness location		0.5/0.5	0.55/0.45	0.6/0.4	0.65/0.35	0.7/0.3	0.75/0.25	0.8/0.2	0.85/0.15	0.9/0.1	0.95/0.05	1/0
Extraction Number	Normalized Location	Average	Average	Average	Average	Average	Average	Average	Average	Average	Average	Average
0	0.000	6.968	6.967	6.974	6.983	6.996	7.006	7.021	7.063	7.403	#N/A	2.578
1	0.027	5.874	5.873	5.879	5.886	5.895	5.903	5.912	5.942	6.218	4.630	2.586
2	0.054	4.973	4.972	4.975	4.982	4.989	4.994	4.999	5.019	5.238	4.202	2.725
3	0.081	4.454	4.453	4.456	4.463	4.466	4.469	4.472	4.487	4.677	3.930	2.745
4	0.108	4.111	4.110	4.113	4.116	4.120	4.123	4.124	4.136	4.306	3.739	2.748
5	0.135	3.861	3.862	3.861	3.864	3.868	3.869	3.870	3.880	4.034	3.595	2.750
6	0.162	3.665	3.663	3.665	3.667	3.671	3.672	3.672	3.681	3.820	3.486	2.757
7	0.189	3.514	3.513	3.514	3.516	3.519	3.520	3.521	3.529	3.655	3.401	2.768
8	0.216	3.390	3.388	3.390	3.392	3.395	3.396	3.396	3.404	3.517	3.334	2.782
9	0.243	3.289	3.287	3.289	3.291	3.293	3.295	3.295	3.303	3.405	3.282	2.798
10	0.270	3.205	3.204	3.206	3.207	3.210	3.212	3.213	3.220	3.312	3.244	2.817
11	0.297	3.135	3.134	3.136	3.137	3.140	3.142	3.143	3.151	3.234	3.211	2.841
12	0.324	3.080	3.079	3.080	3.082	3.085	3.087	3.089	3.096	3.171	3.188	2.865
13	0.351	3.035	3.034	3.035	3.037	3.040	3.042	3.045	3.052	3.121	3.176	2.891
14	0.378	2.999	2.998	2.999	3.001	3.004	3.007	3.010	3.018	3.080	3.166	2.922
15	0.405	2.968	2.967	2.969	2.971	2.974	2.977	2.980	2.988	3.045	3.163	2.956
16	0.432	2.948	2.948	2.949	2.951	2.954	2.957	2.961	2.969	3.023	3.166	2.992
17	0.459	2.935	2.934	2.936	2.938	2.941	2.944	2.948	2.957	3.007	3.176	3.031
18	0.486	2.927	2.927	2.928	2.930	2.934	2.937	2.941	2.950	2.997	3.193	3.076
19	0.514	2.927	2.927	2.928	2.930	2.934	2.938	2.942	2.951	2.996	3.215	3.124
20	0.541	2.935	2.935	2.936	2.938	2.942	2.946	2.950	2.959	3.003	3.244	3.174
21	0.568	2.948	2.948	2.949	2.952	2.956	2.960	2.964	2.974	3.016	3.274	3.232
22	0.595	2.968	2.968	2.969	2.972	2.976	2.980	2.985	2.995	3.036	3.316	3.295
23	0.622	2.999	2.999	3.000	3.003	3.007	3.011	3.016	3.027	3.067	3.364	3.363
24	0.649	3.035	3.035	3.036	3.039	3.043	3.048	3.053	3.064	3.103	3.423	3.439
25	0.676	3.080	3.080	3.081	3.084	3.088	3.093	3.099	3.110	3.149	3.485	3.524
26	0.703	3.135	3.135	3.136	3.139	3.144	3.149	3.155	3.166	3.205	3.562	3.620
27	0.730	3.205	3.205	3.206	3.210	3.214	3.219	3.226	3.238	3.277	3.653	3.723
28	0.757	3.289	3.288	3.290	3.293	3.297	3.303	3.310	3.322	3.362	3.754	3.844
29	0.784	3.390	3.389	3.391	3.394	3.399	3.405	3.412	3.425	3.465	3.876	3.982
30	0.811	3.514	3.514	3.515	3.518	3.523	3.530	3.537	3.551	3.593	4.021	4.141
31	0.838	3.665	3.664	3.665	3.669	3.674	3.681	3.689	3.704	3.746	4.197	4.331
32	0.865	3.861	3.860	3.861	3.864	3.869	3.877	3.886	3.902	3.947	4.412	4.562
33	0.892	4.111	4.110	4.111	4.115	4.120	4.129	4.139	4.156	4.203	4.690	4.856
34	0.919	4.454	4.453	4.453	4.458	4.463	4.473	4.483	4.503	4.553	5.059	5.243
35	0.946	4.973	4.971	4.971	4.977	4.982	4.994	5.006	5.028	5.084	5.579	5.802
36	0.973	5.874	5.871	5.876	5.877	5.883	5.898	5.912	5.939	6.005	6.747	6.775
37	1.000	6.968	6.964	6.962	6.971	6.978	6.997	7.014	7.047	7.125	7.120	6.977

Appendix E Results for Elliptical Crack

Table 26. Raw extraction results for K_1 (MPa √m) about an elliptical crack of depth 0.08 mm

Through thickness location		1		2		3		4		13.75		23.5		33.25		43		52.75		62.5	
Extraction Number	Normalised Location	Normal	Mirror	Normal	Mirror	Normal	Mirror	Normal	Mirror	Normal	Mirror	Normal	Mirror	Normal	Mirror	Normal	Mirror	Normal	Mirror	Normal	Mirror
0	0.000	7.119	7.039	7.030	7.110	6.705	6.837	6.550	6.636	6.552	6.843	7.289	6.385	0.000	0.000	0.000	0.000	0.000	0.000	0.000	0.000
1	0.027	5.853	5.884	5.814	5.882	5.582	5.690	5.528	5.586	0.000	0.000	0.000	0.000	0.000	0.000	0.000	0.000	0.000	0.000	0.000	0.000
2	0.054	4.887	4.906	4.905	4.937	4.802	0.000	4.732	4.760	0.000	0.000	0.000	0.000	0.000	0.000	0.000	0.000	0.000	0.000	0.000	0.000
3	0.081	4.368	4.374	4.462	4.478	4.446	4.470	4.453	4.471	0.000	0.000	0.000	0.000	0.000	0.000	0.000	0.000	0.000	0.000	0.000	0.000
4	0.108	4.020	4.025	4.201	4.213	4.271	4.288	4.350	4.354	0.000	4.655	0.000	4.747	0.000	0.000	0.000	0.000	0.000	0.000	0.000	0.000
5	0.135	3.764	3.766	4.039	4.045	4.185	4.196	4.299	4.301	4.675	4.669	4.752	4.767	0.000	0.000	0.000	0.000	0.000	0.000	0.000	0.000
6	0.162	3.567	3.572	3.935	3.942	4.136	4.148	0.000	4.281	4.679	4.688	4.763	4.757	0.000	0.000	0.000	0.000	0.000	0.000	0.000	0.000
7	0.189	3.413	3.412	3.867	3.870	4.107	4.115	4.270	4.271	4.678	4.680	4.762	4.768	0.000	0.000	0.000	0.000	0.000	0.000	0.000	0.000
8	0.216	3.283	3.288	3.823	3.822	4.096	4.100	4.271	4.271	4.687	4.690	4.778	4.771	0.000	0.000	0.000	0.000	0.000	0.000	0.000	0.000
9	0.243	3.179	3.180	3.784	3.784	4.085	4.094	4.264	4.266	4.688	4.694	4.773	4.766	0.000	0.000	0.000	0.000	0.000	0.000	0.000	0.000
10	0.270	3.092	3.092	3.760	3.766	4.080	4.084	4.266	4.268	4.691	4.691	4.770	4.769	0.000	0.000	0.000	0.000	0.000	0.000	0.000	0.000
11	0.297	3.022	3.020	3.746	3.746	4.080	4.082	4.266	4.267	4.694	4.691	4.776	4.772	0.000	0.000	0.000	0.000	0.000	0.000	0.000	0.000
12	0.324	2.961	2.967	3.735	3.733	4.077	4.078	4.268	4.270	4.697	4.692	4.777	4.776	0.000	0.000	0.000	0.000	0.000	0.000	0.000	0.000
13	0.351	2.914	2.914	3.728	3.727	4.084	4.079	4.270	4.270	4.695	4.698	4.774	4.771	0.000	0.000	0.000	0.000	0.000	0.000	0.000	0.000
14	0.378	2.877	2.879	3.718	3.721	4.079	4.081	4.271	4.273	4.698	4.696	4.778	4.785	0.000	0.000	0.000	0.000	0.000	0.000	0.000	0.000
15	0.405	2.846	2.847	3.716	3.716	4.079	4.079	4.268	4.273	4.693	4.695	4.778	4.779	0.000	0.000	0.000	0.000	0.000	0.000	0.000	0.000
16	0.432	2.827	2.825	3.715	3.714	4.083	4.078	4.273	4.272	4.706	4.699	4.774	4.775	0.000	0.000	0.000	0.000	0.000	0.000	0.000	0.000
17	0.459	2.812	2.810	3.711	3.713	4.078	4.077	4.273	4.273	4.693	4.704	4.774	4.785	0.000	0.000	0.000	0.000	0.000	0.000	0.000	0.000
18	0.486	2.802	2.805	3.711	3.712	4.084	4.078	4.278	4.272	4.701	4.703	4.777	4.781	0.000	0.000	0.000	0.000	0.000	0.000	0.000	0.000
19	0.514	2.805	2.802	3.712	3.711	4.078	4.084	4.272	4.278	4.703	4.701	4.781	4.777	0.000	0.000	0.000	0.000	0.000	0.000	0.000	0.000
20	0.541	2.810	2.812	3.713	3.711	4.077	4.078	4.273	4.273	4.704	4.693	4.785	4.774	0.000	0.000	0.000	0.000	0.000	0.000	0.000	0.000
21	0.568	2.825	2.827	3.714	3.715	4.078	4.083	4.272	4.273	4.699	4.706	4.775	4.774	0.000	0.000	0.000	0.000	0.000	0.000	0.000	0.000
22	0.595	2.847	2.846	3.716	3.716	4.079	4.079	4.273	4.268	4.695	4.693	4.779	4.778	0.000	0.000	0.000	0.000	0.000	0.000	0.000	0.000
23	0.622	2.879	2.877	3.721	3.718	4.081	4.079	4.273	4.271	4.696	4.698	4.785	4.778	0.000	0.000	0.000	0.000	0.000	0.000	0.000	0.000
24	0.649	2.914	2.914	3.727	3.728	4.079	4.084	4.270	4.270	4.698	4.695	4.771	4.774	0.000	0.000	0.000	0.000	0.000	0.000	0.000	0.000
25	0.676	2.967	2.961	3.733	3.735	4.078	4.077	4.270	4.268	4.692	4.697	4.776	4.777	0.000	0.000	0.000	0.000	0.000	0.000	0.000	0.000
26	0.703	3.020	3.022	3.746	3.746	4.082	4.080	4.267	4.266	4.691	4.694	4.772	4.776	0.000	0.000	0.000	0.000	0.000	0.000	0.000	0.000
27	0.730	3.092	3.092	3.766	3.760	4.084	4.080	4.268	4.266	4.691	4.691	4.769	4.770	0.000	0.000	0.000	0.000	0.000	0.000	0.000	0.000
28	0.757	3.180	3.179	3.784	3.784	4.094	4.085	4.266	4.264	4.694	4.688	4.766	4.773	0.000	0.000	0.000	0.000	0.000	0.000	0.000	0.000
29	0.784	3.288	3.283	3.822	3.823	4.100	4.096	4.271	4.271	4.690	4.687	4.771	4.778	0.000	0.000	0.000	0.000	0.000	0.000	0.000	0.000
30	0.811	3.412	3.413	3.870	3.867	4.115	4.107	4.271	4.270	4.680	4.678	4.768	4.762	0.000	0.000	0.000	0.000	0.000	0.000	0.000	0.000
31	0.838	3.572	3.567	3.942	3.935	4.148	4.136	4.281	0.000	4.688	4.679	4.757	4.763	0.000	0.000	0.000	0.000	0.000	0.000	0.000	0.000
32	0.865	3.766	3.764	4.045	4.039	4.196	4.185	4.301	4.299	4.669	4.675	4.767	4.752	0.000	0.000	0.000	0.000	0.000	0.000	0.000	0.000
33	0.892	4.025	4.020	4.213	4.201	4.288	4.271	4.354	4.350	4.655	0.000	4.747	0.000	0.000	0.000	0.000	0.000	0.000	0.000	0.000	0.000
34	0.919	4.374	4.368	4.478	4.462	4.470	4.446	4.471	4.453	0.000	0.000	0.000	0.000	0.000	0.000	0.000	0.000	0.000	0.000	0.000	0.000
35	0.946	4.906	4.887	4.937	4.905	0.000	4.802	4.760	4.732	0.000	0.000	0.000	0.000	0.000	0.000	0.000	0.000	0.000	0.000	0.000	0.000
36	0.973	5.884	5.853	5.882	5.814	5.690	5.582	5.586	5.528	0.000	0.000	0.000	0.000	0.000	0.000	0.000	0.000	0.000	0.000	0.000	0.000
37	1.000	7.039	7.119	7.110	7.030	6.837	6.705	6.636	6.550	6.843	6.552	6.385	7.289	0.000	0.000	0.000	0.000	0.000	0.000	0.000	0.000

Table 27. Raw extraction results for K_1 (MPa √m) about an elliptical crack of depth 0.10 mm

Aspect Ratio		1		2		3		4		11.667		19.33		27		34.66666667		42.33333333		50	
Extraction Number	Normalised Location	Normal	Mirror	Normal	Mirror	Normal	Mirror	Normal	Mirror	Normal	Mirror	Normal	Mirror	Normal	Mirror	Normal	Mirror	Normal	Mirror	Normal	Mirror
0	0.000	7.123	7.042	7.037	7.118	6.716	6.836	6.548	6.634	0.000	0.000	7.269	7.712	7.254	7.209	0.000	0.000	0.000	0.000	0.000	0.000
1	0.027	5.857	5.887	5.819	5.888	5.591	5.690	5.526	5.584	0.000	0.000	0.000	0.000	0.000	0.000	0.000	0.000	0.000	0.000	0.000	0.000
2	0.054	4.890	4.909	4.909	4.941	4.809	0.000	4.731	4.759	0.000	0.000	0.000	0.000	0.000	0.000	0.000	0.000	0.000	0.000	0.000	0.000
3	0.081	4.371	4.377	4.466	4.482	4.451	4.471	4.452	4.470	0.000	0.000	0.000	0.000	0.000	0.000	0.000	0.000	0.000	0.000	0.000	0.000
4	0.108	4.024	4.028	4.204	4.217	4.275	4.289	4.349	4.354	0.000	0.000	0.000	4.726	0.000	4.765	0.000	0.000	0.000	0.000	0.000	0.000
5	0.135	3.767	3.769	4.042	4.049	4.189	4.197	4.298	4.301	0.000	0.000	4.733	4.749	4.775	4.788	0.000	0.000	0.000	0.000	0.000	0.000
6	0.162	3.570	3.575	3.939	3.945	4.140	4.149	0.000	4.281	0.000	0.000	4.745	4.739	4.786	4.778	0.000	0.000	0.000	0.000	0.000	0.000
7	0.189	3.416	3.415	3.870	3.874	4.110	4.117	4.269	4.271	0.000	0.000	4.744	4.750	4.785	4.790	0.000	0.000	0.000	0.000	0.000	0.000
8	0.216	3.286	3.291	3.827	3.826	4.099	4.102	4.271	4.271	0.000	0.000	4.760	4.753	4.800	4.793	0.000	0.000	0.000	0.000	0.000	0.000
9	0.243	3.182	3.183	3.787	3.787	4.088	4.096	4.264	4.267	0.000	0.000	4.755	4.749	4.795	4.787	0.000	0.000	0.000	0.000	0.000	0.000
10	0.270	3.096	3.095	3.764	3.770	4.084	4.086	4.266	4.268	0.000	0.000	4.753	4.751	4.792	4.791	0.000	0.000	0.000	0.000	0.000	0.000
11	0.297	3.025	3.023	3.749	3.750	4.083	4.083	4.266	4.268	0.000	0.000	4.758	4.755	4.798	4.794	0.000	0.000	0.000	0.000	0.000	0.000
12	0.324	2.964	2.970	3.739	3.736	4.080	4.080	4.269	4.270	0.000	0.000	4.760	4.759	4.799	4.797	0.000	0.000	0.000	0.000	0.000	0.000
13	0.351	2.918	2.918	3.732	3.731	4.087	4.082	4.270	4.270	0.000	0.000	4.756	4.754	4.795	4.792	0.000	0.000	0.000	0.000	0.000	0.000
14	0.378	2.880	2.882	3.722	3.724	4.082	4.083	4.271	4.274	0.000	0.000	4.761	4.767	4.797	4.806	0.000	0.000	0.000	0.000	0.000	0.000
15	0.405	2.850	2.850	3.720	3.720	4.083	4.082	4.268	4.274	0.000	0.000	4.761	4.761	4.798	4.800	0.000	0.000	0.000	0.000	0.000	0.000
16	0.432	2.831	2.829	3.719	3.718	4.086	4.081	4.274	4.272	0.000	0.000	4.757	4.758	4.795	4.796	0.000	0.000	0.000	0.000	0.000	0.000
17	0.459	2.815	2.813	3.715	3.717	4.081	4.081	4.274	4.273	0.000	0.000	4.757	4.768	4.794	4.807	0.000	0.000	0.000	0.000	0.000	0.000
18	0.486	2.806	2.808	3.715	3.716	4.087	4.081	4.278	4.273	0.000	0.000	4.760	4.764	4.798	4.802	0.000	0.000	0.000	0.000	0.000	0.000
19	0.514	2.808	2.806	3.716	3.715	4.081	4.087	4.273	4.278	0.000	0.000	4.764	4.760	4.802	4.798	0.000	0.000	0.000	0.000	0.000	0.000
20	0.541	2.813	2.815	3.717	3.715	4.081	4.081	4.273	4.274	0.000	0.000	4.768	4.757	4.807	4.794	0.000	0.000	0.000	0.000	0.000	0.000
21	0.568	2.829	2.831	3.718	3.719	4.081	4.086	4.272	4.274	0.000	0.000	4.758	4.757	4.796	4.795	0.000	0.000	0.000	0.000	0.000	0.000
22	0.595	2.850	2.850	3.720	3.720	4.082	4.083	4.274	4.268	0.000	0.000	4.761	4.761	4.800	4.798	0.000	0.000	0.000	0.000	0.000	0.000
23	0.622	2.882	2.880	3.724	3.722	4.083	4.082	4.274	4.271	0.000	0.000	4.767	4.761	4.806	4.797	0.000	0.000	0.000	0.000	0.000	0.000
24	0.649	2.918	2.918	3.731	3.732	4.082	4.087	4.270	4.270	0.000	0.000	4.754	4.756	4.792	4.795	0.000	0.000	0.000	0.000	0.000	0.000
25	0.676	2.970	2.964	3.736	3.739	4.080	4.080	4.270	4.269	0.000	0.000	4.759	4.760	4.797	4.799	0.000	0.000	0.000	0.000	0.000	0.000
26	0.703	3.023	3.025	3.750	3.749	4.083	4.083	4.268	4.266	0.000	0.000	4.755	4.758	4.794	4.798	0.000	0.000	0.000	0.000	0.000	0.000
27	0.730	3.095	3.096	3.770	3.764	4.086	4.084	4.268	4.266	0.000	0.000	4.751	4.753	4.791	4.792	0.000	0.000	0.000	0.000	0.000	0.000
28	0.757	3.183	3.182	3.787	3.787	4.096	4.088	4.267	4.264	0.000	0.000	4.749	4.755	4.787	4.795	0.000	0.000	0.000	0.000	0.000	0.000
29	0.784	3.291	3.286	3.826	3.827	4.102	4.099	4.271	4.271	0.000	0.000	4.753	4.760	4.793	4.800	0.000	0.000	0.000	0.000	0.000	0.000
30	0.811	3.415	3.416	3.874	3.870	4.117	4.110	4.271	4.269	0.000	0.000	4.750	4.744	4.790	4.785	0.000	0.000	0.000	0.000	0.000	0.000
31	0.838	3.575	3.570	3.945	3.939	4.149	4.140	4.281	0.000	0.000	0.000	4.739	4.745	4.778	4.786	0.000	0.000	0.000	0.000	0.000	0.000
32	0.865	3.769	3.767	4.049	4.042	4.197	4.189	4.301	4.298	0.000	0.000	4.749	4.733	4.788	4.775	0.000	0.000	0.000	0.000	0.000	0.000
33	0.892	4.028	4.024	4.217	4.204	4.289	4.275	4.354	4.349	0.000	0.000	4.726	0.000	4.765	0.000	0.000	0.000	0.000	0.000	0.000	0.000
34	0.919	4.377	4.371	4.482	4.466	4.471	4.451	4.470	4.452	0.000	0.000	0.000	0.000	0.000	0.000	0.000	0.000	0.000	0.000	0.000	0.000
35	0.946	4.909	4.890	4.941	4.909	0.000	4.809	4.759	4.731	0.000	0.000	0.000	0.000	0.000	0.000	0.000	0.000	0.000	0.000	0.000	0.000
36	0.973	5.887	5.857	5.888	5.819	5.690	5.591	5.584	5.526	0.000	0.000	0.000	0.000	0.000	0.000	0.000	0.000	0.000	0.000	0.000	0.000
37	1.000	7.042	7.123	7.118	7.037	6.836	6.716	6.634	6.548	0.000	0.000	7.712	7.269	7.209	7.254	0.000	0.000	0.000	0.000	0.000	0.000

Table 28. Raw extraction results for K_1 (MPa √m) about an elliptical crack of depth 0.20 mm

Aspect Ratio		1		2		3		4		7.5		11		14.5		18		21		25	
Extraction Number	Normalised Location	Normal	Mirror	Normal	Mirror	Normal	Mirror	Normal	Mirror	Normal	Mirror	Normal	Mirror	Normal	Mirror	Normal	Mirror	Normal	Mirror	Normal	Mirror
0	0.000	7.136	7.054	7.053	7.139	6.732	6.856	6.567	6.657	0.000	0.000	0.000	0.000	7.641	7.908	7.771	7.825	0.000	0.000	7.859	7.977
1	0.027	5.868	5.896	5.834	5.906	5.604	5.706	5.543	5.604	0.000	0.000	0.000	0.000	0.000	0.000	0.000	0.000	0.000	0.000	0.000	0.000
2	0.054	4.900	4.918	4.923	4.957	4.821	0.000	4.746	4.776	0.000	0.000	0.000	0.000	0.000	0.000	0.000	0.000	0.000	0.000	0.000	0.000
3	0.081	4.382	4.387	4.479	4.497	4.464	4.485	4.466	4.487	0.000	0.000	0.000	0.000	0.000	0.000	0.000	0.000	0.000	0.000	0.000	0.000
4	0.108	4.034	4.038	4.218	4.232	4.288	4.303	4.363	4.371	0.000	0.000	0.000	0.000	0.000	4.706	0.000	4.755	0.000	0.000	0.000	4.778
5	0.135	3.778	3.780	4.056	4.064	4.203	4.212	4.313	4.318	0.000	0.000	0.000	0.000	4.721	4.714	4.752	4.761	0.000	0.000	4.791	4.805
6	0.162	3.581	3.586	3.953	3.961	4.154	4.164	0.000	4.302	0.000	0.000	0.000	0.000	4.725	4.731	4.766	4.777	0.000	0.000	4.808	4.802
7	0.189	3.428	3.426	3.885	3.890	4.125	4.133	4.286	4.289	0.000	0.000	0.000	0.000	4.724	4.727	4.767	4.772	0.000	0.000	4.813	4.819
8	0.216	3.298	3.303	3.842	3.842	4.114	4.118	4.288	4.290	0.000	0.000	0.000	0.000	4.733	4.730	4.784	4.775	0.000	0.000	4.833	4.826
9	0.243	3.194	3.195	3.803	3.804	4.104	4.113	4.282	4.286	0.000	0.000	0.000	0.000	4.735	4.738	4.780	4.784	0.000	0.000	4.831	4.824
10	0.270	3.108	3.107	3.781	3.787	4.100	4.103	4.284	4.288	0.000	0.000	0.000	0.000	4.738	4.733	4.779	4.775	0.000	0.000	4.830	4.829
11	0.297	3.037	3.035	3.766	3.767	4.100	4.100	4.285	4.288	0.000	0.000	0.000	0.000	4.742	4.740	4.784	4.784	0.000	0.000	4.836	4.833
12	0.324	2.977	2.982	3.756	3.754	4.098	4.098	4.288	4.291	0.000	0.000	0.000	0.000	4.744	4.738	4.786	4.781	0.000	0.000	4.837	4.836
13	0.351	2.930	2.930	3.749	3.749	4.106	4.100	4.290	4.291	0.000	0.000	0.000	0.000	4.740	4.750	4.783	4.793	0.000	0.000	4.833	4.830
14	0.378	2.893	2.895	3.740	3.743	4.101	4.102	4.292	4.295	0.000	0.000	0.000	0.000	4.745	4.745	4.787	4.788	0.000	0.000	4.834	4.843
15	0.405	2.862	2.863	3.738	3.738	4.102	4.101	4.289	4.295	0.000	0.000	0.000	0.000	4.746	4.746	4.787	4.788	0.000	0.000	4.834	4.836
16	0.432	2.843	2.842	3.737	3.736	4.105	4.101	4.295	4.294	0.000	0.000	0.000	0.000	4.741	4.746	4.783	4.788	0.000	0.000	4.830	4.832
17	0.459	2.828	2.826	3.734	3.736	4.100	4.100	4.295	4.295	0.000	0.000	0.000	0.000	4.741	4.753	4.783	4.794	0.000	0.000	4.829	4.842
18	0.486	2.819	2.821	3.733	3.735	4.106	4.101	4.300	4.295	0.000	0.000	0.000	0.000	4.746	4.750	4.787	4.791	0.000	0.000	4.832	4.836
19	0.514	2.821	2.819	3.735	3.733	4.101	4.106	4.295	4.300	0.000	0.000	0.000	0.000	4.750	4.746	4.791	4.787	0.000	0.000	4.836	4.832
20	0.541	2.826	2.828	3.736	3.734	4.100	4.100	4.295	4.295	0.000	0.000	0.000	0.000	4.753	4.741	4.794	4.783	0.000	0.000	4.842	4.829
21	0.568	2.842	2.843	3.736	3.737	4.101	4.105	4.294	4.295	0.000	0.000	0.000	0.000	4.746	4.741	4.788	4.783	0.000	0.000	4.832	4.830
22	0.595	2.863	2.862	3.738	3.738	4.101	4.102	4.295	4.289	0.000	0.000	0.000	0.000	4.746	4.746	4.788	4.787	0.000	0.000	4.836	4.834
23	0.622	2.895	2.893	3.743	3.740	4.102	4.101	4.295	4.292	0.000	0.000	0.000	0.000	4.745	4.745	4.788	4.787	0.000	0.000	4.843	4.834
24	0.649	2.930	2.930	3.749	3.749	4.100	4.106	4.291	4.290	0.000	0.000	0.000	0.000	4.750	4.740	4.793	4.783	0.000	0.000	4.830	4.833
25	0.676	2.982	2.977	3.754	3.756	4.098	4.098	4.291	4.288	0.000	0.000	0.000	0.000	4.738	4.744	4.781	4.786	0.000	0.000	4.836	4.837
26	0.703	3.035	3.037	3.767	3.766	4.100	4.100	4.288	4.285	0.000	0.000	0.000	0.000	4.740	4.742	4.784	4.784	0.000	0.000	4.833	4.836
27	0.730	3.107	3.108	3.787	3.781	4.103	4.100	4.288	4.284	0.000	0.000	0.000	0.000	4.733	4.738	4.775	4.779	0.000	0.000	4.829	4.830
28	0.757	3.195	3.194	3.804	3.803	4.113	4.104	4.286	4.282	0.000	0.000	0.000	0.000	4.738	4.735	4.784	4.780	0.000	0.000	4.824	4.831
29	0.784	3.303	3.298	3.842	3.842	4.118	4.114	4.290	4.288	0.000	0.000	0.000	0.000	4.730	4.733	4.775	4.784	0.000	0.000	4.826	4.833
30	0.811	3.426	3.428	3.890	3.885	4.133	4.125	4.289	4.286	0.000	0.000	0.000	0.000	4.727	4.724	4.772	4.767	0.000	0.000	4.819	4.813
31	0.838	3.586	3.581	3.961	3.953	4.164	4.154	4.302	0.000	0.000	0.000	0.000	0.000	4.731	4.725	4.777	4.766	0.000	0.000	4.802	4.808
32	0.865	3.780	3.778	4.064	4.056	4.212	4.203	4.318	4.313	0.000	0.000	0.000	0.000	4.714	4.721	4.761	4.752	0.000	0.000	4.805	4.791
33	0.892	4.038	4.034	4.232	4.218	4.303	4.288	4.371	4.363	0.000	0.000	0.000	0.000	4.706	0.000	4.755	0.000	0.000	0.000	4.778	0.000
34	0.919	4.387	4.382	4.497	4.479	4.485	4.464	4.487	4.466	0.000	0.000	0.000	0.000	0.000	0.000	0.000	0.000	0.000	0.000	0.000	0.000
35	0.946	4.918	4.900	4.957	4.923	0.000	4.821	4.776	4.746	0.000	0.000	0.000	0.000	0.000	0.000	0.000	0.000	0.000	0.000	0.000	0.000
36	0.973	5.896	5.868	5.906	5.834	5.706	5.604	5.604	5.543	0.000	0.000	0.000	0.000	0.000	0.000	0.000	0.000	0.000	0.000	0.000	0.000
37	1.000	7.054	7.136	7.139	7.053	6.856	6.732	6.657	6.567	0.000	0.000	0.000	0.000	7.908	7.641	7.825	7.771	0.000	0.000	7.977	7.859

Table 29. Raw extraction results for K_1 (MPa √m) about an elliptical crack of depth 0.30 mm

Aspect Ratio		1		2		3		4		6.111		8.22		10.333		12.444		14.556		16.667	
Extraction Number	Normalised Location	Normal	Mirror	Normal	Mirror	Normal	Mirror	Normal	Mirror	Normal	Mirror	Normal	Mirror	Normal	Mirror	Normal	Mirror	Normal	Mirror	Normal	Mirror
0	0.000	7.153	7.073	7.065	7.146	6.748	6.874	6.585	6.679	6.432	6.538	0.000	0.000	0.000	0.000	7.753	7.985	7.708	8.007	7.694	8.057
1	0.027	5.883	5.913	5.844	5.913	5.618	5.722	5.558	5.622	0.000	0.000	0.000	0.000	0.000	0.000	0.000	0.000	0.000	0.000	0.000	0.000
2	0.054	4.914	4.933	4.932	4.964	4.834	0.000	4.760	4.792	0.000	0.000	0.000	0.000	0.000	0.000	0.000	0.000	0.000	0.000	0.000	0.000
3	0.081	4.394	4.401	4.489	4.505	4.477	4.499	4.480	4.502	0.000	4.553	0.000	0.000	0.000	0.000	0.000	0.000	0.000	0.000	0.000	0.000
4	0.108	4.047	4.052	4.228	4.240	4.302	4.317	4.378	4.386	4.509	4.509	0.000	0.000	0.000	0.000	0.000	4.695	0.000	4.737	0.000	4.760
5	0.135	3.791	3.793	4.067	4.073	4.217	4.227	4.328	4.334	4.490	4.501	0.000	0.000	0.000	0.000	4.718	4.713	4.748	4.747	4.776	4.772
6	0.162	3.594	3.600	3.964	3.971	4.169	4.180	0.000	4.315	4.499	4.499	0.000	0.000	0.000	0.000	4.724	4.733	4.755	4.765	4.785	4.795
7	0.189	3.441	3.440	3.897	3.900	4.140	4.149	4.302	4.306	4.500	4.506	0.000	0.000	0.000	0.000	4.725	4.727	4.756	4.763	4.788	4.794
8	0.216	3.311	3.317	3.854	3.853	4.130	4.135	4.305	4.307	4.513	4.508	0.000	0.000	0.000	0.000	4.735	4.739	4.767	4.768	4.801	4.801
9	0.243	3.208	3.209	3.816	3.816	4.121	4.130	4.299	4.304	4.512	4.510	0.000	0.000	0.000	0.000	4.739	4.745	4.771	4.777	4.806	4.811
10	0.270	3.122	3.121	3.794	3.800	4.118	4.121	4.303	4.307	4.515	4.521	0.000	0.000	0.000	0.000	4.742	4.742	4.774	4.772	4.810	4.806
11	0.297	3.052	3.050	3.780	3.781	4.118	4.119	4.304	4.307	4.519	4.516	0.000	0.000	0.000	0.000	4.746	4.743	4.778	4.780	4.814	4.814
12	0.324	2.991	2.997	3.770	3.768	4.117	4.117	4.308	4.311	4.524	4.519	0.000	0.000	0.000	0.000	4.749	4.745	4.781	4.777	4.816	4.810
13	0.351	2.945	2.945	3.764	3.764	4.124	4.119	4.310	4.311	4.530	4.525	0.000	0.000	0.000	0.000	4.748	4.751	4.777	4.789	4.811	4.822
14	0.378	2.908	2.909	3.755	3.757	4.120	4.122	4.312	4.316	4.527	4.533	0.000	0.000	0.000	0.000	4.751	4.749	4.782	4.783	4.815	4.816
15	0.405	2.877	2.878	3.754	3.753	4.121	4.121	4.310	4.316	4.525	4.526	0.000	0.000	0.000	0.000	4.746	4.748	4.782	4.783	4.814	4.815
16	0.432	2.858	2.857	3.753	3.752	4.125	4.121	4.316	4.315	4.530	4.528	0.000	0.000	0.000	0.000	4.759	4.752	4.777	4.783	4.809	4.814
17	0.459	2.843	2.841	3.750	3.751	4.120	4.120	4.316	4.316	4.530	4.529	0.000	0.000	0.000	0.000	4.746	4.756	4.777	4.789	4.809	4.820
18	0.486	2.834	2.836	3.749	3.751	4.127	4.121	4.321	4.316	4.528	4.534	0.000	0.000	0.000	0.000	4.754	4.755	4.782	4.786	4.812	4.816
19	0.514	2.836	2.834	3.751	3.749	4.121	4.127	4.316	4.321	4.534	4.528	0.000	0.000	0.000	0.000	4.755	4.754	4.786	4.782	4.816	4.812
20	0.541	2.841	2.843	3.751	3.750	4.120	4.120	4.316	4.316	4.529	4.530	0.000	0.000	0.000	0.000	4.756	4.746	4.789	4.777	4.820	4.809
21	0.568	2.857	2.858	3.752	3.753	4.121	4.125	4.315	4.316	4.528	4.530	0.000	0.000	0.000	0.000	4.752	4.759	4.783	4.777	4.814	4.809
22	0.595	2.878	2.877	3.753	3.754	4.121	4.121	4.316	4.310	4.526	4.525	0.000	0.000	0.000	0.000	4.748	4.746	4.783	4.782	4.815	4.814
23	0.622	2.909	2.908	3.757	3.755	4.122	4.120	4.316	4.312	4.533	4.527	0.000	0.000	0.000	0.000	4.749	4.751	4.783	4.782	4.816	4.815
24	0.649	2.945	2.945	3.764	3.764	4.119	4.124	4.311	4.310	4.525	4.530	0.000	0.000	0.000	0.000	4.751	4.748	4.789	4.777	4.822	4.811
25	0.676	2.997	2.991	3.768	3.770	4.117	4.117	4.311	4.308	4.519	4.524	0.000	0.000	0.000	0.000	4.745	4.749	4.777	4.781	4.810	4.816
26	0.703	3.050	3.052	3.781	3.780	4.119	4.118	4.307	4.304	4.516	4.519	0.000	0.000	0.000	0.000	4.743	4.746	4.780	4.778	4.814	4.814
27	0.730	3.121	3.122	3.800	3.794	4.121	4.118	4.307	4.303	4.521	4.515	0.000	0.000	0.000	0.000	4.742	4.742	4.772	4.774	4.806	4.810
28	0.757	3.209	3.208	3.816	3.816	4.130	4.121	4.304	4.299	4.510	4.512	0.000	0.000	0.000	0.000	4.745	4.739	4.777	4.771	4.811	4.806
29	0.784	3.317	3.311	3.853	3.854	4.135	4.130	4.307	4.305	4.508	4.513	0.000	0.000	0.000	0.000	4.739	4.735	4.768	4.767	4.801	4.801
30	0.811	3.440	3.441	3.900	3.897	4.149	4.140	4.306	4.302	4.506	4.500	0.000	0.000	0.000	0.000	4.727	4.725	4.763	4.756	4.794	4.788
31	0.838	3.600	3.594	3.971	3.964	4.180	4.169	4.315	0.000	4.499	4.499	0.000	0.000	0.000	0.000	4.733	4.724	4.765	4.755	4.795	4.785
32	0.865	3.793	3.791	4.073	4.067	4.227	4.217	4.334	4.328	4.501	4.490	0.000	0.000	0.000	0.000	4.713	4.718	4.747	4.748	4.772	4.776
33	0.892	4.052	4.047	4.240	4.228	4.317	4.302	4.386	4.378	4.509	4.509	0.000	0.000	0.000	0.000	4.695	0.000	4.737	0.000	4.760	0.000
34	0.919	4.401	4.394	4.505	4.489	4.499	4.477	4.502	4.480	4.553	0.000	0.000	0.000	0.000	0.000	0.000	0.000	0.000	0.000	0.000	0.000
35	0.946	4.933	4.914	4.964	4.932	0.000	4.834	4.792	4.760	0.000	0.000	0.000	0.000	0.000	0.000	0.000	0.000	0.000	0.000	0.000	0.000
36	0.973	5.913	5.883	5.913	5.844	5.722	5.618	5.622	5.558	0.000	0.000	0.000	0.000	0.000	0.000	0.000	0.000	0.000	0.000	0.000	0.000
37	1.000	7.073	7.153	7.146	7.065	6.874	6.748	6.679	6.585	6.538	6.432	0.000	0.000	0.000	0.000	7.985	7.753	8.007	7.708	8.057	7.694

Table 30. Raw extraction results for K_1 (MPa √m) about an elliptical crack of depth 0.50 mm

Aspect Ratio		1		2		3		4		7		8		9		10	
Extraction Number	Normalised Location	Normal	Mirror	Normal	Mirror	Normal	Mirror	Normal	Mirror	Normal	Mirror	Normal	Mirror	Normal	Mirror	Normal	Mirror
0	0.000	7.169	7.091	7.095	7.180	6.778	6.903	6.621	6.717	0.000	0.000	0.000	0.000	0.000	0.000	0.000	0.000
1	0.027	5.898	5.930	5.870	5.941	5.644	5.747	5.590	5.655	0.000	0.000	0.000	0.000	0.000	0.000	0.000	0.000
2	0.054	4.929	4.950	4.957	4.990	4.858	0.000	4.789	4.822	0.000	0.000	0.000	0.000	0.000	0.000	0.000	0.000
3	0.081	4.411	4.418	4.513	4.530	4.501	4.523	4.509	4.532	0.000	0.000	0.000	0.000	0.000	0.000	0.000	0.000
4	0.108	4.064	4.070	4.252	4.266	4.327	4.342	4.408	4.417	0.000	0.000	0.000	0.000	0.000	0.000	0.000	0.000
5	0.135	3.809	3.812	4.092	4.100	4.243	4.253	4.360	4.366	0.000	0.000	0.000	0.000	0.000	0.000	0.000	0.000
6	0.162	3.614	3.620	3.990	3.998	4.196	4.207	0.000	4.349	0.000	0.000	0.000	0.000	0.000	0.000	0.000	0.000
7	0.189	3.461	3.460	3.924	3.929	4.169	4.178	4.338	4.341	0.000	0.000	0.000	0.000	0.000	0.000	0.000	0.000
8	0.216	3.332	3.338	3.883	3.882	4.161	4.165	4.342	4.344	0.000	0.000	0.000	0.000	0.000	0.000	0.000	0.000
9	0.243	3.230	3.231	3.846	3.846	4.153	4.162	4.338	4.342	0.000	0.000	0.000	0.000	0.000	0.000	0.000	0.000
10	0.270	3.144	3.144	3.825	3.831	4.151	4.154	4.343	4.347	0.000	0.000	0.000	0.000	0.000	0.000	0.000	0.000
11	0.297	3.075	3.073	3.812	3.813	4.152	4.153	4.345	4.348	0.000	0.000	0.000	0.000	0.000	0.000	0.000	0.000
12	0.324	3.014	3.021	3.803	3.801	4.152	4.153	4.350	4.353	0.000	0.000	0.000	0.000	0.000	0.000	0.000	0.000
13	0.351	2.969	2.969	3.797	3.797	4.161	4.156	4.353	4.354	0.000	0.000	0.000	0.000	0.000	0.000	0.000	0.000
14	0.378	2.932	2.934	3.789	3.792	4.157	4.159	4.356	4.359	0.000	0.000	0.000	0.000	0.000	0.000	0.000	0.000
15	0.405	2.902	2.902	3.788	3.788	4.159	4.159	4.355	4.361	0.000	0.000	0.000	0.000	0.000	0.000	0.000	0.000
16	0.432	2.883	2.882	3.788	3.787	4.164	4.159	4.361	4.360	0.000	0.000	0.000	0.000	0.000	0.000	0.000	0.000
17	0.459	2.868	2.866	3.785	3.787	4.159	4.159	4.362	4.362	0.000	0.000	0.000	0.000	0.000	0.000	0.000	0.000
18	0.486	2.859	2.861	3.785	3.786	4.166	4.160	4.367	4.361	0.000	0.000	0.000	0.000	0.000	0.000	0.000	0.000
19	0.514	2.861	2.859	3.786	3.785	4.160	4.166	4.361	4.367	0.000	0.000	0.000	0.000	0.000	0.000	0.000	0.000
20	0.541	2.866	2.868	3.787	3.785	4.159	4.159	4.362	4.362	0.000	0.000	0.000	0.000	0.000	0.000	0.000	0.000
21	0.568	2.882	2.883	3.787	3.788	4.159	4.164	4.360	4.361	0.000	0.000	0.000	0.000	0.000	0.000	0.000	0.000
22	0.595	2.902	2.902	3.788	3.788	4.159	4.159	4.361	4.355	0.000	0.000	0.000	0.000	0.000	0.000	0.000	0.000
23	0.622	2.934	2.932	3.792	3.789	4.159	4.157	4.359	4.356	0.000	0.000	0.000	0.000	0.000	0.000	0.000	0.000
24	0.649	2.969	2.969	3.797	3.797	4.156	4.161	4.354	4.353	0.000	0.000	0.000	0.000	0.000	0.000	0.000	0.000
25	0.676	3.021	3.014	3.801	3.803	4.153	4.152	4.353	4.350	0.000	0.000	0.000	0.000	0.000	0.000	0.000	0.000
26	0.703	3.073	3.075	3.813	3.812	4.153	4.152	4.348	4.345	0.000	0.000	0.000	0.000	0.000	0.000	0.000	0.000
27	0.730	3.144	3.144	3.831	3.825	4.154	4.151	4.347	4.343	0.000	0.000	0.000	0.000	0.000	0.000	0.000	0.000
28	0.757	3.231	3.230	3.846	3.846	4.162	4.153	4.342	4.338	0.000	0.000	0.000	0.000	0.000	0.000	0.000	0.000
29	0.784	3.338	3.332	3.882	3.883	4.165	4.161	4.344	4.342	0.000	0.000	0.000	0.000	0.000	0.000	0.000	0.000
30	0.811	3.460	3.461	3.929	3.924	4.178	4.169	4.341	4.338	0.000	0.000	0.000	0.000	0.000	0.000	0.000	0.000
31	0.838	3.620	3.614	3.998	3.990	4.207	4.196	4.349	0.000	0.000	0.000	0.000	0.000	0.000	0.000	0.000	0.000
32	0.865	3.812	3.809	4.100	4.092	4.253	4.243	4.366	4.360	0.000	0.000	0.000	0.000	0.000	0.000	0.000	0.000
33	0.892	4.070	4.064	4.266	4.252	4.342	4.327	4.417	4.408	0.000	0.000	0.000	0.000	0.000	0.000	0.000	0.000
34	0.919	4.418	4.411	4.530	4.513	4.523	4.501	4.532	4.509	0.000	0.000	0.000	0.000	0.000	0.000	0.000	0.000
35	0.946	4.950	4.929	4.990	4.957	0.000	4.858	4.822	4.789	0.000	0.000	0.000	0.000	0.000	0.000	0.000	0.000
36	0.973	5.930	5.898	5.941	5.870	5.747	5.644	5.655	5.590	0.000	0.000	0.000	0.000	0.000	0.000	0.000	0.000
37	1.000	7.091	7.169	7.180	7.095	6.903	6.778	6.717	6.621	0.000	0.000	0.000	0.000	0.000	0.000	0.000	0.000

Table 31. Raw extraction results for K_1 (MPa √m) about an elliptical crack of depth 1.00 mm

Aspect Ratio		1		2		3		4	
Extraction Number	Normalised Location	Normal	Mirror	Normal	Mirror	Normal	Mirror	Normal	Mirror
0	0.000	7.224	7.143	7.176	7.259	6.887	7.012	6.775	6.871
1	0.027	5.948	5.979	5.941	6.011	5.738	5.840	5.720	5.785
2	0.054	4.978	4.997	5.022	5.055	4.943	0.000	4.904	4.937
3	0.081	4.461	4.467	4.578	4.594	4.584	4.605	4.623	4.645
4	0.108	4.116	4.121	4.319	4.331	4.411	4.426	4.524	4.533
5	0.135	3.863	3.865	4.160	4.167	4.330	4.339	4.480	4.485
6	0.162	3.669	3.674	4.062	4.068	4.287	4.297	0.000	4.472
7	0.189	3.519	3.517	3.998	4.002	4.264	4.271	4.465	4.468
8	0.216	3.391	3.397	3.960	3.959	4.259	4.262	4.473	4.475
9	0.243	3.290	3.291	3.926	3.925	4.254	4.263	4.471	4.476
10	0.270	3.206	3.205	3.908	3.913	4.255	4.258	4.479	4.483
11	0.297	3.138	3.136	3.897	3.898	4.259	4.260	4.484	4.487
12	0.324	3.079	3.085	3.891	3.888	4.262	4.262	4.490	4.493
13	0.351	3.035	3.034	3.887	3.887	4.273	4.267	4.495	4.496
14	0.378	2.998	3.000	3.881	3.883	4.271	4.273	4.499	4.502
15	0.405	2.969	2.970	3.882	3.881	4.274	4.274	4.498	4.504
16	0.432	2.951	2.949	3.882	3.881	4.280	4.275	4.505	4.504
17	0.459	2.936	2.934	3.880	3.882	4.276	4.276	4.506	4.506
18	0.486	2.927	2.930	3.880	3.882	4.283	4.277	4.512	4.506
19	0.514	2.930	2.927	3.882	3.880	4.277	4.283	4.506	4.512
20	0.541	2.934	2.936	3.882	3.880	4.276	4.276	4.506	4.506
21	0.568	2.949	2.951	3.881	3.882	4.275	4.280	4.504	4.505
22	0.595	2.970	2.969	3.881	3.882	4.274	4.274	4.504	4.498
23	0.622	3.000	2.998	3.883	3.881	4.273	4.271	4.502	4.499
24	0.649	3.034	3.035	3.887	3.887	4.267	4.273	4.496	4.495
25	0.676	3.085	3.079	3.888	3.891	4.262	4.262	4.493	4.490
26	0.703	3.136	3.138	3.898	3.897	4.260	4.259	4.487	4.484
27	0.730	3.205	3.206	3.913	3.908	4.258	4.255	4.483	4.479
28	0.757	3.291	3.290	3.925	3.926	4.263	4.254	4.476	4.471
29	0.784	3.397	3.391	3.959	3.960	4.262	4.259	4.475	4.473
30	0.811	3.517	3.519	4.002	3.998	4.271	4.264	4.468	4.465
31	0.838	3.674	3.669	4.068	4.062	4.297	4.287	4.472	0.000
32	0.865	3.865	3.863	4.167	4.160	4.339	4.330	4.485	4.480
33	0.892	4.121	4.116	4.331	4.319	4.426	4.411	4.533	4.524
34	0.919	4.467	4.461	4.594	4.578	4.605	4.584	4.645	4.623
35	0.946	4.997	4.978	5.055	5.022	0.000	4.943	4.937	4.904
36	0.973	5.979	5.948	6.011	5.941	5.840	5.738	5.785	5.720
37	1.000	7.143	7.224	7.259	7.176	7.012	6.887	6.871	6.775

Table 32. Processed extraction results for K_1 (MPa √m) about an elliptical crack of depth 0.08 mm

Aspect Ratio		1	2	3	4	13.75	23.5	33.25	43	52.75	62.5
Extraction Number	Normalised Location	Average	Average	Average	Average	Average	Average	Average	Average	Average	Average
0	0.000	7.079	7.070	6.771	6.593	6.698	6.837	#N/A	#N/A	#N/A	#N/A
1	0.027	5.868	5.848	5.636	5.557	#N/A	#N/A	#N/A	#N/A	#N/A	#N/A
2	0.054	4.896	4.921	4.802	4.746	#N/A	#N/A	#N/A	#N/A	#N/A	#N/A
3	0.081	4.371	4.470	4.458	4.462	#N/A	#N/A	#N/A	#N/A	#N/A	#N/A
4	0.108	4.023	4.207	4.279	4.352	4.655	4.747	#N/A	#N/A	#N/A	#N/A
5	0.135	3.765	4.042	4.191	4.300	4.672	4.760	#N/A	#N/A	#N/A	#N/A
6	0.162	3.570	3.938	4.142	4.281	4.683	4.760	#N/A	#N/A	#N/A	#N/A
7	0.189	3.412	3.868	4.111	4.270	4.679	4.765	#N/A	#N/A	#N/A	#N/A
8	0.216	3.286	3.823	4.098	4.271	4.688	4.774	#N/A	#N/A	#N/A	#N/A
9	0.243	3.179	3.784	4.089	4.265	4.691	4.769	#N/A	#N/A	#N/A	#N/A
10	0.270	3.092	3.763	4.082	4.267	4.691	4.769	#N/A	#N/A	#N/A	#N/A
11	0.297	3.021	3.746	4.081	4.267	4.693	4.774	#N/A	#N/A	#N/A	#N/A
12	0.324	2.964	3.734	4.077	4.269	4.694	4.776	#N/A	#N/A	#N/A	#N/A
13	0.351	2.914	3.728	4.081	4.270	4.696	4.772	#N/A	#N/A	#N/A	#N/A
14	0.378	2.878	3.719	4.080	4.272	4.697	4.782	#N/A	#N/A	#N/A	#N/A
15	0.405	2.846	3.716	4.079	4.271	4.694	4.778	#N/A	#N/A	#N/A	#N/A
16	0.432	2.826	3.714	4.081	4.272	4.703	4.774	#N/A	#N/A	#N/A	#N/A
17	0.459	2.811	3.712	4.078	4.273	4.698	4.780	#N/A	#N/A	#N/A	#N/A
18	0.486	2.803	3.711	4.081	4.275	4.702	4.779	#N/A	#N/A	#N/A	#N/A
19	0.514	2.803	3.711	4.081	4.275	4.702	4.779	#N/A	#N/A	#N/A	#N/A
20	0.541	2.811	3.712	4.078	4.273	4.698	4.780	#N/A	#N/A	#N/A	#N/A
21	0.568	2.826	3.714	4.081	4.272	4.703	4.774	#N/A	#N/A	#N/A	#N/A
22	0.595	2.846	3.716	4.079	4.271	4.694	4.778	#N/A	#N/A	#N/A	#N/A
23	0.622	2.878	3.719	4.080	4.272	4.697	4.782	#N/A	#N/A	#N/A	#N/A
24	0.649	2.914	3.728	4.081	4.270	4.696	4.772	#N/A	#N/A	#N/A	#N/A
25	0.676	2.964	3.734	4.077	4.269	4.694	4.776	#N/A	#N/A	#N/A	#N/A
26	0.703	3.021	3.746	4.081	4.267	4.693	4.774	#N/A	#N/A	#N/A	#N/A
27	0.730	3.092	3.763	4.082	4.267	4.691	4.769	#N/A	#N/A	#N/A	#N/A
28	0.757	3.179	3.784	4.089	4.265	4.691	4.769	#N/A	#N/A	#N/A	#N/A
29	0.784	3.286	3.823	4.098	4.271	4.688	4.774	#N/A	#N/A	#N/A	#N/A
30	0.811	3.412	3.868	4.111	4.270	4.679	4.765	#N/A	#N/A	#N/A	#N/A
31	0.838	3.570	3.938	4.142	4.281	4.683	4.760	#N/A	#N/A	#N/A	#N/A
32	0.865	3.765	4.042	4.191	4.300	4.672	4.760	#N/A	#N/A	#N/A	#N/A
33	0.892	4.023	4.207	4.279	4.352	4.655	4.747	#N/A	#N/A	#N/A	#N/A
34	0.919	4.371	4.470	4.458	4.462	#N/A	#N/A	#N/A	#N/A	#N/A	#N/A
35	0.946	4.896	4.921	4.802	4.746	#N/A	#N/A	#N/A	#N/A	#N/A	#N/A
36	0.973	5.868	5.848	5.636	5.557	#N/A	#N/A	#N/A	#N/A	#N/A	#N/A
37	1.000	7.079	7.070	6.771	6.593	6.698	6.837	#N/A	#N/A	#N/A	#N/A

Table 33. Processed extraction results for K_1 (MPa √m) about an elliptical crack of depth 0.10 mm

Aspect Ratio		1	2	3	4	11.67	19.33	27	34.67	42.33	50
Extraction Number	Normalised Location	Average	Average	Average	Average	Average	Average	Average	Average	Average	Average
0	0.000	7.083	7.077	6.776	6.591	#N/A	7.491	7.232	#N/A	#N/A	#N/A
1	0.027	5.872	5.854	5.640	5.555	#N/A	#N/A	#N/A	#N/A	#N/A	#N/A
2	0.054	4.899	4.925	4.809	4.745	#N/A	#N/A	#N/A	#N/A	#N/A	#N/A
3	0.081	4.374	4.474	4.461	4.461	#N/A	#N/A	#N/A	#N/A	#N/A	#N/A
4	0.108	4.026	4.211	4.282	4.351	#N/A	4.726	4.765	#N/A	#N/A	#N/A
5	0.135	3.768	4.046	4.193	4.299	#N/A	4.741	4.782	#N/A	#N/A	#N/A
6	0.162	3.573	3.942	4.145	4.281	#N/A	4.742	4.782	#N/A	#N/A	#N/A
7	0.189	3.416	3.872	4.114	4.270	#N/A	4.747	4.787	#N/A	#N/A	#N/A
8	0.216	3.289	3.826	4.101	4.271	#N/A	4.756	4.796	#N/A	#N/A	#N/A
9	0.243	3.183	3.787	4.092	4.265	#N/A	4.752	4.791	#N/A	#N/A	#N/A
10	0.270	3.095	3.767	4.085	4.267	#N/A	4.752	4.791	#N/A	#N/A	#N/A
11	0.297	3.024	3.750	4.083	4.267	#N/A	4.757	4.796	#N/A	#N/A	#N/A
12	0.324	2.967	3.738	4.080	4.269	#N/A	4.759	4.798	#N/A	#N/A	#N/A
13	0.351	2.918	3.731	4.084	4.270	#N/A	4.755	4.794	#N/A	#N/A	#N/A
14	0.378	2.881	3.723	4.083	4.273	#N/A	4.764	4.802	#N/A	#N/A	#N/A
15	0.405	2.850	3.720	4.082	4.271	#N/A	4.761	4.799	#N/A	#N/A	#N/A
16	0.432	2.830	3.718	4.084	4.273	#N/A	4.757	4.796	#N/A	#N/A	#N/A
17	0.459	2.814	3.716	4.081	4.274	#N/A	4.763	4.801	#N/A	#N/A	#N/A
18	0.486	2.807	3.715	4.084	4.276	#N/A	4.762	4.800	#N/A	#N/A	#N/A
19	0.514	2.807	3.715	4.084	4.276	#N/A	4.762	4.800	#N/A	#N/A	#N/A
20	0.541	2.814	3.716	4.081	4.274	#N/A	4.763	4.801	#N/A	#N/A	#N/A
21	0.568	2.830	3.718	4.084	4.273	#N/A	4.757	4.796	#N/A	#N/A	#N/A
22	0.595	2.850	3.720	4.082	4.271	#N/A	4.761	4.799	#N/A	#N/A	#N/A
23	0.622	2.881	3.723	4.083	4.273	#N/A	4.764	4.802	#N/A	#N/A	#N/A
24	0.649	2.918	3.731	4.084	4.270	#N/A	4.755	4.794	#N/A	#N/A	#N/A
25	0.676	2.967	3.738	4.080	4.269	#N/A	4.759	4.798	#N/A	#N/A	#N/A
26	0.703	3.024	3.750	4.083	4.267	#N/A	4.757	4.796	#N/A	#N/A	#N/A
27	0.730	3.095	3.767	4.085	4.267	#N/A	4.752	4.791	#N/A	#N/A	#N/A
28	0.757	3.183	3.787	4.092	4.265	#N/A	4.752	4.791	#N/A	#N/A	#N/A
29	0.784	3.289	3.826	4.101	4.271	#N/A	4.756	4.796	#N/A	#N/A	#N/A
30	0.811	3.416	3.872	4.114	4.270	#N/A	4.747	4.787	#N/A	#N/A	#N/A
31	0.838	3.573	3.942	4.145	4.281	#N/A	4.742	4.782	#N/A	#N/A	#N/A
32	0.865	3.768	4.046	4.193	4.299	#N/A	4.741	4.782	#N/A	#N/A	#N/A
33	0.892	4.026	4.211	4.282	4.351	#N/A	4.726	4.765	#N/A	#N/A	#N/A
34	0.919	4.374	4.474	4.461	4.461	#N/A	#N/A	#N/A	#N/A	#N/A	#N/A
35	0.946	4.899	4.925	4.809	4.745	#N/A	#N/A	#N/A	#N/A	#N/A	#N/A
36	0.973	5.872	5.854	5.640	5.555	#N/A	#N/A	#N/A	#N/A	#N/A	#N/A
37	1.000	7.083	7.077	6.776	6.591	#N/A	7.491	7.232	#N/A	#N/A	#N/A

Table 34. Processed extraction results for K_1 (MPa √m) about an elliptical crack of depth 0.20 mm

Aspect Ratio		1	2	3	4	7.5	11	14.5	18	21	25
Extraction Number	Normalised Location	Average	Average	Average	Average	Average	Average	Average	Average	Average	Average
0	0.000	7.095	7.096	6.794	6.612	#N/A	#N/A	7.774	7.798	#N/A	7.918
1	0.027	5.882	5.870	5.655	5.573	#N/A	#N/A	#N/A	#N/A	#N/A	#N/A
2	0.054	4.909	4.940	4.821	4.761	#N/A	#N/A	#N/A	#N/A	#N/A	#N/A
3	0.081	4.384	4.488	4.474	4.477	#N/A	#N/A	#N/A	#N/A	#N/A	#N/A
4	0.108	4.036	4.225	4.296	4.367	#N/A	#N/A	4.706	4.755	#N/A	4.778
5	0.135	3.779	4.060	4.207	4.316	#N/A	#N/A	4.717	4.756	#N/A	4.798
6	0.162	3.584	3.957	4.159	4.302	#N/A	#N/A	4.728	4.771	#N/A	4.805
7	0.189	3.427	3.887	4.129	4.287	#N/A	#N/A	4.725	4.770	#N/A	4.816
8	0.216	3.300	3.842	4.116	4.289	#N/A	#N/A	4.732	4.779	#N/A	4.829
9	0.243	3.194	3.803	4.108	4.284	#N/A	#N/A	4.737	4.782	#N/A	4.827
10	0.270	3.107	3.784	4.102	4.286	#N/A	#N/A	4.735	4.777	#N/A	4.829
11	0.297	3.036	3.767	4.100	4.287	#N/A	#N/A	4.741	4.784	#N/A	4.834
12	0.324	2.980	3.755	4.098	4.290	#N/A	#N/A	4.741	4.783	#N/A	4.837
13	0.351	2.930	3.749	4.103	4.291	#N/A	#N/A	4.745	4.788	#N/A	4.832
14	0.378	2.894	3.741	4.101	4.294	#N/A	#N/A	4.745	4.788	#N/A	4.839
15	0.405	2.863	3.738	4.101	4.292	#N/A	#N/A	4.746	4.788	#N/A	4.835
16	0.432	2.843	3.737	4.103	4.294	#N/A	#N/A	4.743	4.785	#N/A	4.831
17	0.459	2.827	3.735	4.100	4.295	#N/A	#N/A	4.747	4.789	#N/A	4.835
18	0.486	2.820	3.734	4.104	4.297	#N/A	#N/A	4.748	4.789	#N/A	4.834
19	0.514	2.820	3.734	4.104	4.297	#N/A	#N/A	4.748	4.789	#N/A	4.834
20	0.541	2.827	3.735	4.100	4.295	#N/A	#N/A	4.747	4.789	#N/A	4.835
21	0.568	2.843	3.737	4.103	4.294	#N/A	#N/A	4.743	4.785	#N/A	4.831
22	0.595	2.863	3.738	4.101	4.292	#N/A	#N/A	4.746	4.788	#N/A	4.835
23	0.622	2.894	3.741	4.101	4.294	#N/A	#N/A	4.745	4.788	#N/A	4.839
24	0.649	2.930	3.749	4.103	4.291	#N/A	#N/A	4.745	4.788	#N/A	4.832
25	0.676	2.980	3.755	4.098	4.290	#N/A	#N/A	4.741	4.783	#N/A	4.837
26	0.703	3.036	3.767	4.100	4.287	#N/A	#N/A	4.741	4.784	#N/A	4.834
27	0.730	3.107	3.784	4.102	4.286	#N/A	#N/A	4.735	4.777	#N/A	4.829
28	0.757	3.194	3.803	4.108	4.284	#N/A	#N/A	4.737	4.782	#N/A	4.827
29	0.784	3.300	3.842	4.116	4.289	#N/A	#N/A	4.732	4.779	#N/A	4.829
30	0.811	3.427	3.887	4.129	4.287	#N/A	#N/A	4.725	4.770	#N/A	4.816
31	0.838	3.584	3.957	4.159	4.302	#N/A	#N/A	4.728	4.771	#N/A	4.805
32	0.865	3.779	4.060	4.207	4.316	#N/A	#N/A	4.717	4.756	#N/A	4.798
33	0.892	4.036	4.225	4.296	4.367	#N/A	#N/A	4.706	4.755	#N/A	4.778
34	0.919	4.384	4.488	4.474	4.477	#N/A	#N/A	#N/A	#N/A	#N/A	#N/A
35	0.946	4.909	4.940	4.821	4.761	#N/A	#N/A	#N/A	#N/A	#N/A	#N/A
36	0.973	5.882	5.870	5.655	5.573	#N/A	#N/A	#N/A	#N/A	#N/A	#N/A
37	1.000	7.095	7.096	6.794	6.612	#N/A	#N/A	7.774	7.798	#N/A	7.918

Table 35. Processed extraction results for K_1 (MPa √m) about an elliptical crack of depth 0.30 mm

Aspect Ratio		1	2	3	4	6.111	8.22	10.33	12.44	14.56	16.67
Extraction Number	Normalised Location	Average	Average	Average	Average	Average	Average	Average	Average	Average	Average
0	0.000	7.113	7.106	6.811	6.632	6.485	#N/A	#N/A	7.869	7.857	7.875
1	0.027	5.898	5.878	5.670	5.590	#N/A	#N/A	#N/A	#N/A	#N/A	#N/A
2	0.054	4.923	4.948	4.834	4.776	#N/A	#N/A	#N/A	#N/A	#N/A	#N/A
3	0.081	4.398	4.497	4.488	4.491	4.553	#N/A	#N/A	#N/A	#N/A	#N/A
4	0.108	4.050	4.234	4.310	4.382	4.509	#N/A	#N/A	4.695	4.737	4.760
5	0.135	3.792	4.070	4.222	4.331	4.496	#N/A	#N/A	4.715	4.747	4.774
6	0.162	3.597	3.967	4.174	4.315	4.499	#N/A	#N/A	4.729	4.760	4.790
7	0.189	3.440	3.898	4.145	4.304	4.503	#N/A	#N/A	4.726	4.760	4.791
8	0.216	3.314	3.854	4.132	4.306	4.511	#N/A	#N/A	4.737	4.768	4.801
9	0.243	3.208	3.816	4.125	4.302	4.511	#N/A	#N/A	4.742	4.774	4.808
10	0.270	3.121	3.797	4.119	4.305	4.518	#N/A	#N/A	4.742	4.773	4.808
11	0.297	3.051	3.780	4.118	4.306	4.518	#N/A	#N/A	4.745	4.779	4.814
12	0.324	2.994	3.769	4.117	4.309	4.521	#N/A	#N/A	4.747	4.779	4.813
13	0.351	2.945	3.764	4.122	4.311	4.527	#N/A	#N/A	4.749	4.783	4.816
14	0.378	2.908	3.756	4.121	4.314	4.530	#N/A	#N/A	4.750	4.783	4.816
15	0.405	2.877	3.753	4.121	4.313	4.525	#N/A	#N/A	4.747	4.783	4.815
16	0.432	2.858	3.752	4.123	4.315	4.529	#N/A	#N/A	4.756	4.780	4.812
17	0.459	2.842	3.750	4.120	4.316	4.530	#N/A	#N/A	4.751	4.783	4.815
18	0.486	2.835	3.750	4.124	4.319	4.531	#N/A	#N/A	4.755	4.784	4.814
19	0.514	2.835	3.750	4.124	4.319	4.531	#N/A	#N/A	4.755	4.784	4.814
20	0.541	2.842	3.750	4.120	4.316	4.530	#N/A	#N/A	4.751	4.783	4.815
21	0.568	2.858	3.752	4.123	4.315	4.529	#N/A	#N/A	4.756	4.780	4.812
22	0.595	2.877	3.753	4.121	4.313	4.525	#N/A	#N/A	4.747	4.783	4.815
23	0.622	2.908	3.756	4.121	4.314	4.530	#N/A	#N/A	4.750	4.783	4.816
24	0.649	2.945	3.764	4.122	4.311	4.527	#N/A	#N/A	4.749	4.783	4.816
25	0.676	2.994	3.769	4.117	4.309	4.521	#N/A	#N/A	4.747	4.779	4.813
26	0.703	3.051	3.780	4.118	4.306	4.518	#N/A	#N/A	4.745	4.779	4.814
27	0.730	3.121	3.797	4.119	4.305	4.518	#N/A	#N/A	4.742	4.773	4.808
28	0.757	3.208	3.816	4.125	4.302	4.511	#N/A	#N/A	4.742	4.774	4.808
29	0.784	3.314	3.854	4.132	4.306	4.511	#N/A	#N/A	4.737	4.768	4.801
30	0.811	3.440	3.898	4.145	4.304	4.503	#N/A	#N/A	4.726	4.760	4.791
31	0.838	3.597	3.967	4.174	4.315	4.499	#N/A	#N/A	4.729	4.760	4.790
32	0.865	3.792	4.070	4.222	4.331	4.496	#N/A	#N/A	4.715	4.747	4.774
33	0.892	4.050	4.234	4.310	4.382	4.509	#N/A	#N/A	4.695	4.737	4.760
34	0.919	4.398	4.497	4.488	4.491	4.553	#N/A	#N/A	#N/A	#N/A	#N/A
35	0.946	4.923	4.948	4.834	4.776	#N/A	#N/A	#N/A	#N/A	#N/A	#N/A
36	0.973	5.898	5.878	5.670	5.590	#N/A	#N/A	#N/A	#N/A	#N/A	#N/A
37	1.000	7.113	7.106	6.811	6.632	6.485	#N/A	#N/A	7.869	7.857	7.875

Table 36. Processed extraction results for K_1 (MPa √m) about an elliptical crack of depth 0.50 mm

Aspect Ratio		1	2	3	4	7	8	9	10
Extraction Number	Normalised Location	Average	Average	Average	Average	Average	Average	Average	Average
0	0.000	7.130	7.138	6.841	6.669	#N/A	#N/A	#N/A	#N/A
1	0.027	5.914	5.906	5.696	5.622	#N/A	#N/A	#N/A	#N/A
2	0.054	4.939	4.973	4.858	4.805	#N/A	#N/A	#N/A	#N/A
3	0.081	4.415	4.522	4.512	4.521	#N/A	#N/A	#N/A	#N/A
4	0.108	4.067	4.259	4.335	4.413	#N/A	#N/A	#N/A	#N/A
5	0.135	3.811	4.096	4.248	4.363	#N/A	#N/A	#N/A	#N/A
6	0.162	3.617	3.994	4.202	4.349	#N/A	#N/A	#N/A	#N/A
7	0.189	3.461	3.926	4.174	4.339	#N/A	#N/A	#N/A	#N/A
8	0.216	3.335	3.883	4.163	4.343	#N/A	#N/A	#N/A	#N/A
9	0.243	3.230	3.846	4.157	4.340	#N/A	#N/A	#N/A	#N/A
10	0.270	3.144	3.828	4.153	4.345	#N/A	#N/A	#N/A	#N/A
11	0.297	3.074	3.812	4.153	4.347	#N/A	#N/A	#N/A	#N/A
12	0.324	3.018	3.802	4.152	4.351	#N/A	#N/A	#N/A	#N/A
13	0.351	2.969	3.797	4.158	4.354	#N/A	#N/A	#N/A	#N/A
14	0.378	2.933	3.791	4.158	4.358	#N/A	#N/A	#N/A	#N/A
15	0.405	2.902	3.788	4.159	4.358	#N/A	#N/A	#N/A	#N/A
16	0.432	2.883	3.787	4.162	4.360	#N/A	#N/A	#N/A	#N/A
17	0.459	2.867	3.786	4.159	4.362	#N/A	#N/A	#N/A	#N/A
18	0.486	2.860	3.786	4.163	4.364	#N/A	#N/A	#N/A	#N/A
19	0.514	2.860	3.786	4.163	4.364	#N/A	#N/A	#N/A	#N/A
20	0.541	2.867	3.786	4.159	4.362	#N/A	#N/A	#N/A	#N/A
21	0.568	2.883	3.787	4.162	4.360	#N/A	#N/A	#N/A	#N/A
22	0.595	2.902	3.788	4.159	4.358	#N/A	#N/A	#N/A	#N/A
23	0.622	2.933	3.791	4.158	4.358	#N/A	#N/A	#N/A	#N/A
24	0.649	2.969	3.797	4.158	4.354	#N/A	#N/A	#N/A	#N/A
25	0.676	3.018	3.802	4.152	4.351	#N/A	#N/A	#N/A	#N/A
26	0.703	3.074	3.812	4.153	4.347	#N/A	#N/A	#N/A	#N/A
27	0.730	3.144	3.828	4.153	4.345	#N/A	#N/A	#N/A	#N/A
28	0.757	3.230	3.846	4.157	4.340	#N/A	#N/A	#N/A	#N/A
29	0.784	3.335	3.883	4.163	4.343	#N/A	#N/A	#N/A	#N/A
30	0.811	3.461	3.926	4.174	4.339	#N/A	#N/A	#N/A	#N/A
31	0.838	3.617	3.994	4.202	4.349	#N/A	#N/A	#N/A	#N/A
32	0.865	3.811	4.096	4.248	4.363	#N/A	#N/A	#N/A	#N/A
33	0.892	4.067	4.259	4.335	4.413	#N/A	#N/A	#N/A	#N/A
34	0.919	4.415	4.522	4.512	4.521	#N/A	#N/A	#N/A	#N/A
35	0.946	4.939	4.973	4.858	4.805	#N/A	#N/A	#N/A	#N/A
36	0.973	5.914	5.906	5.696	5.622	#N/A	#N/A	#N/A	#N/A
37	1.000	7.130	7.138	6.841	6.669	#N/A	#N/A	#N/A	#N/A

Table 37. Processed extraction results for K_1 (MPa √m) about an elliptical crack of depth 1.00 mm

Aspect Ratio		1	2	3	4
Extraction Number	Normalised Location	Average	Average	Average	Average
0	0.000	7.184	7.217	6.949	6.823
1	0.027	5.964	5.976	5.789	5.752
2	0.054	4.988	5.039	4.943	4.920
3	0.081	4.464	4.586	4.594	4.634
4	0.108	4.119	4.325	4.419	4.528
5	0.135	3.864	4.164	4.335	4.482
6	0.162	3.672	4.065	4.292	4.472
7	0.189	3.518	4.000	4.267	4.466
8	0.216	3.394	3.959	4.261	4.474
9	0.243	3.291	3.926	4.258	4.474
10	0.270	3.206	3.911	4.257	4.481
11	0.297	3.137	3.898	4.260	4.485
12	0.324	3.082	3.890	4.262	4.492
13	0.351	3.034	3.887	4.270	4.496
14	0.378	2.999	3.882	4.272	4.501
15	0.405	2.969	3.881	4.274	4.501
16	0.432	2.950	3.882	4.278	4.505
17	0.459	2.935	3.881	4.276	4.506
18	0.486	2.928	3.881	4.280	4.509
19	0.514	2.928	3.881	4.280	4.509
20	0.541	2.935	3.881	4.276	4.506
21	0.568	2.950	3.882	4.278	4.505
22	0.595	2.969	3.881	4.274	4.501
23	0.622	2.999	3.882	4.272	4.501
24	0.649	3.034	3.887	4.270	4.496
25	0.676	3.082	3.890	4.262	4.492
26	0.703	3.137	3.898	4.260	4.485
27	0.730	3.206	3.911	4.257	4.481
28	0.757	3.291	3.926	4.258	4.474
29	0.784	3.394	3.959	4.261	4.474
30	0.811	3.518	4.000	4.267	4.466
31	0.838	3.672	4.065	4.292	4.472
32	0.865	3.864	4.164	4.335	4.482
33	0.892	4.119	4.325	4.419	4.528
34	0.919	4.464	4.586	4.594	4.634
35	0.946	4.988	5.039	4.943	4.920
36	0.973	5.964	5.976	5.789	5.752
37	1.000	7.184	7.217	6.949	6.823

Appendix F Results for Through Crack

Table 38. Raw and processed extraction results for K_1 (MPa √m) along a through crack of various depths

Depth (mm)		0.08			0.1			0.2			0.3			0.5			1		
Extraction Number	Normalised Location	Normal	Mirror	Average	Normal	Mirror	Average	Normal	Mirror	Average	Normal	Mirror	Average	Normal	Mirror	Average	Normal	Mirror	Average
0	0.000	3.469	3.466	3.468	3.419	3.415	3.417	3.494	3.494	3.494	3.598	3.596	3.597	3.758	3.750	3.754	3.992	3.994	3.993
1	0.027	4.568	4.570	4.569	4.570	4.574	4.572	4.597	4.602	4.599	4.621	4.622	4.621	4.665	4.658	4.662	4.747	4.747	4.747
2	0.054	4.726	4.716	4.721	4.720	4.724	4.722	4.742	4.737	4.740	4.758	4.749	4.754	4.791	4.775	4.783	4.856	4.851	4.854
3	0.081	4.783	4.782	4.782	4.781	4.791	4.786	4.799	4.803	4.801	4.811	4.812	4.812	4.840	4.834	4.837	4.900	4.901	4.901
4	0.108	4.830	4.819	4.824	4.819	4.831	4.825	4.842	4.841	4.842	4.854	4.852	4.853	4.879	4.872	4.875	4.931	4.934	4.932
5	0.135	4.846	4.843	4.844	4.845	4.849	4.847	4.861	4.860	4.860	4.872	4.869	4.870	4.894	4.887	4.891	4.944	4.945	4.944
6	0.162	4.857	4.851	4.854	4.859	4.860	4.860	4.873	4.871	4.872	4.885	4.880	4.883	4.908	4.898	4.903	4.956	4.957	4.956
7	0.189	4.876	4.867	4.872	4.873	4.872	4.873	4.887	4.883	4.885	4.898	4.892	4.895	4.921	4.909	4.915	4.969	4.965	4.967
8	0.216	4.872	4.876	4.874	4.871	4.879	4.875	4.888	4.892	4.890	4.899	4.901	4.900	4.922	4.919	4.920	4.971	4.973	4.972
9	0.243	4.875	4.870	4.872	4.873	4.882	4.878	4.889	4.893	4.891	4.900	4.903	4.901	4.922	4.922	4.922	4.971	4.978	4.974
10	0.270	4.879	4.872	4.875	4.878	4.883	4.881	4.894	4.896	4.895	4.904	4.904	4.904	4.926	4.922	4.924	4.975	4.975	4.975
11	0.297	4.885	4.878	4.881	4.885	4.881	4.883	4.895	4.892	4.894	4.906	4.901	4.904	4.928	4.921	4.924	4.977	4.976	4.977
12	0.324	4.869	4.875	4.872	4.872	4.878	4.875	4.887	4.890	4.889	4.898	4.899	4.899	4.922	4.917	4.920	4.974	4.972	4.973
13	0.351	4.877	4.865	4.871	4.877	4.874	4.876	4.892	4.887	4.889	4.903	4.896	4.900	4.925	4.916	4.921	4.978	4.972	4.975
14	0.378	4.873	4.868	4.870	4.874	4.880	4.877	4.886	4.892	4.889	4.896	4.903	4.900	4.919	4.923	4.921	4.973	4.976	4.974
15	0.405	4.878	4.871	4.875	4.877	4.876	4.876	4.890	4.893	4.892	4.900	4.903	4.902	4.921	4.923	4.922	4.972	4.977	4.975
16	0.432	4.871	4.880	4.876	4.872	4.881	4.876	4.885	4.895	4.890	4.895	4.904	4.900	4.917	4.924	4.920	4.970	4.977	4.974
17	0.459	4.872	4.870	4.871	4.873	4.874	4.874	4.887	4.887	4.887	4.897	4.897	4.897	4.917	4.917	4.917	4.970	4.969	4.970
18	0.486	4.867	4.880	4.874	4.869	4.884	4.876	4.883	4.895	4.889	4.893	4.905	4.899	4.915	4.925	4.920	4.970	4.974	4.972
19	0.514	4.880	4.867	4.874	4.884	4.869	4.876	4.895	4.883	4.889	4.905	4.893	4.899	4.925	4.915	4.920	4.974	4.970	4.972
20	0.541	4.870	4.872	4.871	4.874	4.873	4.874	4.887	4.887	4.887	4.897	4.897	4.897	4.917	4.917	4.917	4.969	4.970	4.970
21	0.568	4.880	4.871	4.876	4.881	4.872	4.876	4.895	4.885	4.890	4.904	4.895	4.900	4.924	4.917	4.920	4.977	4.970	4.974
22	0.595	4.871	4.878	4.875	4.876	4.877	4.876	4.893	4.890	4.892	4.903	4.900	4.902	4.923	4.921	4.922	4.977	4.972	4.975
23	0.622	4.868	4.873	4.870	4.880	4.874	4.877	4.892	4.886	4.889	4.903	4.896	4.900	4.923	4.919	4.921	4.976	4.973	4.974
24	0.649	4.865	4.877	4.871	4.874	4.877	4.876	4.887	4.892	4.889	4.896	4.903	4.900	4.916	4.925	4.921	4.972	4.978	4.975
25	0.676	4.875	4.869	4.872	4.878	4.872	4.875	4.890	4.887	4.889	4.899	4.898	4.899	4.917	4.922	4.920	4.972	4.974	4.973
26	0.703	4.878	4.885	4.881	4.881	4.885	4.883	4.892	4.895	4.894	4.901	4.906	4.904	4.921	4.928	4.924	4.976	4.977	4.977
27	0.730	4.872	4.879	4.875	4.883	4.878	4.881	4.896	4.894	4.895	4.904	4.904	4.904	4.922	4.926	4.924	4.975	4.975	4.975
28	0.757	4.870	4.875	4.872	4.882	4.873	4.878	4.893	4.889	4.891	4.903	4.900	4.901	4.922	4.922	4.922	4.978	4.971	4.974
29	0.784	4.876	4.872	4.874	4.879	4.871	4.875	4.892	4.888	4.890	4.901	4.899	4.900	4.919	4.922	4.920	4.973	4.971	4.972
30	0.811	4.867	4.876	4.872	4.872	4.873	4.873	4.883	4.887	4.885	4.892	4.898	4.895	4.909	4.921	4.915	4.965	4.969	4.967
31	0.838	4.851	4.857	4.854	4.860	4.859	4.860	4.871	4.873	4.872	4.880	4.885	4.883	4.898	4.908	4.903	4.957	4.956	4.956
32	0.865	4.843	4.846	4.844	4.849	4.845	4.847	4.860	4.861	4.860	4.869	4.872	4.870	4.887	4.894	4.891	4.945	4.944	4.944
33	0.892	4.819	4.830	4.824	4.831	4.819	4.825	4.841	4.842	4.842	4.852	4.854	4.853	4.872	4.879	4.875	4.934	4.931	4.932
34	0.919	4.782	4.783	4.782	4.791	4.781	4.786	4.803	4.799	4.801	4.812	4.811	4.812	4.834	4.840	4.837	4.901	4.900	4.901
35	0.946	4.716	4.726	4.721	4.724	4.720	4.722	4.737	4.742	4.740	4.749	4.758	4.754	4.775	4.791	4.783	4.851	4.856	4.854
36	0.973	4.570	4.568	4.569	4.574	4.570	4.572	4.602	4.597	4.599	4.622	4.621	4.621	4.658	4.665	4.662	4.747	4.747	4.747
37	1.000	3.466	3.469	3.468	3.415	3.419	3.417	3.494	3.494	3.494	3.596	3.598	3.597	3.750	3.758	3.754	3.994	3.992	3.993

This page is intentionally blank

DEFENCE SCIENCE AND TECHNOLOGY ORGANISATION
DOCUMENT CONTROL DATA

1. PRIVACY MARKING/CAVEAT (OF DOCUMENT)

2. TITLE

Determination of Small Crack Stress Intensity Factors for an American Society for Testing Materials (ASTM) Middle Tension Test Specimen by Finite Element Method

3. SECURITY CLASSIFICATION (FOR UNCLASSIFIED REPORTS THAT ARE LIMITED RELEASE USE (L) NEXT TO DOCUMENT CLASSIFICATION)

Document	(U)
Title	(U)
Abstract	(U)

4. AUTHOR(S)

Callum Wright

5. CORPORATE AUTHOR

DSTO Defence Science and Technology Organisation
506 Lorimer St
Fishermans Bend Victoria 3207 Australia

6a. DSTO NUMBER	6b. AR NUMBER	6c. TYPE OF REPORT	7. DOCUMENT DATE
DSTO-TR-2628	AR-015-156	Technical Report	November 2011

8. FILE NUMBER	9. TASK NUMBER	10. TASK SPONSOR	11. NO. OF PAGES	12. NO. OF REFERENCES
2009/1000722/1	07/250	CAVD	86	13

13. DSTO Publications Repository

http://dspace.dsto.defence.gov.au/dspace/

14. RELEASE AUTHORITY

Chief, Air Vehicles Division

15. SECONDARY RELEASE STATEMENT OF THIS DOCUMENT

Approved for public release

OVERSEAS ENQUIRIES OUTSIDE STATED LIMITATIONS SHOULD BE REFERRED THROUGH DOCUMENT EXCHANGE, PO BOX 1500, EDINBURGH, SA 5111

16. DELIBERATE ANNOUNCEMENT

No limitations.

17. CITATION IN OTHER DOCUMENTS Yes

18. DSTO RESEARCH LIBRARY THESAURUS http://web-vic.dsto.defence.gov.au/workareas/library/resources/dsto_thesaurus.shtml

Finite element analysis, fatigue, stress intensity factors

19. ABSTRACT

Improved small-crack stress intensity factors are important for accurate fatigue crack growth prediction. This report presents accurate small-crack stress intensity factor distributions for the American Society for Testing Materials middle tension test specimen, derived in three dimensions utilising the advanced finite element method code StressCheck for a parametric study of a range of small crack sizes and shapes. This information was not readily available in reference books. The results have been presented in tabulated normalised form for future reference and clearly show the influence of the specimen notch on the variation of stress intensity factors.